ISSN 0973-8916

Current Trends in Biotechnology and Pharmacy

Volume 5 Issue 4 October 2011

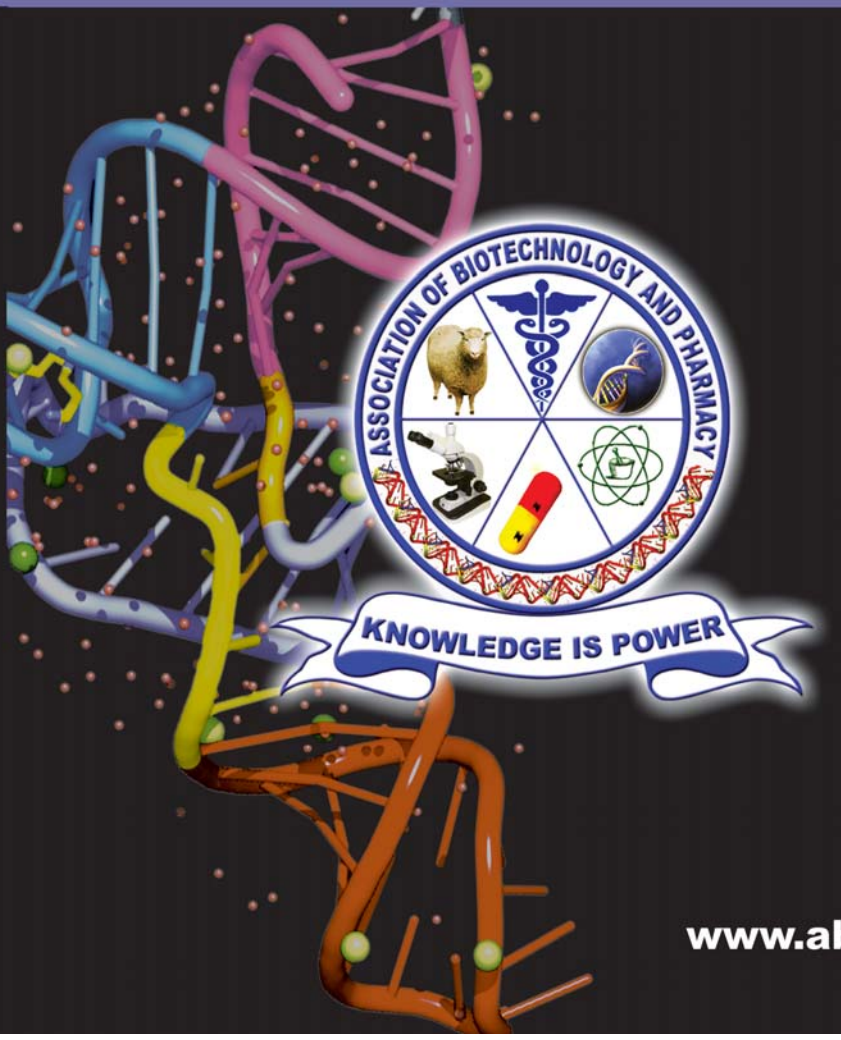

www.abap.co.in

Current Trends in Biotechnology and Pharmacy
ISSN 0973-8916 (Print), 2230-7303 (Online)

Editors

Prof. K.R.S. Sambasiva Rao, India
krssrao@abap.co.in

Prof. Karnam S. Murthy, USA
skarnam@vcu.edu

Editorial Board

Assistant Editors

(Electronic Version)
www.abap.co.in

ISSN 0973-8916

Current Trends in Biotechnology and Pharmacy

(An International Scientific Journal)

Volume 5 Issue 4 October 2011

www.abap.co.in

Indexed in Chemical Abstracts, EMBASE, ProQuest, Academic SearchTM, DOAJ, CAB Abstracts, Index Copernicus, Ulrich's Periodicals Directory, Open J-Gate Pharmoinfonet.in Indianjournals.com and Indian Science Abstracts.

Association of Biotechnology and Pharmacy

(Regn. No. 28 OF 2007)

The *Association of Biotechnology and Pharmacy (ABAP)* was established for promoting the science of Biotechnology and Pharmacy. The objective of the Association is to advance and disseminate the knowledge and information in the areas of Biotechnology and Pharmacy by organising annual scientific meetings, seminars and symposia.

Members

The persons involved in research, teaching and work can become members of Association by paying membership fees to Association.

The members of the Association are allowed to write the title ***MABAP*** (Member of the Association of Biotechnology and Pharmacy) with their names.

Fellows

Every year, the Association will award Fellowships to the limited number of members of the Association with a distinguished academic and scientific career to be as Fellows of the Association during annual convention. The fellows can write the title ***FABAP*** (Fellow of the Association of Biotechnology and Pharmacy) with their names.

Membership details

(Membership and Journal)		India	SAARC	Others
Individuals	– 1 year	Rs. 600	Rs. 1000	$100
	LifeMember	Rs. 4000	Rs. 6000	$500
Institutions (Journal only)	– 1 year	Rs. 1500	Rs. 2000	$200
	Life member	Rs.10000	Rs.12000	$1200

Individuals can pay in two instalments, however the membership certificate will be issued on payment of full amount. All the members and Fellows will receive a copy of the journal free

Association of Biotechnology and Pharmacy
(Regn. No. 28 OF 2007)
#5-69-64; 6/19, Brodipet
Guntur – 522 002, Andhra Pradesh, India

Current Trends in Biotechnology and Pharmacy
Vol. 5 (4) October 2011, ISSN 0973-8916 (Print), 2230-7303 (Online)

Current Trends in Biotechnology and Pharmacy

ISSN 0973-8916

Volume 5 (4) **October - 2011**

CONTENTS

Information to Authors

The *Current Trends in Biotechnology and Pharmacy* is an official international journal of *Association of Biotechnology and Pharmacy*. It is a peer reviewed quarterly journal dedicated to publish high quality original research articles in biotechnology and pharmacy. The journal will accept contributions from all areas of biotechnology and pharmacy including plant, animal, industrial, microbial, medical, pharmaceutical and analytical biotechnologies, immunology, proteomics, genomics, metabolomics, bioinformatics and different areas in pharmacy such as, pharmaceutics, pharmacology, pharmaceutical chemistry, pharma analysis and pharmacognosy. In addition to the original research papers, review articles in the above mentioned fields will also be considered.

Call for papers

The Association is inviting original research or review papers and short comunications in any of the above mentioned research areas for publication in Current Trends in Biotechnology and Pharmacy. The manuscripts should be concise, typed in double space in a general format containing a title page with a short running title and the names and addresses of the authors for correspondence followed by Abstract (350 words), 3 – 5 key words, Introduction, Materials and Methods, Results and Discussion, Conclusion, References, followed by the tables, figures and graphs on separate sheets. For quoting references in the text one has to follow the numbering of references in parentheses and full references with appropriate numbers at the end of the text in the same order. References have to be cited in the format below.

Mahavadi, S., Rao, R.S.S.K. and Murthy, K.S. (2007). Cross-regulation of VAPC2 receptor internalization by m2 receptors via c-Src-mediated phosphorylation of GRK2. Regulatory Peptides, 139: 109-114.

Lehninger, A.L., Nelson, D.L. and Cox, M.M. (2004). Lehninger Principles of Biochemistry, (4th edition), W.H. Freeman & Co., New York, USA, pp. 73-111.

Authors have to submit the figures, graphs and tables of the related research paper/article in Adobe Photoshop of the latest version for good illumination and allignment.

Authors can submit their papers and articles either to the editor or any of the editorial board members for onward transmission to the editorial office. Members of the editorial board are authorized to accept papers and can recommend for publication after the peer reviewing process. The email address of editorial board members are available in website www.abap.in. For submission of the articles directly, the authors are advised to submit by email to krssrao@abap.co.in or krssrao@yahoo.com.

Authors are solely responsible for the data, presentation and conclusions made in their articles/ research papers. It is the responsibility of the advertisers for the statements made in the advertisements.

Current Trends in Biotechnology and Pharmacy
Vol. 5 (4) 1372-1382 October 2011, ISSN 0973-8916 (Print), 2230-7303 (Online)

Nexus between Hepatic Enzyme Modulation and Cancer

Cinoy Maliakal[1], Hima Pius[2], Chris M. Lee[1] and Umesh T. Sankpal[1]*
[1]Cancer Research Institute, MD Anderson Cancer Center Orlando
Orlando, FL 32827 USA
[2]Florida State University College of Medicine
Tallahassee, FL 32306, USA
*For Correspondence - umesh.sankpal@orlandohealth.com

Abstract

The risk of developing cancer caused by environmental carcinogens lies in the balance between phase I carcinogen-activating enzymes and phase II detoxifying enzymes. Potentially genotoxic chemicals to which we are exposed to may require metabolic activation to exhibit their mutagenic and carcinogenic effects. Most of the enzyme systems, involved in carcinogen bioactivation, are concentrated in liver, but many extrahepatic organs and tissues have appreciable quantities of such enzymes. Most chemical carcinogens are activated in humans by specific cytochrome P450 (CYP) species, mainly CYP1A1, CYP1A2, CYP2E, and CYP3A. Activation of chemical carcinogens follows various metabolic pathways. The difference could range from only a single oxidation step or several sequential enzymatic steps. Polymorphic differences in carcinogen metabolism may result in difference in carcinogen risk since fast activators and/or slow detoxifiers may have higher steady state tissue concentration of the causative agent than slow activator and/or fast detoxifiers. Cancer prevention through better diet and nutrition has received considerable attention in the past and continues to show promise even today." It has become increasingly apparent that adopting a diet may allow reduction in cancer incidence worldwide by functioning as inhibitors of tumor initiation, promotion, and progression, which may be mediated by either selective induction or inhibition of the hepatic xenobiotic metabolizing enzymes.

Key Words: Bioactivation, carcinogens, cytochrome P450, cancer prevention, hepatic enzymes

How are carcinogens assimilated in the body?

Carcinogens act through electrophilic entities which bind covalently to specific sites in DNA. Whereas some electrophilic chemicals may function as direct carcinogens, most DNA-damaging carcinogens act via formation of reactive intermediates generated by metabolic reactions in the body. A number of carcinogens, however, appear to act via mechanisms that are not related to genotoxic effect. For these diverse structure entities, no clear cut pattern of metabolic involvement is discernible. Some chemicals with promoting activity such as phorbol ester function via the un-metabolized parent compound, whereas other promoters may cause tissue proliferation by forming metabolic products (1, 2). Most of the metabolic reactions that convert chemically-stable pre-carcinogens to electrophilic, DNA-damaging species are carried out by cytochrome P450 (CYP) (3). Many forms of CYP exist with varying substrate

Vol. 5 (4) 1372-1382 October 2011, ISSN 0973-8916 (Print), 2230-7303 (Online)

specificities, organ specificities, and inter-individual difference in their distribution. Furthermore, expression of enzymes may be altered by the administration of carcinogens themselves (auto-induction), by chemical co-exposure or by nutritional influences. In addition to the CYP-mediated activation reaction, a number of other enzyme systems have been implicated in the metabolic formation of electrophilic products. These include oxidative enzyme like flavin monooxygenase (FMO), and prostaglandin H synthetase, hydrolytic enzymes such as epoxide hydrolase and carboxyl amidase, and conjugative enzymes such as glutathione-*S*-transferase, sulfotransferase, and acetyl transferases.

Carcinogenesis is thought to be a multistep process. This fact precludes any direct linkage between the formation of reactive intermediates, covalent binding to macromolecules, and the final outcome - uncontrolled growth. Covalent interactions of reactive intermediates with DNA may be expected to have a direct correlation with mutagenesis, except when reactive intermediates generate free radicals that cause DNA damage without covalent binding of the metabolite (4). Activation of chemical carcinogens occurs by various reactions. For some carcinogens, only a single oxidation step (aflatoxin B1, vinyl chloride) or single oxidation step followed by spontaneous chemical reaction (short chain alkyl N-nitrosamines) may be needed. For other carcinogens, different sequential enzymatic steps (polycyclic aromatic hydrocarbons) or sequential enzymatic steps followed by spontaneous reactions (2-naphthylamine) appears to be crucial (5). Most of the enzyme systems involved in carcinogen bioactivation are concentrated in liver, but many extrahepatic organs and tissues have appreciable quantities of such enzymes. Since many carcinogens induce cancer in extrahepatic tissue, those that act through reactive forms must either be converted metabolically to such forms from the parent compound or a stable metabolite in the extrahepatic tissues themselves, or they must be activated in the liver and then transported to the extrahepatic tissues. Because tumor development in most instances is dose related, it follows that, for those carcinogens that act through reactive intermediates, the sites, routes and rates of the enzymatic reactions involved may influence tumor rate. It should be realised that other steps in the carcinogenic process, such as DNA-adduct repair and promotion, may be rate-determining in the overall process.

Carcinogen metabolizing enzymes **:** Most of the xenobiotics (drugs and exogenous compounds) to which humans are exposed undergo biotransformation by xenobiotic-metabolizing enzymes in the liver and extrahepatic tissues, and are eliminated by excretion as hydrophilic metabolites. Metabolic enzymes have been classified as belonging to either Phase-I or Phase-II pathways of metabolism. Phase-I biotransformations include oxidation, reduction and hydrolysis which result in the formation of functional groups and “reaction centers” on substrates. These reactions are catalyzed mainly by a super family of enzymes known as cytochrome P450 (CYP). In addition to cytochrome P450, oxidation of drugs and other xenobiotics can also be mediated by non-P450 enzymes, the most significant of which are flavin monooxygenase, monoamine oxidase, alcohol dehydrogenase, aldehyde dehydrogenase, aldehyde oxidase and xanthine oxidase (6). Phase-II biotransformations involve the conjugation of parent chemicals, or their phase-I metabolites, with small endogenous molecules such as glucuronide sulphate, glutathione, amino acids or methyl groups. Phase-I and phase-II enzymes are found most abundantly in the liver, the principal organ of biotransformation.

However, many other tissues such as the gastrointestinal tract, kidneys, lungs, skin, brain, and nasal mucosa also possess these enzymes (7). At the subcellular level, the major enzymes of biotransformation are either anchored in the membranes of the endoplasmic reticulum (P450, epoxide hydrolase, glucuronyl-transferases) or are cytosolic enzymes (aldehyde oxidase, acetyltransferases, sulfotransferases, xanthine oxidase).

Mostly, chemical carcinogens have been environmental contaminants that may be routinely ingested by humans in the diet, such as the food-derived heterocyclic amines, or less frequently chemicals given for their therapeutic value, as in the case of the synthetic estrogen, diethylstilboestrol (8). Enzymes that metabolize foreign compounds exhibit a large degree of inter-individual variability in their levels of expression (9). Inter-individual variability in drug metabolism has been shown to directly influence drug efficacy and toxicity.

The Majority of chemical carcinogens are activated in humans by specific CYP species, mainly CYP1A1, CYP1A2, CYP2E and CYP3A (10) (Table 1). Human CYP1A2 and CYP3A4 appear to be the most important enzymes with respect to activation of a number of pre-carcinogens to mutagenic species. Inter-individual susceptibility to cancer may be associated with genetic variations in these activating enzymes, and in the enzymes that catalyze detoxification of carcinogens. The highly potent hepato-carcinogen, 3-methoxy-4-aminobenzene, although selectively inducing rat CYP1A2, is itself bioactivated by rat CYP1A1,

Table 1. Major Carcinogen metabolising cytochrome P450 isozymes in human (10)

P450 enzymes	Site	Induced by	Carcinogens activated
CYP 1A1	Extrahepatic	PAH, TCDD	BP,2-AAF AFB, 2AAF
CYP 1A2	liver	isosafrole	Tyro-P-2,IQ
CYP 2A6	Liver	PAH	AFB, DEN
CYP 2B7	Liver	Phenobarbital	AFB
CYP 2C7	Live	Phenobarbital, Retionids	AFB
CYP 2C10	Liver		AFB
CYP 2D6	Liver	Phenobarbital, Dexamethasone	AFB
CYP 2E1	Liver	Acetone, ethanol	DEN,DMN
CYP 2F1	Liver		Styrene, Naphthalene
CYP3A3	Liver	Dexamethasone, Rifampicin, Phenobarbital	AFB
CYP 3A4	Liver	Dexamethasone, Rifampicin, Phenobarbital	AFBBP-7
CYP 3A5	Liver	Dexamethasone, Rifampicin, Phenobarbital	8-diol AFB
CYP 3A7	Liver	Dexamethasone, Rifampicin, Phenobarbital	IQ
CYP4B1	Placenta, lung	Clofibrate	

Abbreviations: AFB=AflatoxinB1; BP=Benzo[*a*]pyrene; 2-AAF=2-acetylamidofluorene; Trp-P-2, and IQ=food pyrolysis, mutagenic heterocyclic amines; DEN and DMN=diethyl and dimethyl nitrosamines; PAH=Polycyclic Aromatic Hydrocarbon; TCDD=tetrachloro-dibenzo-p-dioxin.

1A2, 2B1, 2E1 and 3A1 and by human CYP1A2, 2E1 and 3A4 (10). Aromatic amine carcinogens are preferentially activated by CYP1A2; these include 2-aminofluorene, 2-naphthylamine, 4-amino-biphenyl and several heterocyclic amines. CYP3A4 is involved mainly in the activation of carcinogens such as aflatoxins, sterigmatocystine, 2,3-dibromopropyl phosphate and several dihydrodiols of polycyclic aromatic hydrocarbons (PAH). Human CYP2E1 seems to play an important role in the oxidation of short-chain, N-alkyl nitrosamines, benzene, carbon tetrachloride, chloroform, dichloromethane, vinyl chloride, urethane, etc.

***Polycyclic Aromatic Hydrocarbons*:** Polycyclic aromatic hydrocarbons (PAH) are commonly present in the environment as a result of industrial combustion processes and in tobacco products. Carcinogenic PAH form DNA adducts via a complex metabolic activation pathway that includes CYP1A1, whereas intermediate metabolites can be detoxified by conjugation through pathways including glutathione-S-transferase (GST). There is evidence that diol epoxides are the ultimate carcinogenic metabolite of a number of PAHs. Such epoxides are formed by three sequential catalytic reactions involving CYP and epoxide hydrolase. In rats and mice, CYP1A1 enzymes play predominant roles in both epoxidation reactions and benzo[a]pyrene activation (11). Whereas the initial oxidation of benzo[*a*]pyrene is catalyzed by CYP1A1, further activation is performed by CYP3A4 in human liver (Fig. 1). Cigarette smoke contains a wide variety of polycyclic hydrocarbons (Table 2), nitrosamines, and aromatic amines. There is a highly significant correlation between the amount of immunoreactive CYP and high affinity component of phenacetin-*O*-deethylase (CYP1A2) activity in both smokers and non-smokers. A dramatic increase of benzo[*a*]pyrene hydroxylation in human placenta is also seen in smokers (12). 6-Nitrochrysene is present in environmental sources such as diesel exhaust particulate and has been shown to be a potent liver and lung carcinogen in newborn mice. The formation of proximate carcinogen trans-1,2-dihydro-1,2-dihydroxy-6-nitrochrysene is the most abundant metabolite of 6-nitrochrysene in human microsomes, and is preferentially catalysed by CYP1A2 (13).

***Arylamines*:** Humans are frequently exposed to arylamines such as 2-naphthylamine and 4-aminobiphenyl, found in coal and shale-derived oils and in agricultural chemicals. 4-aminobiphenyl is regarded as the most potent of the arylamine human pro-carcinogens and is primarily activated by CYP1A2 to a reactive hydroxylated metabolite that can enter the circulation and be transported to the urinary bladder where reabsorption into the bladder epithelium and arylamine-DNA adduct formation can occur (14).

***Aromatic amines*:** 2-Acetylaminofluorene (AAF) is a model carcinogenic aromatic amine. This shows considerable species difference with respect to hepato-carcinogenecity. Rats are much more susceptible than mice or hamster whereas guinea pig has been found resistant (15). It is extensively metabolised by human liver microsomes, and is activated by N-hydroxylation to ultimate carcinogen.

***Nitrosamines*:** Nitrosamines require metabolic activation to initiate the carcinogenic response. For example, nitrosodimethylamine (NDMA) is hydroxylated by CYP at its a-carbon atom to yield an unstable metabolite, which decomposes to give a reactive metabolite (16). Of 11 reconstituted mono-oxygenase systems containing individual purified rat P450 enzymes, only CYP2E1 has high activity for N-demethylation of NDMA (17). Human CYP2E1

Vol. 5 (4) 1372-1382 October 2011, ISSN 0973-8916 (Print), 2230-7303 (Online)

also appears to play an important role in the metabolic activation of NDMA and other short chain nitrosamines.

***Mycotoxins*:** The mycotoxin, aflatoxin B_1 is a very potent liver carcinogen in rats. Metabolic activation of aflatoxin B_1 appears to be one step oxidation reaction to form the epoxide. In human, rat, and hamster, the major CYP enzymes involved in aflatoxin activation are CYP3A4, CYP1A2, CYP2C11 and CYP2A3, respectively (18). CYP1A2 has also been found to be primarily responsible for activation of aflatoxin B_1 under ordinary conditions of human exposure. Aflatoxin B_1 is produced by some strains of *Aspergillus,* which grow on a variety of agricultural products, such as peanuts. Numerous outbreaks of human acute aflatoxicosis involving liver failure and gastrointestinal bleeding have occurred in Southeast Asia and Africa.

***Food Mutagens*:** Epidemiological studies have revealed a strong association between diet and a variety of human cancers. Heterocyclic aromatic amines (HAAs) are formed when meat juices are pyrolyzed. In humans, HAAs are activated *in vivo* by CYP1A2 and N-acetyltransferase (NAT) to mutagens or carcinogens (19). While activity of NAT is non-inducible, exposure to cruciferous vegetables containing indole-3-carbinol, caffeine, and some forms of green tea have been shown to induce CYP1A2 activity in humans.

Variations in Carcinogen Metabolism

***Polymorphism*:** Polymorphic differences in carcinogen metabolism may result in difference in carcinogen risk since fast activators and/or slow detoxifiers may have higher steady state tissue concentration of the causative agent than slow activator and/or fast detoxifiers. There is some evidence that differences in cancer risk are related to polymorphic variations in P450 N-acetyltransferase or glutathione transferase enzymes (20, 21). Similarly, for PAH-DNA (polycyclic aromatic hydrocarbon–DNA) adducts in white blood cells, the range of binding levels was 3-9 fold among smokers and 2-7 fold among non-smokers (22, 23)

***P450 enzyme content*:** Changes in CYP composition can influence tumor initiation in experimental animal systems. Indirect evidence for role of CYP is provided by experiments in which *in vitro* mutagenesis and DNA adduct formation are affected by changes in CYP composition, which can be brought about by genetic means or by enzyme induction with reconstituted purified enzymes (24). Although increases in CYP enzyme activity occur in liver and extrahepatic tissue of genetically-responsive mice, only extrahepatic tissues show enhanced tumor formation and these experiments have been restricted to PAH. Most of the PAHs were used in single dose complete carcinogen bioassays, and the possibility must be considered that their effect might not only be on initiation. Any experiments designed to show roles of enzymes in tumor initiation must be carefully constructed to show that the enzyme inducers are truly acting as co-carcinogens and not as promoters (some barbiturates and hydantoins are inducers but not promoters).

***Tumor promoters*:** Tumor promoters are chemicals which increase the number of tumors when administered after initiating carcinogens at doses which, by themselves, do not produce tumors, and are distinguished from co-carcinogens, which must be administered very close to the time of initiation. There is a possibility that the formation of electrophilic metabolites of carcinogens can play a role in their tumor-promoting activities (25)

***Non-hepatic P450 enzymes*:** In some extrahepatic tissues CYPs are highly localized in particular regions or cell types so that local

Vol. 5 (4) 1372-1382 October 2011, ISSN 0973-8916 (Print), 2230-7303 (Online)

concentration may approach that found in liver. These tissue specific differences in CYP can be major determinants in extrahepatic carcinogenesis, since these CYPs can activate chemicals in close proximity to targets. On the other hand, evidence exists that some of the ultimate carcinogens can migrate throughout the body. It should also be pointed out that, in extrahepatic tissues, high levels of FMO and prostaglandin synthase can be found. Often these enzymes form the same products that are encountered in CYP reactions, and caution should be exercised in assignment of the various enzymes.

***Difference between metabolism of carcinogens in humans and animals*:** Evidence of association of cancer risk with CYP composition is not well established in humans than in experimental animals. How adequate are the animal models for prediction of events in a human? If it is hypothesized that CYP and other enzymes have major role in the activation of chemicals to ultimate carcinogens, then it must be asked what similarity of enzymes encounter in animal models to those of interest in human population at risk. Elovaara et al reported a good correlation between the level of lymphocyte aryl hydrocarbon hydroxylase (CYP1A) activity and incidence of lung cancer (26).

***Dietary influence*:** Food contains a variety of specifically healthful or harmful components and hence the incidence of cancer has a strong relationship to the food we ingest. The knowledge of nutrition's role in the pathogenesis of cancer has recently continued to increase with evidence coming from ecological correlation, particularly in the United States, and Japan, where several types of cancer differ greatly in its incidence (27).

A variety of highly sensitive analytical techniques can detect food-borne carcinogenic chemicals. Aflatoxins, which are potent carcinogenic mycotoxins produced by fungi, were not discovered until 1960, but were probably at significant levels in certain crops such as corn or peanuts prior that time (28). Aflatoxins have been associated with liver cancer in Asian and African countries, where exposure is high, and chronic hepatitis also contributes. During the cooking of food, a variety of heterocyclic amines are formed in the browning reactions (29). These DNA–reactive agents are potent multi-organ and multi-species carcinogens, in many species including primates. It has been postulated that they may be the initiating agents for breast, prostate, pancreas, and colon cancers in western societies (30).

Table 2. Examples of polycyclic hydrocarbons (PAH) present in cigarette smoke (40)

3,4-Benzo[a]pyrene	Naphthalene
Dibenzo[a,e]pyrene	Acenaphthylene
Dibenz[a,h]anthracene	Acenaphthene
1,2-Benzanthracene	Fluorene
1,2,5,6-Dibenzanthracene	Phenanthrene
Chrysene	Fluoranthene
3,4-Benzofluorene	Pyerene
Anthracene	Benzo[b]fluoranthene
Cyclophenta[c,d]pyrene	Perylene
Indeno[1,2,-cd]pyrene	Coronene
Benzo[ghi]perylene	

Vol. 5 (4) 1372-1382 October 2011, ISSN 0973-8916 (Print), 2230-7303 (Online)

Consumption of well-done red meat, a source of heterocyclic amines, has been associated with an increased risk of colorectal adenomas, (precursors of carcinomas). In the stomach, nitrosation reactions involving nitrates and other components in the diet give rise to nitrosamides and nitrosamines. These carcinogens are postulated to be initiating agents for stomach and esophageal cancer. Among beverages, alcohol consumed in excessive amounts is clearly associated with liver disease and increased risk of liver cancer, as well as esophageal cancer linked with cigarette smoking. Increased risk of colon cancer is also reported to be associated with alcohol consumption. Coffee has also been discussed as a risk factor, particularly for bladder cancer, but a causal association has not been established. In fact, caffeine may possibly be antimutagenic (31).

***Prevention of Cancer*:** Early diagnosis, novel therapy as well as cancer chemoprevention is needed, if the battle against cancer is to be won. Chemoprevention in recent years has emerged as a potential strategy for control of cancer. Chemoprevention is a means by which the use of naturally-occurring and/or synthetic compounds completely prevents, blocks or reverses occurrence of the disease (32-34). Cancer chemoprevention is also defined as the prevention, inhibition, or reversal of carcinogenesis by administration of one or more chemical entities, either as individual drugs or as naturally-occurring constituents of the diet. Cancer prevention through better diet and nutrition has received considerable attention in the recent past and also promises to be a particularly important issue now. In this new millennium it has become increasingly apparent that an era where the option of adopting a diet that may allow reduction in cancer incidence worldwide has been entered. Almost one third of cancers are caused by dietary substances and the strategy of manipulation of diet is being increasingly recognized as a practical approach for cancer prevention. It is one of the novel approaches of controlling cancer by alternative therapy that has some limitations and drawbacks in patient treatment. It is important to find a way to neutralize carcinogens or protect against deleterious effects they exert. In this respect, chemoprevention offers a realistic promise to reducing the incidence of human cancer.

For many chemopreventive agents, mechanistic details of how they act are not fully elucidated. Many agents may act through more than one mechanism, making it difficult, if not impossible, to establish the most effective mode of action. Conventional classification of chemopreventive agents is based on the underlying mechanism by which they exert protective effects on a specific stage of multi-step carcinogenesis, where tumor development has been generally considered to consist of three distinct steps-initiation, promotion, and progression. Chemopreventive agents may be classified as inhibitors of carcinogen formation, blocking agents and suppressing agents. Blocking agents are inhibitors of tumor initiation, while suppressing agents are inhibitors of tumor promotion/ progression. Inhibitors of Carcinogen formation predominantly prevent the formation of nitrosamines from amine and nitrite in an acidic medium. These inhibitors of carcinogen formation include reductive acids like ascorbic acid, phenolic compounds like caffeic acid, gallic acid, sulfhydryl compounds such as N-acetylcysteine and amino acids like proline (35-37). Blocking agents act by chemical intervention at the initiation stage of carcinogen. They could be classified as inhibitors of CYP enzymes; inducers of CYP enzymes; inducers of phase-II enzymes or scavengers of electrophiles and free radicals; inducers of DNA repair. Suppressing agents can be classified as compounds that inhibit

polyamine metabolism; induce terminal cell differentiation; modulate signal transduction; modulate hormonal/growth factor activity; inhibit oncogene activity; promote intercellular communication; restore immune response; induce apoptosis; correct DNA methylation imbalance; inhibit basement membrane degradation; and inhibit arachidonic acid metabolism (38, 39).

Conclusion

Modulation of carcinogen metabolism is often considered by many investigators as a mechanistic basis for protective effect of many types of chemopreventive phytochemicals in the initiation stage of carcinogenesis. However, inhibition of initiation alone is less of a practical approach to chemoprevention, since there are diverse types of initiators present in environment. It is not feasible to find a chemopreventive agent that can nullify the initiating activity of all carcinogens to which humans are exposed. Therefore, recent chemopreventive strategies are more concerned with identifying substances with anti-proliferative or anti-progressive activity that can suppress transformation of initiated or precancerous cells to malignant ones. More studies should investigate the mechanisms which include modulation of signal transduction, inhibition of oncogene activation, inhibition of polyamine metabolism, inhibition of angiogenesis etc. Judicious utilization of current advances in molecular biology and tissue culture techniques would help achieve this objective more quickly. It is widely agreed that conducting intervention trials of chemopreventive agents on human cancer is an important approach to elucidate any protective effect. It is important to know the levels of putative active components in target tissues and whether such levels are capable of inhibiting cancer formation and growth.

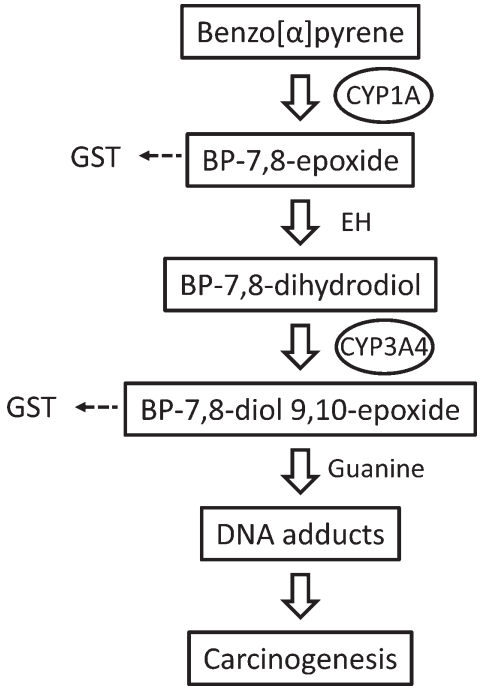

Fig. 1. Metabolism and activation of polycyclic aromatic hydrocarbons. Metabolic enzymes cytochrome P450 (CYP1A, CYP3A4) and microsomal epoxide hydrolase (EH) activate Benzopyrene to BP-diol-epoxide that forms stable DNA adducts leading to carcinogenesis.

References

1. Bogi, K., Lorenzo, P.S., Szallasi, Z., Acs, P., Wagner, G.S. and Blumberg, P.M. (1998). Differential selectivity of ligands for the C1a and C1b phorbol ester binding domains of protein kinase Cdelta: possible correlation with tumor-promoting activity. Cancer Res, 58(7): 1423-1428.

2. Dybing, E. and Huitfeldt, H.S. 1992). Species differences in carcinogen metabolism and interspecies extrapolation. IARC Sci Publ, (116): 501-522.

3. Guengerich, F.P. (2000). Metabolism of chemical carcinogens. Carcinogenesis, 21(3): 345-51.

Vol. 5 (4) 1372-1382 October 2011, ISSN 0973-8916 (Print), 2230-7303 (Online)

4. Liu, W.B., Liu, J.Y., Ao, L., Zhou, Z.Y., Zhou, Y.H., Cui, Z.H., Yang, H. and Cao, J. (2009). Dynamic changes in DNA methylation during multistep rat lung carcinogenesis induced by 3-methylcholanthrene and diethylnitrosamine. Toxicol Lett, 189(1): 5-13.

5. Levin, W., Wood, A., Chang, R., Ryan, D., Thomas, P., Yagi, H., Thakker, D., Vyas, K., Boyd, C., Chu, S.Y., Conney, A. and Jerina, D. (1982). Oxidative metabolism of polycyclic aromatic hydrocarbons to ultimate carcinogens. Drug Metab Rev, 13(4): 555-80.

6. Beedham, C. (1997). The role of non-P450 enzymes in drug oxidation. Pharm World Sci, 19(6): p. 255-63.

7. Rendic, S. and Di Carlo, F.J. (1997). Human cytochrome P450 enzymes: a status report summarizing their reactions, substrates, inducers, and inhibitors. Drug Metab Rev, 29(1-2): 413-580.

8. Roberts-Thomson, S.J., McManus, M.E., Tukey, R.H. Gonzalez, F.J. and Holder, G.M. (1995). Metabolism of polycyclic aza-aromatic carcinogens catalyzed by four expressed human cytochromes P450. Cancer Res, 1995. **55**(5): p. 1052-9.

9. Espinosa-Aguirre, J.J., Rubio, J., Cassani, M., Nosti, R., Caballero, S., Gonzalez, I. and Martinez, G. (1996). Induction of microsomal enzymes in liver of rats treated with cyclohexanol. Mutat Res, 368(2): p. 103-7.

10. Ioannides, C. and Parke, D.V. (1993). Induction of cytochrome P4501 as an indicator of potential chemical carcinogenesis. Drug Metab Rev, 1993. **25**(4): p. 485-501.

11. Li, D.N., Seidel, A., Pritchard, M.P., Wolf, C.R. and Friedberg, T. (2000). Polymorphisms in P450 CYP1B1 affect the conversion of estradiol to the potentially carcinogenic metabolite 4-hydroxyestradiol. Pharmacogenetics, 10(4): 343-53.

12. Sesardic, D., Boobis, A.R., Edwards, R.J. and Davies, D.S. (1988). A form of cytochrome P450 in man, orthologous to form d in the rat, catalyses the O-deethylation of phenacetin and is inducible by cigarette smoking. Br J Clin Pharmacol, 26(4): 363-72.

13. Chen, Z.Y., White, C.C., He, C.Y., Liu, Y.F. and Eaton, D.L. (1995). Zonal differences in DNA synthesis activity and cytochrome P450 gene expression in livers of male F344 rats treated with five nongenotoxic carcinogens. J Environ Pathol Toxicol Oncol, 14(2): 83-99.

14. Eaton, D.L., Gallagher, E.P., Bammler, T.K. and Kunze, K.L. (1995). Role of cytochrome P4501A2 in chemical carcinogenesis: implications for human variability in expression and enzyme activity. Pharmacogenetics, **5**(5): 259-74.

15. Holme, J.A. and Soderlund, E.J. (1985). Species differences in the cytotoxic and genotoxic effects of 2-acetylaminofluorene and its primary metabolites 2-aminofluorene and N-OH-2-acetylaminofluorene. Carcinogenesis, 6(3): 421-425.

16. Fujita, K. and Kamataki, T. (2001). Role of human cytochrome P450 (CYP) in the metabolic activation of N-alkylnitrosamines: application of genetically engineered Salmonella typhimurium YG7108 expressing each

form of CYP together with human NADPH-cytochrome P450 reductase. Mutat Res, 483(1-2): 35-41.

17. Dey, A., Dhawan, A., Kishore Seth, P. and Parmar, D. (2005). Evidence for cytochrome P450 2E1 catalytic activity and expression in rat blood lymphocytes. Life Sci, 77(10): 1082-1093.

18. Crespi, C.L., Penman, B.W., Steimel, D.T., Gelboin, H.V. and Gonzalez, F.J. (1991). The development of a human cell line stably expressing human CYP3A4: role in the metabolic activation of aflatoxin B1 and comparison to CYP1A2 and CYP2A3. Carcinogenesis, 12(2): 355-359.

19. Bechtel, Y.C., Haffen, E., Lelouet, H. Brientini, M.P., Paintaud, G., Miguet, J.P. and Bechtel, P.R. (2000). Relationship between the severity of alcoholic liver cirrhosis and the metabolism of caffeine in 226 patients. Int J Clin Pharmacol Ther, 38(10): 467-75.

20. Zhou, S.F., Liu, J.P. and Chowbay, B. (2009). Polymorphism of human cytochrome P450 enzymes and its clinical impact. Drug Metab Rev, 41(2): p. 89-295.

21. Ruwali, M., M.C. Pant, P.P. Shah, B.N. Mishra, and D. Parmar, Polymorphism in cytochrome P450 2A6 and glutathione S-transferase P1 modifies head and neck cancer risk and treatment outcome. Mutat Res, 2009. 669(1-2): p. 36-41.

22. McCarty, K.M., R.M. Santella, S.E. Steck, R.J. Cleveland, J. Ahn, C.B. Ambrosone, K. North, S.K. Sagiv, S.M. Eng, S.L. Teitelbaum, A.I. Neugut, and M.D. Gammon, PAH-DNA adducts, cigarette smoking, GST polymorphisms, and breast cancer risk. Environ Health Perspect, 2009. 117(4): p. 552-8.

23. Nock, N.L., D. Tang, A. Rundle, C. Neslund-Dudas, A.T. Savera, C.H. Bock, K.G. Monaghan, A. Koprowski, N. Mitrache, J.J. Yang, and B.A. Rybicki, Associations between smoking, polymorphisms in polycyclic aromatic hydrocarbon (PAH) metabolism and conjugation genes and PAH-DNA adducts in prostate tumors differ by race. Cancer Epidemiol Biomarkers Prev, 2007. 16(6): p. 1236-45.

24. Guengerich, F.P., Characterization of human cytochrome P450 enzymes. FASEB J, 1992. 6(2): p. 745-8.

25. Thompson, J.A., J.L. Bolton, and A.M. Malkinson, Relationship between the metabolism of butylated hydroxytoluene (BHT) and lung tumor promotion in mice. Exp Lung Res, 1991. 17(2): p. 439-53.

26. Elovaara, E., J. Mikkola, H. Stockmann-Juvala, L. Luukkanen, H. Keski-Hynnila, R. Kostiainen, M. Pasanen, O. Pelkonen, and H. Vainio, Polycyclic aromatic hydrocarbon (PAH) metabolizing enzyme activities in human lung, and their inducibility by exposure to naphthalene, phenanthrene, pyrene, chrysene, and benzo(a)pyrene as shown in the rat lung and liver. Arch Toxicol, 2007. 81(3): p. 169-82.

27. Williams, G.M., C.L. Williams, and J.H. Weisburger, Diet and cancer prevention: the fiber first diet. Toxicol Sci, 1999. 52(2 Suppl): p. 72-86.

28. Wang, J., X.M. Liu, and Z.Q. Zhang, [Exposure assessment of liver cancer attributed to dietary aflatoxins exposure in Chinese residents]. Zhonghua Yu Fang Yi Xue Za Zhi, 2009. 43(6): p. 478-81.

29. Liao, G.Z., G.Y. Wang, X.L. Xu, and G.H. Zhou, Effect of cooking methods on the formation of heterocyclic aromatic amines in chicken and duck breast. Meat Sci. 85(1): p. 149-54.

30. Williams, C., R.L. Shattuck-Brandt, and R.N. DuBois, The role of COX-2 in intestinal cancer. Ann N Y Acad Sci, 1999. 889: p. 72-83.

31. Weisburger, J.H., L. Dolan, and B. Pittman, Inhibition of PhIP mutagenicity by caffeine, lycopene, daidzein, and genistein. Mutat Res, 1998. 416(1-2): p. 125-8.

32. Shukla, S. and S. Gupta, Dietary agents in the chemoprevention of prostate cancer. Nutr Cancer, 2005. 53(1): p. 18-32.

33. Khan, N., F. Afaq, and H. Mukhtar, Cancer chemoprevention through dietary antioxidants: progress and promise. Antioxid Redox Signal, 2008. 10(3): p. 475-510.

34. Mukhtar, H. and N. Ahmad, Green tea in chemoprevention of cancer. Toxicol Sci, 1999. 52(2 Suppl): p. 111-7.

35. Morse, M.A. and G.D. Stoner, Cancer chemoprevention: principles and prospects. Carcinogenesis, 1993. 14(9): p. 1737-46.

36. Stoner, G.D., L.S. Wang, and T. Chen, Chemoprevention of esophageal squamous cell carcinoma. Toxicol Appl Pharmacol, 2007. 224(3): p. 337-49.

37. Stoner, G.D., M.A. Morse, and G.J. Kelloff, Perspectives in cancer chemoprevention. Environ Health Perspect, 1997. 105 Suppl 4: p. 945-54.

38. Pompeia, C., J.J. Freitas, J.S. Kim, S.B. Zyngier, and R. Curi, Arachidonic acid cytotoxicity in leukocytes: implications of oxidative stress and eicosanoid synthesis. Biol Cell, 2002. 94(4-5): p. 251-65.

39. Myzak, M.C. and R.H. Dashwood, Chemoprotection by sulforaphane: keep one eye beyond Keap1. Cancer Lett, 2006. 233(2): p. 208-18.

40. Lee, H.L., D.P. Hsieh, and L.A. Li, Polycyclic aromatic hydrocarbons in cigarette sidestream smoke particulates from a Taiwanese brand and their carcinogenic relevance. Chemosphere, 2011. 82(3): p. 477-82.

Current Trends in Biotechnology and Pharmacy
Vol. 5 (4) 1383-1396 October 2011, ISSN 0973-8916 (Print), 2230-7303 (Online)

Influence of Poly (ethylene glycol) in Cyclosporine A Loaded PVM/MA Nanoparticles and Oral Absorption of the Drug

Marisin Pecchio[1,2], Maria Jesús Renedo Omaechevarria[1] and M. Carmen Dios-Viéitez[1]
[1]Department of Pharmacy and Pharmaceutical Technology. School of Pharmacy
University of Navarra. Irunlarrea, 1, 31008, Pamplona, Spain
[2]Center for Drug Discovery, Institute for Scientific Research and High Technology Services (INDICASATAIP)
City of Knowledge, Republic of Panama
*For Correspondence - mpecchio@indicasat.org.pa

Abstract

Cyclosporine A (CsA) has been widely used as a potent immunosuppressive agent in spite of its low oral bioavailability and formulation problems. Thus, we have developed a novel nanoformulation named CsANP-6, containing cyclosporine A associated to poly(methyl vinyl ether-co-maleic) anhydride (PVM/MA) nanoparticles by inclusion of poly(ethylene glycol) 2000 (PEG2000). The new nanoformulation for oral administration presented uniform sizes and zeta potentials for an efficient interaction with the mucosa of the gastrointestinal tract. The addition of PEG2000 to the formulation of PVM/MA nanoparticles increased the efficiency of CsA encapsulation. The release of CsA from CsANP-6 presented the typical biphasic profile of a nanoparticulated system, i.e. a rapid initial release, which could be explained as if a certain amount of CsA remains adsorbed on the surface of the nanoparticles, and then released slowed and steadily. Stability studies of CsANP-6 show that these systems are stable at 5 °C up to 1 year. Our results suggest that CsANP-6 can be an alternative to commercial formulations of CsA for oral administration without the adverse effects caused by the vehicle, Cremophor® EL.

Key words: Cyclosporine A, Bioavailability, PVM/MA, Poly (ethylene glycol), Nanoparticles, Pharmacokinetic.

Introduction

Cyclosporine A (CsA) is a calcineurin inhibitor used as an immunosuppressor for organ transplantation (1, 2). It causes suppression of the cell-mediated immune response by selective inhibition of interleukin-2 release during the activation of T-cells. The resultant immunosuppression is non-toxic and reversible when treatment is stopped (3). CsA shows low and variable oral bioavailability due to its high molecular weight and rigid cyclic structure which reduce its aqueous solubility and intestinal permeability (4,5). Bioavailability of CsA can be affected by an extensive pre-systemic metabolism in the gut wall and liver where cytochromes involved in CsA biotransformation (CYP3A) are present (6). The amount of bioavailable CsA can also be reduced by P-glycoprotein (P-gp) mediated efflux of CsA from the enterocyte back into the lumen enabling the enzymatic activity of CYP3A4 and thus CsA biotransformation (7). Currently available formulations of CsA such as Sandimmun® i.v. and Sandimmun Neoral® contain Cremophor EL® as a formulation vehicle to improve aqueous solubility and biovailability of CsA (8,9). Several side effects have been associated to the use of Cremophor EL® including anaphylactoid hypersensitivity reactions, abnormal lipoprotein patterns, hyperlipidemia, peripheral neuropathy,

Vol. 5 (4) 1383-1396 October 2011, ISSN 0973-8916 (Print), 2230-7303 (Online)

aggregation of erythrocytes and gastrointestinal side effects (10,11).

Nanoparticles have been successfully used as drug carriers for oral administration of molecules with poor bioavailability (12). Polymeric nanoparticles, such as chitosan (13) poly(alkyl-cyanocrylate) (14), poly(iso-hexyl-cyanocrylate) (15) and poly(methyl vinyl ether-co-maleic) anhydride (PVM/MA) (16), and solid lipid nanoparticles (17) have been developed to improve oral bioavailability of drugs with poor absorption and low permeability protecting the entrapped drug from enzymatic degradation. PVM/MA carriers are widely used because of its low cost and its capacity to develop strong bioadhesive interactions with a portion of the intestinal mucosa promoting absorption of drugs by the pre-sytemic metabolism (16). Moreover, PVM/MA forms homogeneous populations of nanoparticles which improves the distribution and transport of active substances to its site of action by increasing its penetration into target cells (16). However, association of CsA to this type of polymer is not possible because of CsA low water solubility. This is why, the inclusion of an excipient like poly(ethylene glycol) (PEG) is needed. PEG is a polymer widely used to improve macromolecule solubility with no side effects (18). It is also biocompatible, non-toxic and has been approved for human oral, dermal and intravenous administrations (18). Association of PEG to PVM/MA nanoparticles presents additional advantages like improvement of bioadhesive properties to intestinal mucosa (19,20) and inhibition of P-gp and cytocrome P450 which would facilitate oral absorption of CsA (21,22).

The objective of this research is to develop a strategy to encapsulate CsA in PVM/MA nanoparticles and to evaluate the ability of this carrier to transport CsA through the intestinal mucosa. To achieve this objective it was necessary to carry out the physicochemical and pharmacokinetical characterization of these nanoparticles. The present work includes X-ray diffraction studies and differential thermal analysis of CsANP-6 and its components for a better understanding of the nature of the interaction between components of the formulation in PVM/MA nanoparticles. Sandimmun Neoral® was chosen as the reference formulation to determine relative bioavailability of CsA in magnitude and velocity after oral administration of the new nanoformulation.

Materials and Methods

***Material*:** CsA Ph. Eu. (Roig Farma, Barcelona), phosphate buffered saline (PBS) pH=7.4 (Gibco, New York), distilled water (Pamplona, Navarra), copolymers PVM/MA (ISP, Barcelona), acetone, sodium chloride, potassium chloride, potassium dihydrogen phosphate, disodium hydrogen phosphate, acetonitrile and ethanol grade HPLC (Merck, Darmstadt), PEG2000 (Sigma-Aldrich Chemie, Steinheim), mannitol (Roquete, Lestrem), hydrochloric acid 2 N (Panreac, Barcelona), sodium hidroxide 5 mol/l (Sharlau Chemie, Barcelona). Sandimmun Neoral® 100 mg/ml and Sandimmun® i.v. was kindly gifted by Pharmacy Service of the Clinical University of Navarra. Emit® 2000 CsA specific assay, Emit® 2000 CsA sample pre-treatment reagent and Emit® 2000 CsA specific calibrators were from Siemens, Newark NJ.

***CsA loaded PVM/MA nanoparticles*:** CsA loaded PVM/MA nanoparticles were prepared by a desolvation method previously described (16) with modifications as follows. The organic phase was prepared dissolving different quantities of CsA (2.5, 5.0, 7.5, 10.0, 12.5, 15.0, 17.5 or 20.0 mg), 12.5 mg PEG2000 and 100 mg PVM/MA in 9 ml acetone and stirred during 1 h. Nanosuspensions were formed after addition of 3 ml water to the organic phase by stirring

Vol. 5 (4) 1383-1396 October 2011, ISSN 0973-8916 (Print), 2230-7303 (Online)

(300 rpm). Then, acetone was removed by evaporation under reduced pressure. CsA loaded PVM/MA nanoparticles were purified twice by ultracentrifugation at 17,000 rpm for 20 min. After purification, 200 mg of mannitol was used as cryoprotector agent. Finally, nanosupensions were freeze dried. All formulations were prepared in triplicate.

***Efficiency of encapsulated CsA*:** In order to determine the efficiency of encapsulated CsA in CsANP-1, CsANP-2, CsANP-3, CsANP-4, CsANP-5 and CsANP-6, freeze dried formulations were suspended in 3 mL water to form new nanosuspensions, which then were dissolved in 7.5-19.5 ml acetonitrile. CsA concentration in the resulting solution was analyzed by High Performance Liquid Chromatography (HPLC) equipped with a C-18 column (5µm, 250 x 4.6 mm) and an UV detector. The mobile phase consisted of acetonitrile/water in gradient mixture (6 min of 100% acetonitrile, 4 min of 80% acetonitrile) with a flow rate of 1.0 ml/min; the column was heated and kept at 70 °C. Encapsulation efficiency was expressed in percentage (%) of the ratio between encapsulated drug in the nanoparticles and the quantity of CsA initially added to the formulations.

***Particle size and zeta potential*:** Particle size distribution, index of polydispersity and zeta potential of nanoparticles were measured using a laser diffraction particle sizer (Zetasizer, Malvern Instrument, UK). For the procedure, 10 µl of nanosuspension were diluted in 2 ml water and stirred for 30 s before the analysis. Particle size and zeta potential were measured in triplicate.

***Product yield*:** Nanoparticles yield was expressed as the ratio between quantities of CsA loaded PVM/MA nanoparticles obtained after freeze drying and the initial quantity of PVM/MA added to the nanoformulation.

***In vitro release*:** *In vitro* release studies were carried out at 37°C using PBS artificial gastric and intestinal simulated medium with pH 7.4, 1.7 and 6.8, respectively. The formulation CsANP-6 (1.5 mg) was suspended in 15 ml of each medium, this volume of medium is enough to maintain sink condition (at least three times the volume required to form a saturated solution of CsA). *In vitro* release of CsA in PBS medium was measured at 1, 5, 15, 30, 60, 120 and 240 min. While, in artificial gastric and intestinal simulated medium was measured at 5, 30, 60, 90, 120, 150, 180, 210 and 240 min. At each specific time samples were centrifuged (4°C, 17000 rpm for 20 min) and CsA release into the medium was determined by HPLC.

***Amount of CsA associated to PVM/MA*:** CsA associated to PVM/MA was expressed in *µg CsA/mg PVM/MA* and calculated as follows:

$$\mu g\ CsA / mg\ polymer = \frac{amount\ of\ CsA\ in\ nanoparticles\ (\mu g)}{PVM\ /\ MA\ yield\ (mg)}$$

***Characterization of solid state of CsANP-6 and its components*:** The solid physical state of commercial CsA, PEG2000, mannitol, PVM/MA and CsANP-6 were explored by X-ray diffraction, thermogravimetric and differential thermal analysis (DTA/TGA). Powder X-ray diffractometry was carried out in a Bruker axs D8 Advance X-ray diffractometer (Herzogenrath, Germany) with a Cu-K_{a1} radiation, 0.02° increments and 1 s/step, sweep 2–40°, 2q. Thermogravimetric and differential thermal analysis were performed using a simultaneous DTA/TGA 851^e thermoanalyser (Mettler Toledo, Spain). All samples were weighted, sealed in aluminium pans and heated at scanning rate of 5°C/min between 20°C and 250°C under static air atmosphere.

Vol. 5 (4) 1383-1396 October 2011, ISSN 0973-8916 (Print), 2230-7303 (Online)

***Storage Stability*:** Stability studies were performed in long, intermediate and short-term storage during 12, 6 and 2 months, respectively. The evaluated parameters to determine stability of the samples were particle size and quantity of CsA associated to the PVM/MA. A coefficient of variation (CV) bellow 20 % and a variation of CsA associated to PVM/MA of 4.5% were considered acceptable for particle size and quantity of drug associated to PVM/MA, respectively. In long, intermediate and short-term storage, samples were stored at 60 ± 5% relative humidity; and at 5 ± 3 °C, 25 ± 6 °C and 40 ± 2 °C, respectively.

***Pharmacokinetic studies*:** Male Wistar rats with free access to water were fasted for 24 h prior to the experiment. The experiment was performed according to the policies and guidelines of the responsible Committee at the University of Navarra in line with the European legislation on animal experiments (86/609/EU). All experiments were conducted according to the Guiding 034/09 approved by the responsible Committee of the University of Navarra. For the pharmacokinetic studies, the rats were randomly divided into three groups (n = 6). Rats of the same sex (males) and similar weights (240 ± 20 g) were chosen for the experiment to avoid possible variations. The first group received Sandimmun® i.v. diluted with PBS (10 mg/kg) by intravenous injection into the tail vein. The other two groups of animals received orally 15 mg/kg of CsA in CsANP-6 formulation and Sandimmun Neoral®. The blood samples (0.150 ml) were collected from the the tail vein at predetermined intervals up to 48 and 72 h after intravenous and oral administration of CsA, respectively. CsA concentration in blood was determined by Emit® 2000 CsA specific assay (23). Calibration curves were obtained for each set of samples and quality control of the methods was evaluated with control samples provided by the manufacturer. Pharmacokinetic parameters were determined by compartmental model using WinNonlin 1.5 software (Scientific Consulting, EEUU). Blood CsA concentration of 6 rats were simultaneously analyzed in every study. Total area under the curve after intravenous or oral administration (AUC_{iv} or AUC_{oral}), maximum concentration (C_{max}), the time to C_{max} (t_{max}), volumen of distribution (V) and cleareance (CL) were obtained from whole blood data. Furthermore, the absolute bioavailability (F) of CsA was estimated using the ratio of dose-normalized AUC values after oral and i.v. administrations [Eq. (1)]

$$F = \frac{AUC_{oral}}{AUC_{iv}} \bullet \frac{D_{iv}}{D_{oral}} \quad (1)$$

where AUC_{oral} and $AUC_{i.v.}$ were the area under the concentration–time curve after the oral and i.v. administration of CsA, respectively.

Also the relative bioavailability (Fr) of CsA was estimated using the ratio of dose-normalized AUC values after oral administrations [Eq. (2)]

$$Fr = \frac{AUC_{fd}}{AUC_{sn}} \bullet \frac{D_{sn}}{D_{fd}} \quad (2)$$

where AUC_{fd} and AUC_{sn} were the area under the CsA concentration–time curve after administration of CsANP-6 and Sandimmun Neoral®, respectively.

Besides the mean transit time (MTT) was calculated after the oral administration of CsA as follows [Eq. (3)]:

$$MTT_{oral} = \frac{AUMC_{oral}}{AUC_{oral}} \quad (3)$$

where $AUMC_{oral}$ is the area under the first moment curve and AUC_{oral} is the area under the concentration–time curve after the oral administration of CsANP-6 and Sandimmun Neoral®.

Statistical analysis: The Wilcoxon-test, Mann–Whitney U-test and Kruskal-Wallis-test were used to determine statistical differences. In all cases, $p < 0.05$ was considered to be statistically significant. All data processing was performed using the SPSS® statistical software program (SPSS® 10, Microsoft, USA).

Results

***Characteristics of nanoparticles CsA loaded PVM/MA*:** Six CsA loaded PVM/MA nanoparticles base formulations were developed containing PEG2000 to improve the amount of CsA associated to PVM/MA and the bioavailability of CsA. The new CsA loaded PVM/MA nanoparticles were characterized in terms of mean particle size, zeta potential, and product yield and encapsulation efficiency (Table 1). All formulations were adequate for oral administration respect to particle size and zeta potential (24, 25). All formulations presented index of polydispersity of less than 0.2 indicating a homogeneous systems. The amount of CsA associated to PVM/MA and encapsulation efficiency obtained were considered acceptable. Formulation CsANP-6 was selected for further analysis because of its high quantity of CsA associated to PVM/MA (Table 1).

When PVM/MA nanoparticles were prepared without PEG2000, precipitation of CsA during the formation of nanoparticles was observed. This was not seen when PEG2000 was included in the process, except when ≥ 17.5 mg of CsA were used to prepare the nanoparticles (Data not shown).

***In vitro release studies*:** Fig. 1 shows the CsA release profile from the formulation CsANP-6. The study shows a biphasic release profile characterized by a burst effect up to 1 or 5 min depending of the medium, followed by a phase of slow release. A fast release of CsA from the nanoparticle was observed in the three media, followed by a continue release of CsA. This rapid initial release may be due to an adsorbed fraction of the drug on the surface of the nanoparticle. This biphasic release profile (rapid in the early stages and then slow) shows the behavior of a typical drug in a nano-delivery system (16).

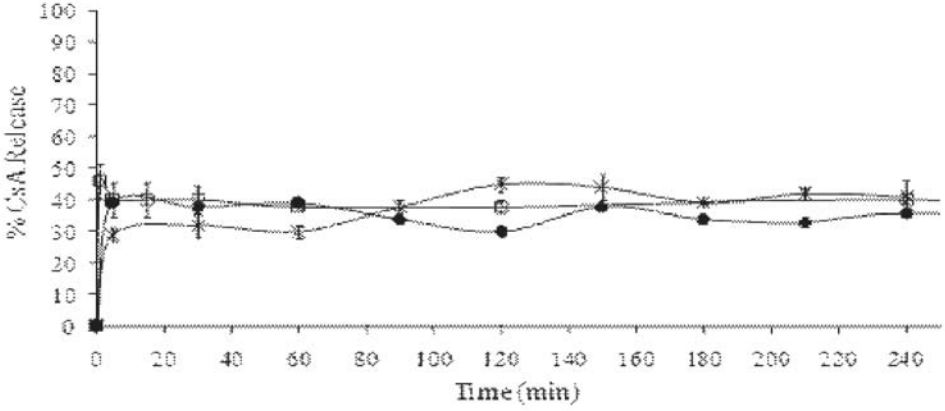

Fig. 1. *In vitro* release of CsA from PVM/MA nanoparticles (CsANP-6) in (-∗-) Artificial gastric simulated medium, pH 1.7, (-□-) PBS medium, pH=7.4 and (-•-) artificial intestinal medium, pH 6.8. Data represents the mean of the standard deviation (SD) of three independent measurements.

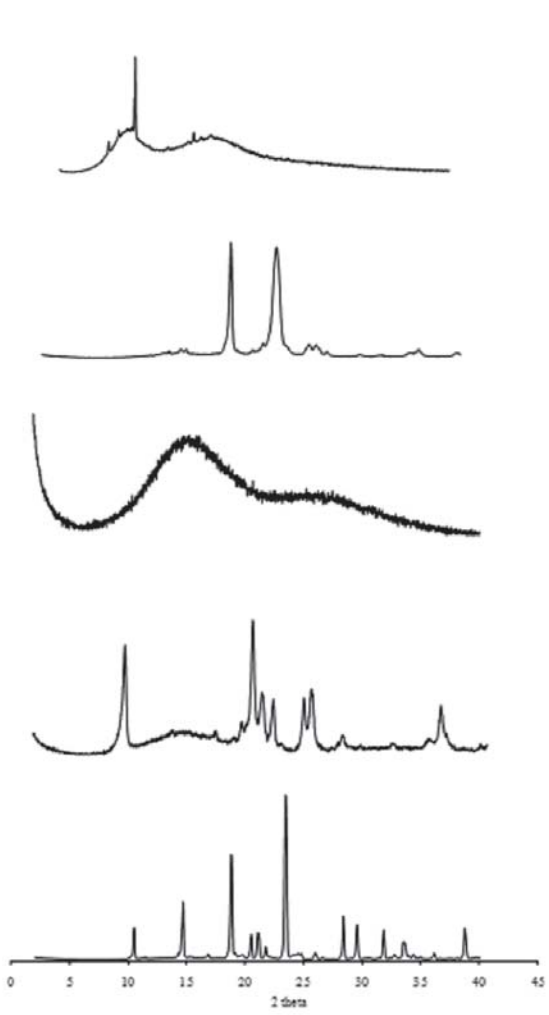

Fig. 2. Powder X-ray diffraction diagrams of A) Commercial CsA, B) PEG2000, C) CsANP-6, D) PVM/MA and E) Mannitol.

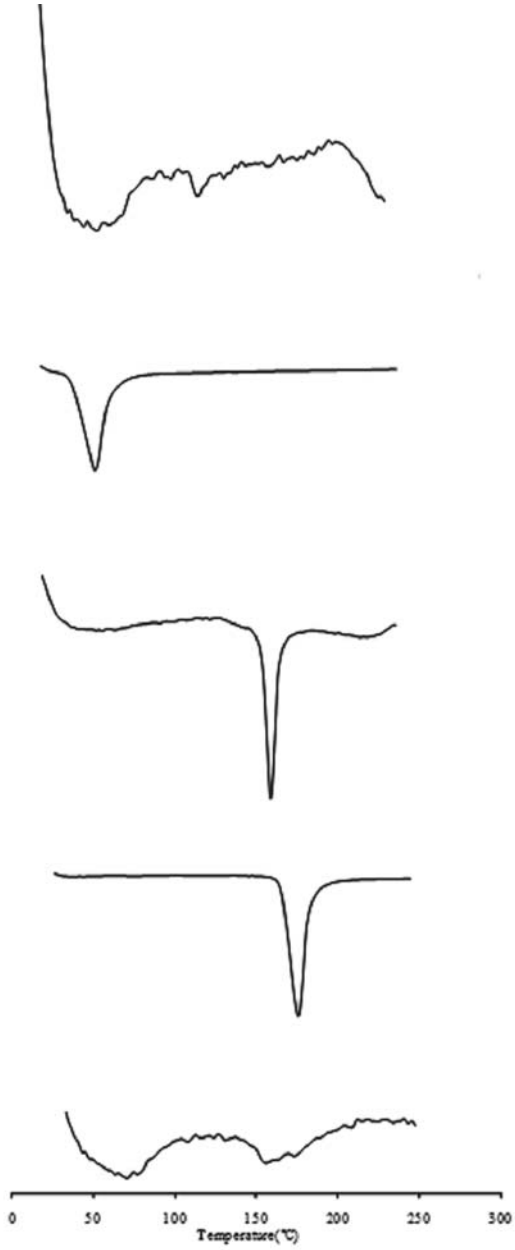

Fig. 3. DTA/TGA thermograms of. A) Commercial CsA, B) PEG2000, C) PVM/MA, D) Mannitol and E) CsANP-6.

Vol. 5 (4) 1383-1396 October 2011, ISSN 0973-8916 (Print), 2230-7303 (Online)

Characterization of solid state of CsA loaded nanoparticles and its components: X-ray diffraction diagrams and DTA/TGA thermograms of formulation CsANP-6 and its components are shown in Figs. 2 and 3, respectively. Diffraction diagram of CsA after very high exposure of radiation (10 s every 0.02 ° 2 θ), showed some reflections and a weak signal was detected at 10 ° 2θ (Fig. 2-A). PEG2000 showed two reflections at 19.1 and 23.2° 2θ (Fig. 2-B). PVM/MA (Fig. 2-D) and mannitol (Fig. 2-E) showed numerous reflections indicating that these polymers are crystalline solid state. However, X-ray diagrams of CsANP-6 formulation showed an amorphous solid state (Fig. 2-C). DTA/TGA thermograms of PEG2000 and PVM/MA showed endothermic responses between 50 and 70 °C (Fig. 3-B) and 170 ° C (Fig. 3-C), respectively, while CsANP-6 formulation did not show an endothermic responses (Fig. 3-E). These results suggest that CsANP-6 is an amorphous solid state which corresponds to the solid-solid interaction characteristic of this nanoparticle system.

***Storage Stability*:** Particle size of the CsANP-6 did not change significantly (CV <20%) and the quantity of CsA associated to PVM/MA did not show loss of the drug in more than 4.5% during long term storage (up to 48 weeks). Following the same criteria variation of the particle size and the quantity of CsA associated to PVM/MA were considered acceptable during 7 weeks in intermediate- and short- term storage, respectively (Table 2).

***Pharmacokinetics studies*:** The pharmacokinetic analysis shown in Fig. 4 represents a compartmental model of biphasic nature. Blood concentration profile of CsA after intravenous

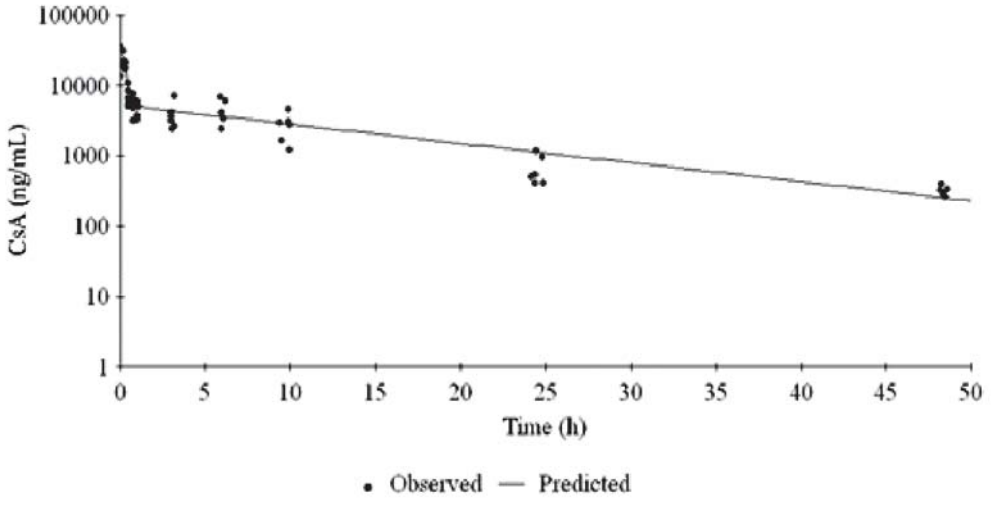

Fig. 4. Pharmacokinetic profile of CsA in blood after intravenous administration of 10 mg/kg of Sandimmun® i.v. A two-compartment model describes CsA concentration in blood. Dots (•) represent experimental data and the predicted profile is show by lines (-). Experimental data show six independent measurements.

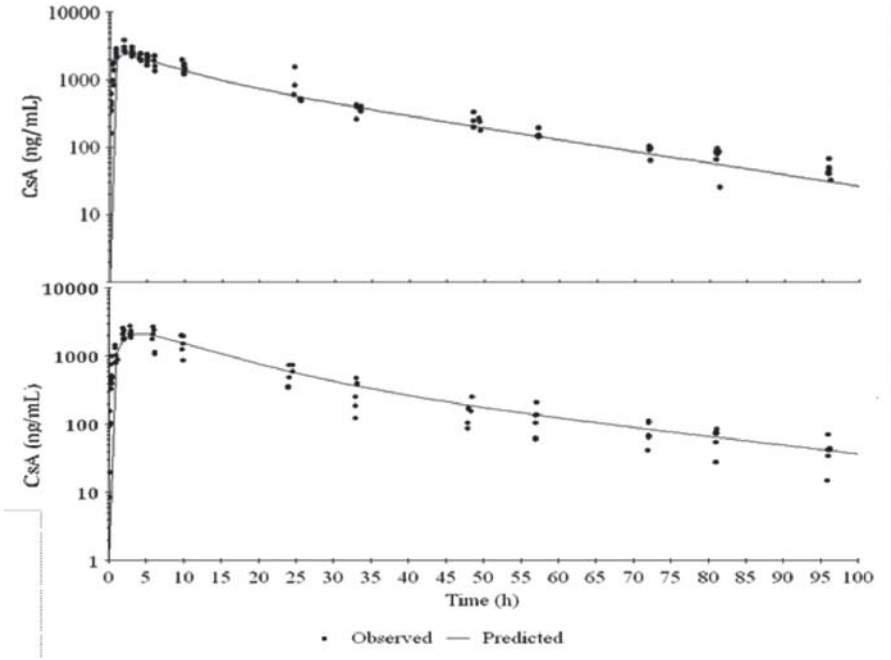

Fig. 5. Pharmacokinetic profile of CsA in blood, using a two-compartment model to describe CsA concentration in blood including lag time, after A) Oral administration of 15 mg/kg of Sandimmun Neoral® and B) Oral administration of 15mg/kg of CsANP-6. Experimental data show six independent measurements. Dots (•) represent experemental data and the predicted profile is shown by lines (-).

administration of Sandimmun® i.v. showed a biphasic decline of CsA, fast in the early days (α or distributive phase) and then slow (β or phase postdistributive) (Fig. 4). This indicates that the drug has a clear dynamic distribution, faster access to some areas of the body (central compartment) than others (compartment (s) peripheral (s)). Pharmacokinetic analysis of blood CsA concentration showed that drug disposition in the rat could be adequately characterized by a two-compartment model after intravenous administration of Sandimmun® i.v. (Fig. 4).

The pharmacokinetic profile of CsA, after oral administration of Sandimmun Neoral® (Figure 5-A) or CsANP-6 (Fig. 5-B), showed that a two-compartment model with a lag time describes adequately CsA concentration in blood in both cases. Lag times consist in the time between drug administration and the onset of drug absorption (26) and are a reflection of the processes associated with the absorption phase, for example drug release from the delivery system and drug migration to the absorbing surface (27).

Pharmacokinetic parameters of CsA in CsANP-6, Sandimmun® i.v. and Sandimmun Neoral® are shown in Table 3. The area under the curve of CsA was similar when given in both Sandimmun Neoral® (AUC_{oral} = 45190.88 ng/ml) and CsANP-6 (AUC_{oral} = 45490.39 ng/ml) oral formulations. However, considerable differences were observed for the t_{max} obtained after administration of CsANP-6 (4.11 h) and Sandimmun Neoral® (1.97 h). When CsA was administered in CsANP-6, t_{max} was 2.09 times

Vol. 5 (4) 1383-1396 October 2011, ISSN 0973-8916 (Print), 2230-7303 (Online)

Table 1. Physicochemical characteristics of the CsA loaded PVM/MA nanoparticles. Data represents the mean of the standard deviation (SD) of three independent measurements.

Formulation	mg CsA	Particle size (nm)	Index of Polydispersity	Zeta Potential (mV)	Nanoparticles yield (%)	E.E (%)	µg CsA/mg PVM/MA
CsANP-1	2.5	110.1 (±16.60)	0.096 (±0.023)	-42.5 (±5.20)	84.50 (±2.05)	52.90 (±10.10)	15.70 (±3.40)
CsANP-2	5.0	111.0 (±2.60)	0.110 (±0.022)	-49.1 (±5.00)	84.06 (±1.54)	71.53 (±2.92)	34.99 (±9.80)
CsANP-3	7.5	113.2 (±5.90)	0.103 (±0.017)	-48.4 (±9.50)	81.50 (±1.08)	58.90 (±0.14)	54.21 (±0.78)
CsANP-4	10.0	110.0 (±7.70)	0.112 (±0.026)	-39.4 (±1.97)	75.03 (±1.27)	61.42 (±3.58)	81.85 (±4.40)
CsANP-5	12.5	129.9 (±6.40)	0.085 (±0.008)	-55.5 (±4.90)	78.72 (±0.62)	45.37 (±2.54)	72.10 (±4.62)
CsANP-6	15.0	135.4 (±3.50)	0.083 (±0.009)	-53.7 (±4.40)	78.13 (±0.62)	44.04 (±1.50)	83.84 (±2.20)

higher than Sandimmun Neoral® which means more sustained levels of the drug after giving CsA in CsANP-6. Moreover, MTT increase when CsA was administered in CsANP-6 (29.64 h) compared with Sandimmun Neoral® (23.42 h); this result confirms significant sustained release of CsA from the nanoparticles.

Discussion

***Physicochemical characteristics of CsA loaded PVM/MA nanoparticles*:** There are evidences that PVM/MA nanoparticles have bioadhesive properties (16). CsA loaded PVM/MA nanoparticles possessed suitable sizes (d" 150 nm) for oral administration and were negatively charged on the surface. The results shown in this study suggest that particles with these characteristic could interact with the intestinal mucosa when its components have bioadhesive properties. Formulation CsANP-6 was selected for the *in vivo* studies, because of the higher association between CsA and PVM/MA. Additionally, CsA loaded PVM/MA nanoparticles containing PEG2000 were systems of long-term stable release at 5 ± 3 °C and 60 ± 5% relative humidity during one year. This is in line with previous formulations where PEG was successfully used as a stabilizer (28).

***Characterization of solid state of CsA loaded PVM/MA nanoparticles and its components*:** X-ray diffraction diagrams and DTA / TGA thermograms showed the amorphous solid state of CsANP-6 and there was no signal of crystalline solid state of its components. Absence of this signal suggests that these components form covalent bonds, as is described for poly(lactic acid-poly(ethylene oxide) nanoparticles (29). An amorphous state suggests that PEG2000 is not physically adsorbed to PVM/MA (30). From these findings, CsANP-6 appears as a pegylated nanoparticle with extending chains of PEG2000 which could cause steric hindrance and lower levels of mucin protein chain interactions with nanoparticles (19, 20). The latest characteristic is desired for a maximal interaction of nanoparticles and the intestinal mucosa (20).

***Pharmacokinetics studies*:** The rate of oral absorption of CsA after its administration in PVM/MA nanoparticles was sustained in this study. This is expected, because drugs encapsulated in nanoparticles show sustained levels in blood through time (31). The values of t_{max} and MTT of CsA in CsANP-6 were higher than Sandimmun Neoral®, suggesting a sustained release of CsA from PVM/MA nanoparticles (Table 3). Additionally, the relative bioavailability (Fr) of CsANP-6 was 107% which is close to the reference formulation (Sandimmun Neoral®).

Moreover, the volume of distribution (Vee) and cleareance (Cls) of CsA in CsANP-6 and Sandimmun® i.v. were similar. These results suggest

Table 2. Stability studies of CsANP-6 after long, intermediate and short-term storage at 60 ± 5% relative humidity and 5 ± 3 °C, 25 ± 6 °C and 40 ± 2 °C, respectively.

CsANP-6			
Time (week)	**Particle Size (SD)**	**% Loss of CsA**	***P***
Long-term storage			
1	196.50 (±1.52)	1.75	0.127
2	207.00 (± 1.17)	3.36	0.083
3	179.80 (±2.38)	3.60	0.127
4	186.00 (±3.37)	3.95	0.127
5	188.00 (±1.00)	3.23	0.513
6	190.90 (±0.69)	4.50	0.827
7	226.10 (±2.85)	3.94	0.127
8	170.80 (±0.37)	3.33	0.127
12	165.00 (±2.27)	3.91	0.083
16	185.00 (±1.36)	3.83	0.083
20	163.30 (±1.31)	3.65	0.083
24	167.70 (±1.68)	3.39	0.083
36	194.20 (±2.33)	3.74	0.083
48	193.40 (±0.75)	4.08	0.180
% CV	**9.61**		
Intermediate-term storage			
1	166.10 (±1.09)	3.89	0.827
2	175.20 (±0.51)	3.91	0.513
3	217.70 (±4.38)	3.35	0.513
4	195.30 (±1.28)	2.61	0.827
5	200.30 (±1.59)	3.23	0.513
6	199.80 (±1.25)	3.70	0.827
7	205.40 (±3.11)	3.86	0.513
% CV	**9.74**		
8	214.70 (±2.07)	4.80	0.564
12	275.30 (±1.07)	8.20	0.050
16	278.70 (±5.24)	18.91	0.050
20	314.40 (±4.31)	25.90	0.050
24	361.10 (±5.32)	32.71	0.050
% CV	**27.02**		
Short-term storage			
1	166.70 (±2.88)	3.29	0.827
2	203.00 (±2.41)	4.04	0.513
3	211.00 (±3.58)	4.57	0.827
4	180.40 (±3.15)	3.77	0.083
5	219.70 (±2.49)	4.07	0.083
6	252.70 (±1.36)	3.43	0.827
7	252.70 (±1.36)	3.43	0.827
8	253.30 (±2.67)	4.69	0.127
% CV	**19.97**		

Table 3. Pharmacokinetics values and parameter of CsA after intravenous administration of 10 mg/kg of Sandimmun® i.v. and oral administration of 15 mg/kg of Sandimmun Neoral® and CsANP-6. Data represents simultaneously analysis of six measurements. C_{max}: The maximum concentration. t_{max}: Time of maximum observed concentration. t_o: lag time. V_{ee}/F: Volume of distribution at steady state based on the absolute bioavailability. Cl_s/F: Clearance based on the absolute bioavailability. F: The absolute bioavailability. Fr: The relative bioavailability. V_{ee}: Volume of distribution at steady state. CLs: Clearance. Co: Initial concentration after i.v. administration. α: Constant associated at distribution phase. β: Constant associated at elimination phase. $t_{1/2}\alpha$: Half-life associated at distribution phase. $t_{1/2}\beta$: Half-life associated at elimination phase. $k_{10:}$ The elimination rate. k_{12}: Constant of distribution when CsA enters to peripheral compartment from central compartment. k_{21}: Constant of distribution when CsA return of peripheral compartment to central compartment. V_c: Volume of distribution. $AUC_{oral:}$ Total area under the curve after oral administration. AUC_{iv}: Total area under the curve after intravenous administration. MTT_{oral}: Mean transit time after oral administration. $AUMC_{oral}$: The area under the first moment curve. %CV: Coefficient of variation.

Parameter	Unit	Sandimmun Neoral® oral		CsANP-6 oral		Sandimmun® i.v.	
		n=6	% CV	n=6	%CV	n=6	%CV
C_{max}	ng/ml	2485.03	6.47	2133.45	9.04	-	-
t_{max}	h	1.97	10.66	4.11	11.41	-	-
α	min	15	4.68	8	11.05	-	-
β	ml	1331.90	11.57	1277.76	18.33	-	-
V_{ee}/F	ml/h	84.64	4.12	82.65	6.52	-	-
Cl_s/F	(ng/ml)h	45190.88	4.12	45490.39	6.51	-	-
AUC_{oral}	$(ng/ml)h^2$	1262181.28	-	1348323.60	-	-	-
$AUMC_{oral}$	-	0.33	-	0.33	-	-	-
F	-	-	-	1.07	-	-	-
Fr	h	23.42	-	29.64	-	-	-
MTT_{oral}	ml	439.53	-	421.66	-	385.91	7.48
V_{ee}	ml/h	27.93	-	27.27	-	26.55	5.46
CLs	ng/ml	-	-	-	-	45692.10	20.77
Co	h^{-1}	-	-	-	-	4.758	18.91
α	h^{-1}	-	-	-	-	0.063	5.89
β	h	-	-	-	-	0.146	18.89
$t_{1/2}\alpha$	h	-	-	-	-	11.08	5.89
$t_{1/2}\beta$	h^{-1}	-	-	-	-	0.495	19.66
k_{10}	h^{-1}	-	-	-	-	3.724	21.27
k_{12}	h^{-1}	-	-	-	-	0.601	15.32
k_{21}	ml	-	-	-	-	53.62	20.76
V_c	$(ng/ml)h$	-	-	-	-	92284.72	5.46
AUC_{iv}							

Vol. 5 (4) 1383-1396 October 2011, ISSN 0973-8916 (Print), 2230-7303 (Online)

that CsA loaded PVM/MA nanoparticles remained at the absorption site in the gastrointestinal tract for a period of time and did not pass into the systemic circulation, which is in agreement with results obtained by Agüero et al. after studying *in vivo* distribution of such nanoparticles (32). Our novel "pegylated nanoparticles" can carry CsA to the surface of the intestinal mucosa where they remain in contact with the membrane of the enterocyte and release their content.

The components of the new formulation can also facilitate drug absorption due to the inhibitory properties of PEG2000 on P-glycoprotein and cytochrome P450, resulting in a decreased gut-wall metabolism of CsA.

Conclusions

CsA loaded PVM/MA nanoparticles for oral administration presented uniform sizes and zeta potentials for an efficient interaction with the mucosa of the gastrointestinal tract. The addition of PEG2000 to the formulation of PVM/MA nanoparticles increased the efficiency of CsA encapsulation. The release of CsA from CsANP-6 presented the typical biphasic profile of a nanoparticulated system, i.e. a rapid initial release, which could be explained as if a certain amount of CsA remains adsorbed on the surface of the nanoparticles, and then released slow and steadily. Stability studies of CsANP-6 show that these systems are stable at 5 °C during at least 1 year. Our results suggest that CsANP-6 can be an alternative to commercial formulations of CsA for oral administration without the adverse effects caused by the vehicle, Cremophor® EL.

Acknowledgements

This work was supported by FUNDACION CAJA NAVARRA and M. Pecchio received fellowship of SENACYT-IFARHU of GOVERNMENT OF PANAMA. We would like to thanks to Dr. L. Zufía from the Pharmacy Service (University Clinic of Navarra) and Dr. C. Martínez from Department of Chemistry and Soil Sciences, School of Sciences (University of Navarra) for all their help in the development of this project. Thank are also due to Dr. Catherina Caballero for kind dedication to review this paper.

References

1. Italia, J.L., Bhardwaj, V. and Kumar, M.N.V.R. (2006). Disease, destination, dose and delivery aspects of ciclosporin: the state of the art. Drug Discov. Today, 11: 846–854.

2. Sommerer, C., Giese, T., Meuer, S. and Zeier, M. (2010). New concepts to individualize calcineurin inhibitor therapy in renal allograft recipients. Saudi J Kidney Dis Transpl. 21(6):1030-1037.

3. Drugge, R.J. and Handschumacher, R.E., (1988). Cyclosporine: Mechanism of action. Transplant Proc., 20: 301-309.

4. Choc, M.G. (1997). Bioavailability and pharmacokinetics of cyclosporine formulations: Neoral® vs Sandimmun®. Int J Dermatol., 36(1): 1-6.

5. Noble S. and Markham A. (1995). Cyclosporin. A review of the pharmacokinetic properties, clinical efficacy and tolerability of a microemulsion-based formulation (Neoral). Drugs., 50: 924–941.

6. Kolars, J.C, Awni, W.M., Merion, R.M. and Watkins, P.B. (1991). First-pass metabolism of cyclosporin by the gut. Lancet, 338:1488–1490.

7. Hebert, M.F. (1997). Contributions of hepatic and intestinal matabolism and P-glycoprotein to cyclosporin ans tacrolimus oral drug delivery. Adv. Drug. Deliv. Rev., 27: 201–214.

8. Vonderscher, J. and Meinzer, A., (1994). The Neoral formula of cyclosporine. Transplant Proc., 26: 2925-2927.

9. Ran, Y., Zhao, L., Xu, Q. and Yalkowsky, S.H. (2001). Solubilization of cyclosporin A. AAPS PharmSciTech., 2(1): E2.

10. Gelderblom, H., Verweij, J. and Nooter, K. (2001). Cremophor EL: the drawbacks and advantages of vehicle selection for drug formulation. Eur J Cancer.,37(13):1590-1598.

11. Ten Tije, A.J., Verweij, J., Loos, W.J. and Sparreboom, A. (2003). Pharmacological effectts of formulation vehicles: implications for cancer chemotherapy. Clin Pharmacokinet., 42(7): 665-685.

12. Kreuter, J. (1991). Peroral administration of nanoparticles. Adv. Drug Deliv. Rev., 7: 71–86.

13. Takeuchi, H., Yamamoto, H., Niwa, T., Hino, T. and Kawashima, Y. (1996). Enteral absorption of insulin in rats from mucoadhesive chitosan-coated liposomes. Pharm. Res., 13 :896–901.

14. Damgé, C. Vranckx, H. Balschmidt, P. and Couvreur, P. (1997). Poly(alkyl cyanoacrylate) nanospheres for oral administration of insulin. J. Pharm. Sci., 86 :1403–1409.

15. Dembri, A., Montisci, M.J., Gantier, J.C. Chacun, H. and Ponchel, G. (2001). Targeting of 32 -azido-32 deoxythymidine (AZT)-loaded poly(isohexylcyanoacrylate) nanospheres to the gastrointestinal mucosa and associated lymphoid tissues. Pharm. Res., 18: 467–472.

16. Arbós, P., Campanero, M.A., Arango, M.A. and Irache, J.M. (2004). Nanoparticles with specific bioadhesive properties to circumvent the pre-systemic degradation of fluorinated pyrimidines. J Control Release., 96:55-65.

17. Yang, S., Zhu, j. Lu, Y. Liang, B. and Yang, C. (1999). Body distribution of camptothecin solid lipid nanoparticles after oral administration. Pharm. Res., 16 :751–757.

18. Greenwald, R.B., (2001). PEG drugs: an overview. J Control Release, 74(1-3): 159-171.

19. Yoncheva, K., Guembe, L., Campanero, M.A. and Irache, J.M. (2007). Evaluation of bioadhesive potential and intestinal transport of pegylated poly(anhydride) nanoparticles. Int J Pharm., 334(1-2): 156-165.

20. Yoncheva, K., Lizarraga, E. and Irache, J.M. (2005). Pegylated nanoparticles based on poly(methyl vinyl ether-co-maleic anhydride): preparation and evaluation of their bioadhesive properties. Eur J Pharm Sci., 24(5): 411-419.

21. Shen, Q., Lin, Y., Handa, T., Doi, M., Sugie, M., Wakayama, K., Okada, N., Fujita, T. and Yamamoto, A. (2006). Modulation of intestinal P-glycoprotein function by polyethylene glycols and their derivatives by in vitro transport and in situ absorption studies. Int J Pharm., 313(1-2): 49-56.

22. Mudra, D. and Borchardt, R. (2009). Absorption barriers in the rat intestinal mucosa. 3. Effects of polyethoxylated solubilizing agents on drug permeation and metabolism. J Pharm Sci., 99(2): 1016-1027.

23. Siemens Healthcare Diagnostic, (2008). Emit 2000 Cyclosporine Specific Assay.

Siemens Healthcare Diagnosctic Ltd. Camberley, UK.

24. Desai, M.P., Labhasetwar, V., Amidon, G.L. and Levy, R.J. (1996). Gastrointestinal uptake of biodegradable microparticles: Effect of particle size. Pharm Res., 13(12): 1838-1845.

25. Desai, M., Labhasetwar, V., Walter, E., Levy, R. and Amidon, G. (1997). The mechanism of uptake of biodegradable microparticles in Caco-2 cells is size dependent. Pharm Res, 14(11):1568-1573.

26. WinNonlin Glossary. WinNonlin® version 1.5 Pharmacokinetic Analysis Software (1995). Scientific Consulting Inc. USA.

27. Nerella, N.G., Block, L.H. and Noonan, P.K. (1993). The impact of lag time on the estimation of pharmacokinetic parameters. I. One-Compartment Open Model. Pharm Res, 10 (7): 1031-1036.

28. Liu, W., Yang, A., Li, Z., Xu, H. and Yang, X. (2007). PEGylated PLGA nanoparticles as tumor necrosis factor-alpha receptor blocking peptide carriers: Preparation, characterization and release in vitro. Journal of Wuhan University of Technology, 22(1): 112-116.

29. De Jaeghere F, Allemann E, Feijen J, Kissel T, Doelker E, Gurny R.J. (2000). Cellular uptake of PEO surface-modified nanoparticles: evaluation of nanoparticles made of PLA:PEO diblock and triblock copolymers. J Drug Target., 8(3):143-153.

30. Stolnik, S., Illum, L. and Davis, S. (1995). Long circulating microparticulate drug carriers. Adv Drug Deliv Rev., 16(2-3): 195-214.

31. Wang, X.Q., Dai, J.D., Chen, Z., Zhang, T., Xia, G.M., Nagai, T. and Zhang, Q. (2004). Bioavailability and pharmacokinetics of cyclosporine A-loaded pH-sensitive nanoparticles for oral administration. J Control Release., 97(3): 421-429.

32. Agüeros, M., Zabaleta, V., Espuelas, S., Campanero, M.A., Irache, J.M. (2010) Increased oral bioavailability of paclitaxel by its encapsulation through complex formation with cyclodextrins in poly(anhydride) nanoparticles. J Control Release. 145(1):2-8.

Current Trends in Biotechnology and Pharmacy
Vol. 5 (4) 1397-1409 October 2011, ISSN 0973-8916 (Print), 2230-7303 (Online)

Comparative *In vivo* Evaluation of Aripiprazole Coprecipitate, Nanoparticles and Marketed Tablets in Healthy Human Volunteers and *In vitro-In vivo* Correlation

Aly A. Abdelbary[1], Ahmed H. Elshafeey[2, 3], Mohamed El-Nabarawi[2], Abdelhalim Elassasy[2], Xiaoling Li[1] and Bhaskara Jasti[1*]

[1]Thomas J. Long School of Pharmacy & Health Sciences, University of the Paciûc
3601 Paciûc Avenue, Stockton, CA 95211, United States
[2] Faculty of Pharmacy, Cairo University, Kasr El-Aini Street, *Cairo* 11562, Egypt
[3] Genuine Research Center, Cairo, Egypt
[*]For Correspondence - bjasti@pacific.edu

Abstract

The aim of this study was to evaluate the bioavailability of two aripiprazole tablets, coprecipitate (CP) and nanoparticles (NP) when compared to the market tablets. A single-dose, randomized, three period crossover design under fasting conditions in healthy human volunteers was studied. The dissolution rate of the CP, NP and market tablets was determined. In order to investigate the feasibility of in vitro data as a tool for predicting in vivo results, two types of in vitro-in vivo correlation (IVIVC), level C and multiple level C, were studied. Almost 75% of aripiprazole was dissolved from the nanoparticles tablets within 10 minutes compared with 20% and 46% for coprecipitate and market tablets, respectively. The mean $AUC_{0\text{-}72}$ value of aripiprazole from the NP tablets (6136.35 ± 421.29 ng.hr/mL) was significantly higher than both CP tablets (3216.12 ± 525.02 ng.hr/mL) and market tablets (5215.57 ± 457.28 ng.hr/mL) (p d" 0.05). The relative bioavailability of aripiprazole after oral administration of the CP and NP tablets was 61.66% and 117.65%, respectively. The higher dissolution rate of NP tablets resulted in rapid absorption of aripiprazole and consequently higher bioavailability. Multiple level C IVIVC showed the bioequivalence of NP and bioinequivalence of the CP tablets in comparison to market tablets.

Keywords: Aripiprazole; Coprecipitate; Nanoparticles; Bioequivalence; Volunteers.

Introduction

Solubility of a drug is essential for its effectiveness, independent of the route (1). Dissolution is the rate limiting step in the absorption of BCS class II drugs across the gastrointestinal tract (2). Since poor aqueous solubility is associated with poor dissolution characteristics, solubility has become a challenging problem in drug formulation development (3, 4). Nanomilling and coprecipitation are two particle engineering approaches commonly used for enhancing the dissolution rate of poorly water soluble drugs (5, 6).

The increase in dissolution rate is hypothesized to increase both the rate and extent of absorption resulting in higher bioavailability and faster onset of action (7). The increase in dissolution rate of nanomilled drug powders can be explained using the Noyes Whitney equation as smaller particles result in an increase in surface area and through the Prandtl equation as the particles will have smaller diffusional thickness. In case of coprecipitation, the

Vol. 5 (4) 1397-1409 October 2011, ISSN 0973-8916 (Print), 2230-7303 (Online)

dissolution rate was found to increase due to reduction in crystallinity and subsequent lowered energy to break up crystalline lattice of the drug. Moreover, the drug solubility and wettability may be increased by surrounding hydrophilic polymer matrices (8, 9).

The enhancement of the bioavailability of poorly water soluble drugs by nanomilling and coprecipitation has been reported earlier. For example, nanomilling enhanced the AUC and C_{max} of NVS-102 by a factor of 9 and 5, respectively (10), the AUC of MK-0869 by a factor of 4 (11) and resulted in 86% of the absolute bioavailability of cilostazol (12). Similarly, coprecipitation enhanced the bioavailability of KRN633 7.5 times (13), the C_{max} and AUC of ER-34122 by 100 times (14), C_{max} of ritonavir 15 times (15) and resulted in 95% of the absolute bioavailability of albendazole (16).

Aripiprazole is a novel atypical antipsychotic agent with a pharmacological mechanism that is distinct from currently available antipsychotic agents (17). It acts as a potent partial dopamine D_2 receptor agonist, a partial serotonin 5-HT_{1A} agonist, and 5-HT_{2A} receptor antagonist (18). Aripiprazole is currently approved for schizophrenia and the acute treatment of manic or mixed manic/depressive episodes of bipolar disorder (19). Aripiprazole has a poor aqueous solubility (10.98 ± 1.39 ng/mL) and is classified as BCS class II (6, 20). Hence, aripiprazole was used as a model drug to compare the effect of nanomilling and coprecipitation on the dissolution rate and in vivo bioavailability of poorly water soluble drugs.

In vitro-in vivo correlations (IVIVC) are generally observed when the dissolution is the rate-limiting step in absorption and appearance of the drug in the circulation (21, 22). Four categories of IVIVC have been described in the literature: level A, B, C and multiple level C (23). A good correlation is a tool for predicting in vivo results based on in vitro data (24). In this respect, dissolution tests may be considered as surrogate markers of availability of a drug in the systemic circulation for drugs with dissolution rate limited absorption (25).

In our previous work, nanomilling resulted in a significant increase in intrinsic dissolution rate of aripiprazole (2 to 9 folds) when compared to coprecipitation (6). This increase in dissolution rate was hypothesized to enhance the in vivo bioavailability in the same rank order. To verify this hypothesis, the pharmacokinetics of 2 aripiprazole tablets containing, coprecipitate (CP) and nanoparticles (NP), respectively were assessed after administration to healthy human volunteers and compared to the market tablets. In addition, two levels of in vitro-in vivo correlation, C and multiple level C were also investigated.

Materials and Methods

***Materials*:** Aripiprazole was purchased from Hetero Labs Limited, India. Acetonitrile, Formic acid and water (HPLC grade) were purchased from Fisher Scientific Co., Pittsburgh, PA, USA. Pluronic F127 was purchased from BASF, Florham Park, NJ, USA. Escitalopram (internal standard) was provided by Alkan Pharma Co., Egypt. Abilify® 10 mg tablets, used as reference, were purchased from Egypt Otsuka Pharmaceutical Co., and referred to in the manuscript as market tablets.

***Preparation of coprecipitate composition*:** The coprecipitate of aripiprazole with Pluronic F127 (1:1) was prepared by solvent evaporation method (26, 27). Briefly, aripiprazole and Pluronic F127 were accurately weighed and each was transferred to a beaker containing dichloromethane:methanol (9:1). The solvent

was evaporated in rotary evaporator (Rotavapor® R-300, Bûchi, Switzerland) at reduced pressure and the resulting coprecipitate composition of aripiprazole was stored in a desiccator until further study.

***Preparation of nanoparticles composition*:** The nanosuspension of aripiprazole with Pluronic F127 (1:1) was prepared by media milling using a Dyno®-Mill Multilab (Glenmills, Clifton, NJ) utilizing 200 G zirconia grinding beads at a speed of 4180 rpm for 2 hours. The nanosuspension was lyophilized after preparation. First the nanosuspension was poured into glass flasks and prefrozen using an ultra cold freezer (Thermo Scientific Revco, Waltham, MA, USA) at -80 °C for 12 hours, then the samples were freeze-dried using a Flexi-Dry™ MP Freeze Dryer (SP Scientific, Stone Ridge, NY, USA) at -90 °C and 380 mT of pressure for 48 hours to yield dry nanoparticle powder. Prior to freezing, sucrose (1.67% w/v) was added into the suspension as a cryoprotective agent.

***Particle size analysis of the compositions*:** The particle size was determined by introducing an aliquot of the prepared compositions into the water-filled sample cell of a Horiba LA-930 laser light scattering particle size and distribution analyzer (Horiba Instruments, Irvine, CA, USA). The measured particle size distribution values were reported based on volume-weighted analyses (28). For the analysis of particle size of the freeze-dried nanosuspension, the samples were first reconstituted in water. The measurement is based on Mie scattering theory and has a wide range of 0.02–2000 μm (29). All the measurements were made in triplicate.

***Preparation of the tablets*:** The coprecipitate and nanoparticles compositions of aripiprazole with Pluronic F127 were mixed with excipients; Ac-Di-Sol, Avicel pH 102 and magnesium stearate (Table 1). The tablets were prepared by direct compression using a single punch tablet machine (Stokes, Pennwalt Chemical Corp., Warminster, PA, USA). The tablets containing coprecipitate and nanoparticles will be referred to in the discussion as CP and NP tablets, respectively.

***Dissolution study of the prepared tablets*:** The CP, NP, and market tablets were immersed in a USP II dissolution apparatus (Hanson Research Corp., Los Angeles, CA, USA) containing 900 mL 0.1 N HCl as dissolution medium at 37 °C and stirred at 60 rpm. At predetermined time intervals, aliquots of 5 mL were withdrawn, filtered and replaced by fresh medium. The samples were analyzed by HPLC and the percentage of aripiprazole dissolved was plotted as a function of time.

The dissolution characteristics selected for the in vitro-in vivo correlation (IVIVC) calculations were mean percentages of the unit dose dissolved at given time points in minutes,

Table 1. Aripiprazole tablet compositions.

Tablets	Pluronic F127	Sucrose	Ac-Di-Sol	Avicel pH 102	Magnesium stearate
CP tablets	10 mg	-	7.5 mg	121 mg	1.5 mg
NP tablets	10 mg	83.45 mg	7.5 mg	37.55 mg	1.5 mg

*Total tablet weight: 150 mg, aripiprazole = 10 mg in both tablets.

expressed as D values. For example, D30 means the mean percentage dissolved after 30 minutes (30).

***HPLC analysis of aripiprazole*:** An isocratic HPLC method was employed for the quantification of aripiprazole (31). A Thermo Separation HPLC system (Fremont, CA, USA) equipped with a P4000 *pump* unit, an AS3000 *autosampler including an injection valve with a sample loop of 50 µL volume*, and a UV2000 detector was used. A Zorbax Extend-C18 column (4.6 mm x 250 mm) containing 3.5 µm size adsorbent as stationary phase (Agilent technologies, Santa Clara, CA, USA) was used for chromatographic separation. The column was maintained at room temperature (25± 2°C). The mobile phase consisted of a mixture of 10 mM ammonium buffer (adjusted to pH 8.35 with sodium hydroxide 6 mol/L) and acetonitrile (25:75). The flow rate and the UV detector were set at 1.0 mL/min and 254 nm, respectively. Aripiprazole was eluted at 6.6 min under the conditions described above. An external calibration curve was established in the range of 0.1-20 µg/mL.

Pharmacokinetic study in healthy human volunteers

***Study design and subjects*:** A single-dose, randomized, three period crossover design was adopted to evaluate the pharmacokinetic parameters of CP and NP tablets compared to the market tablets, Abilify® 10 mg tablets (Egypt Otsuka Pharmaceutical Co.). Six healthy adult male volunteers participated in this comparative study. Their mean age was 47.17 ± 5.71 years, mean body weight 77.17 ± 8.45 Kg and mean height 171 ± 9.63 cm. The purpose of the study was fully explained, and volunteers had given their written consent. The volunteers were instructed to abstain from taking any drug, including over-the-counter (OTC), for 2 weeks prior to and during the study period. The study was performed according to the revised Declaration of Helsinki for biomedical research involving human subjects and the rules of Good Clinical Practices (GCP). The study protocol was reviewed and approved by the Cairo University protection of human subjects committee.

***Drug administration and sample collection*:** The volunteers were checked-in a hospital at 9:00 P.M. and had a standard dinner at the clinical site. After an overnight fast (at least 10 hr), volunteers were given a single oral dose of the CP tablet, NP tablet and market tablet according to a randomization schedule.

Food and drink (other than water, which was allowed after 2 hr) were not allowed until 4 hr after dosing and then a standard breakfast, lunch and dinner were given to all volunteers according to a time schedule. Beverages and food containing caffeine were not permitted over the entire course of study. The volunteers were under continual medical supervision at the study site. Adverse events including abnormal laboratory values were spontaneously reported or observed either by the volunteers or the resident physician and were recorded, tabulated and evaluated. Approximately 5 mL blood samples for aripiprazole analysis were drawn into evacuated heparinized glass tubes through an indwelling cannula at 0.0, 0.5, 1.0, 1.5, 2.0, 2.5, 3.0, 3.5, 4.0, 4.5, 5.0, 5.5, 6.0, 8.0, 10.0, 12.0, 24.0, 48.0 and 72.0 hours post dose. All the samples were collected and centrifuged at 3500 rpm for 10 min at 4°C and the plasma was transferred directly into 5 mL plastic tubes and stored at -70 °C until the analysis. Plasma samples labeled by protocol number, subject number, study phase and the designated sample number were forwarded to the analysis laboratory. After 21 days washout period, the

study was repeated in the same manner to complete the crossover design.

***Sample preparation*:** All frozen plasma samples were thawed at ambient temperature. A solvent extraction procedure was used. 1 mL of human plasma samples and 100 µL of escitalopram (internal standard) solution were placed in 10 mL glass tubes, and vortexed for 1 min using a vortex mixer (Julabo *Para Mix II*, Munich, Germany). Four mL Ethyl Acetate was added and samples were vortexed for 2 min. The tubes were centrifuged for 10 min at 4000 rpm using a Centrifuge R32 A (Remi Laboratory Equipment, Bombay, India). The upper organic phases were then transferred to clean glass tubes and evaporated to dryness using centrifugal vacuum concentrator Vacufuge® 5301 (Eppendorf AG, Hamburg, Germany) at 40 °C. Dry residues were reconstituted by dissolving in 200 µL of (50% acetonitrile + 50% water) and vortexing for 1 min.

***Liquid chromatography/tandem mass spectrometry (LC-MS/MS) method for the determination of aripiprazole in human plasma*:** Plasma samples were analyzed using a sensitive, reproducible and accurate LC-MS/MS method, developed and validated before the study (32). Escitalopram (internal standard) stock solution was prepared by dissolving 40 mg of escitalopram in 100 mL (50% acetonitrile + 50% water) and serially diluted to give a final working concentration of 40 ng/mL. A shimadzu Prominence (Shimadzu, Japan) series LC system equipped with degasser (DGU-20A3), solvent delivery unit (LC-20AB) along with autosampler (SIL-20 AC) was used to inject 30 ìL aliquots of the processed samples on a Luna C_{18} column (4.6 x 50 mm) containing 5 µm size adsorbent as stationary phase (Phenomenex, Inc., Torrance, CA, USA). The Guard column used was Phenomenex C_{18} (4.0 x 5 mm), 5 µm particle size. Analysis was carried out at room temperature (25 ±2 °C). The isocratic mobile phase consisted of acetonitrile and water (70:30) and 0.1% formic acid, which was delivered at a flow rate of 1.0 mL/min into the mass spectrometer's electrospray ionization chamber. Quantitation was achieved by LC-MS/MS detection in positive ion mode for both aripiprazole and escitalopram, using an API-3200 mass spectrometer (MDS Sciex, Foster City, CA, USA) equipped with a Turbo ionspray™ interface at 400°C. The ion spray voltage was set at 5500 V. The common parameters: nebulizer gas, curtain gas, auxiliary gas, and collision gas were set at 60, 23, 50, and 12 PSI, respectively. The compound parameters: declustering potential, collision energy, entrance potential, and collision exit potential were 51, 19, 9, and 4 V, respectively, for aripiprazole and 72, 28, 18, and 4 V for escitalopram. Detection of the ions was performed in the multiple reaction monitoring (MRM) mode, analyzing the transition of the *m/z* 447.89 precursor ion to *m/z* 285.20 for aripiprazole and the *m/z* 324.98 precursor ion to *m/z* 109.10 for escitalopram. Quadrupoles Q1 and Q3 were set on unit resolution. The analytical data were processed using Analyst software version 1.4.2 (Applied Biosystems Inc., Foster City, CA, USA).

***Pharmacokinetic and statistical analysis*:** Plasma concentration-time data of aripiprazole was analyzed for each subject by non-compartmental pharmacokinetic models using kinetica® software version 4.4.1 (Thermo Fisher Scientific Inc., Waltham, MA, USA). The peak plasma concentrations (C_{max}) and the time of their occurrence (T_{max}) were directly obtained from the concentration-time data. The area under the plasma concentration-time curve (AUC) from time zero to last measured concentration (AUC_{0-72}) was calculated according to the linear trapezoidal method. Two-way analysis of

variance (ANOVA GLM procedure; Kinetica ™ 2000 Computer program for a crossover design) was used to assess the effect of formulation, period, and subjects on C_{max} and AUC_{0-t}. Differences between two related parameters were considered statistically significant for p-value equal to or less than 0.05.

***In vitro-in vivo correlation (IVIVC)*:** Two levels of in vitro-in vivo correlation, C and multiple level C, were studied (23). Level C IVIVC was investigated for each of the in vitro dissolution D values (D10, D20 and D30) versus C_{max} (30). Multiple level C IVIVC was studied by correlating partial AUCs (AUC_{0-1hr}, AUC_{0-2hr}, and AUC_{0-3hr}) versus D10, D20 and D30 (33). The partial AUCs were also calculated according to the linear trapezoidal method. In vitro and in vivo results were taken as independent (*x*) and dependent (*y*) variables, respectively. The correlation coefficient and the slope were calculated and interpreted using linear regression analysis (Microsoft Excel software).

Results and Discussion

***Dissolution study of the tablets*:** The particle size of the freshly prepared nanosuspension (0.41 ±13.70 µm), resuspended nanoparticles (0.39 ±16.45 µm) was comparable and significantly lower than the coprecipitate composition (11.08 ±0.31 µm) (p d" 0.05). The nanoparticles compressed tablets (NP) showed a significant increase in the rate and extent of dissolution and the dissolution rate was maintained at higher level throughout all time intervals compared to coprecipitate (CP) and market tablets. The rank order increase in dissolution rate was as follows: NP tablets > Market tablets > CP tablets (Fig. 1). Within 10 minutes, almost 75% of aripiprazole was dissolved from the NP tablets compared with 20% and 46% for CP tablets and market tablets, respectively. After 45 minutes, the dissolution was almost complete (99.5%) for NP tablets compared to only 72% and 82% for CP and market tablets, respectively.

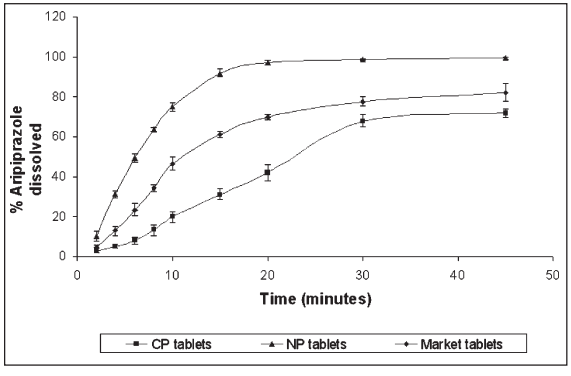

Fig. 1. The dissolution profile of nanoparticles tablets compared to coprecipitate and market tablets. Data points are means ± SD. All studies were conducted in triplicate.

The increase in dissolution rate from NP tablets was similar to the intrinsic dissolution rate of aripiprazole nanoparticles based on the disruption of the crystalline structure of aripiprazole and conversion into amorphous (6). In addition, after the disintegration of NP tablets, the increased surface area described by Noyes Whitney equation (34, 35, 36, 37, 38) and higher surface to volume ratio enabled hydration over larger surface area and consequently resulted in increased drug dissolution (39). Moreover, the increase in dissolution rate caused due to particle size reduction can be explained by the decrease in diffusion layer thickness (40). This decrease in diffusional thickness *h* leads to an increase in the concentration gradient *(Cs-Ct)/h* which consequently increases the dissolution rate.

***Pharmacokinetic study in healthy human volunteers*:** All volunteers fully completed the study. No adverse reactions were reported by any of the subjects.

The LC-MS/MS assay has been validated and a good linearity from 1-500 ng/mL with acceptable within and between day

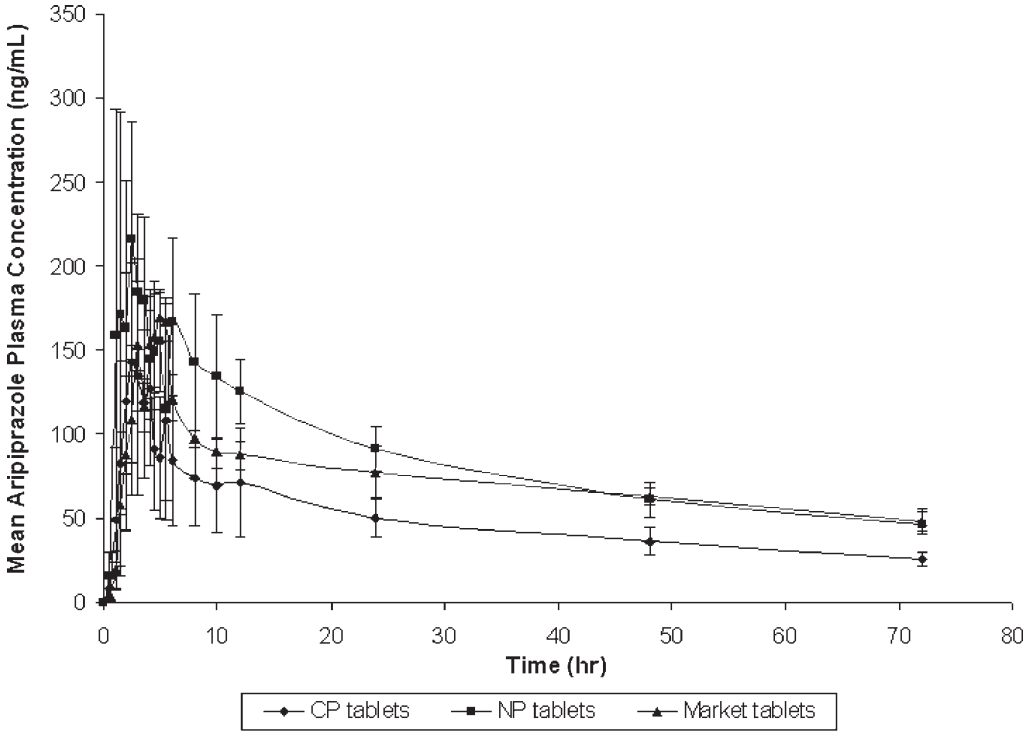

Fig. 2. Mean aripiprazole plasma concentration after single oral dose administration of 10 mg tablets (CP, NP, and Market tablets) to six healthy adult male volunteers. Data are means ± SD.

reproducibility was observed. The lower limit of aripiprazole quantification in plasma was 1 ng/mL.

The aripiprazole mean plasma concentration-time profiles following single oral administration of CP tablets, NP tablets, and market tablets to six healthy human volunteers are shown in Fig. 2. Corresponding pharmacokinetic parameters are summarized in Table 2.

The mean C_{max} value of aripiprazole from the NP tablets was numerically higher than both the CP tablets and the market tablets. However, statistical analysis showed that the mean C_{max} value of NP tablets was significantly higher than the CP tablets but not significant between the NP and the market tablets (p d" 0.05). The mean AUC_{0-72} value of aripiprazole from the NP tablets was significantly higher than both the CP tablets and market tablets (p d" 0.05). This indicated that the extent of absorption of aripiprazole from the NP tablets is significantly higher than that of the other tablets. The rate of absorption of aripiprazole from the CP tablets (T_{max} = 2.42 ±0.38 hr) and NP tablets (T_{max} = 2.25 ±1.08 hr) was comparable and significantly higher than the market tablets (T_{max} = 3.83 ±1.03 hr) (p d" 0.05). The calculated relative bioavailability of aripiprazole after oral administration of the CP and NP tablets was 61.66% and 117.65%, respectively compared to the market tablets. This shows that NP tablet was bioequivalent with the market tablet while the CP tablet was bioinequivalent.

Table 2. Pharmacokinetic parameters of aripiprazole after single oral dose administration of 10 mg tablets (CP, NP, and Market tablets) to six healthy adult male volunteers.

Pharmacokinetic parameter	CP tablets	NP tablets	Market tablets
C_{max} (ng/ml) ± SD	159.97 ± 55.59	223.50 ± 71.78	186.17 ± 18.36
T_{max} (hr) ± SD	2.42 ± 0.38	2.25 ± 1.08	3.83 ± 1.03
AUC 0-72 (ng.hr/ml) ± SD	3216.12 ± 525.02	6136.35 ± 421.29	5215.57 ± 457.28
Relative bioavailability (%)	61.66%	117.65%	100%

*Market tablets are used as reference standard.
*Relative bioavailability for CP and NP tablets was calculated as follows: $\frac{AUC_{test}}{AUC_{reference}} \times \frac{Dose_{reference}}{Dose_{test}}$

The higher C_{max} and AUC_{0-72} following the oral administration of the NP tablets compared to CP tablets are due to the higher dissolution rate and consequently rapid absorption of aripiprazole from the gastrointestinal tract. This resulted in higher bioavailability (117.65%) (1, 3, 12, 41, 42).

***Evaluation of the in vitro- in vivo correlation (IVIVC)*:** In level C correlation, one single in vitro dissolution time point is related to one single pharmacokinetic parameter (23, 43). It is most applicable to immediate release tablets (30). Multiple level C correlation relates one or several pharmacokinetic parameters of interest to the amount of drug dissolved at several time points of the dissolution profile (23, 33). Multiple level C correlation can be as useful as level A correlation from a regulatory point of view, although the later is the most desirable (33, 44).

C_{max} is one of the pharmacokinetic parameters primarily related to the absorption phase and has been selected as the pharmacokinetic parameter of choice in bioequivalence testing (30, 45). D values as in vitro data were shown to be good estimates of the rate of dissolution (30, 46, 47, 48). Hence, D values were correlated with C_{max}.
The relationships between each of the in vitro dissolution D values (D10, D20 and D30) versus C_{max} are shown in Figs. 3-5. A high correlation

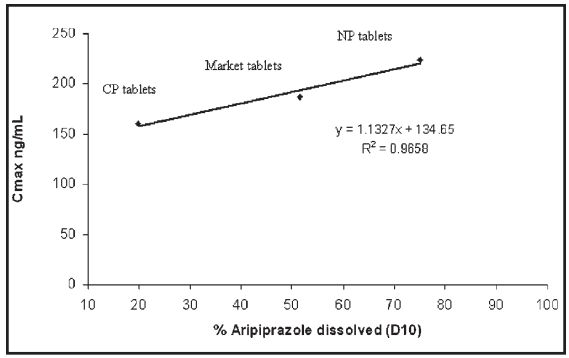

Fig. 3. Level C IVIVC between C_{max} and the percentage of aripiprazole dissolved in vitro at 10 min.

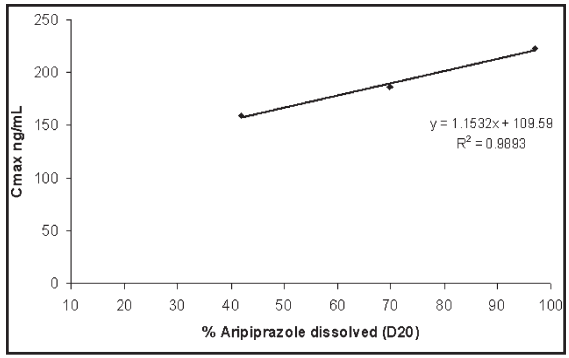

Fig. 4. Level C IVIVC between C_{max} and the percentage of aripiprazole dissolved in vitro at 20 min.

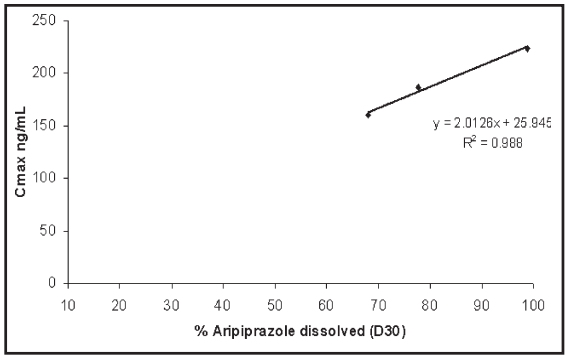

Fig. 5. Level C IVIVC between C_{max} and the percentage of aripiprazole dissolved in vitro at 30 min.

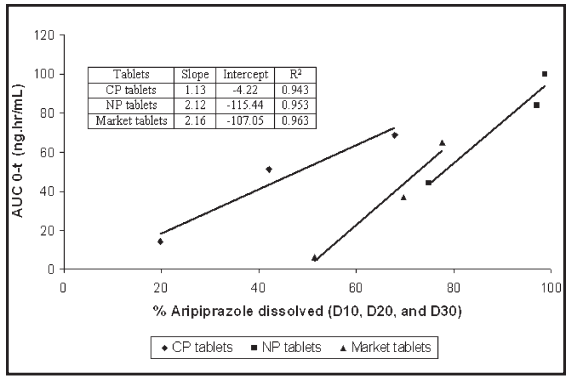

Fig. 6. Multiple level C IVIVC between AUC_{0-t} for 1, 2, and 3 hrs as a function of the amount of aripiprazole dissolved at different times (D10, D20, and D30).

was observed. This indicates that C_{max} can be well predicted at D10, D20 and D30 as evident from the high in vitro-in vivo correlation (30). In addition, the rank order increase in C_{max} was similar to the in vitro dissolution curves, NP tablets > Market tablets > CP tablets (Fig. 3).

In immediate release dosage forms, the in vitro and in vivo sampling time points are different. Therefore, in order to establish a multiple level C correlation between the in vitro and in vivo data that were collected at different time periods, a time scale factor is needed (33, 43, 49). Hence, the partial AUC obtained in the first three hours (60, 120, and 180 min) were compared with the amount dissolved at in vitro times six-fold lower (10, 20, and 30 min) (33). The correlation between partial AUC (AUC_{0-1hr}, AUC_{0-2hr}, and AUC_{0-3hr}) and percentage of aripiprazole dissolved at different time intervals (D10, D20 and D30) is shown in Fig. 4. The intercepts and slopes were calculated for the three tablets and the correlation coefficients were higher than 0.94 (Fig. 5). The similarity between the intercept and slope of NP tablet and market tablet supported that the two tablets were bioequivalent (33). On the other hand, the slope and intercept of the CP tablet were different than that of market tablet supporting bioinequivalence.

Conclusion

A significant increase in the in vivo bioavailability of aripiprazole (~2 folds) due to nanomilling was achieved when compared to coprecipitation. This higher bioavailability of the NP tablets (117.65%) was due to the higher dissolution rate and consequently rapid absorption of aripiprazole from the gastrointestinal tract. A high level C IVIVC was found between each of the in vitro dissolution D values and C_{max}. Furthermore, multiple level C IVIVC supported the bioequivalence and bioinequivalence of the NP and CP tablets, respectively compared to the market tablets.

References

1. Kocbek, P., Baumgartner, S. and Kristl, J. (2006). Preparation and evaluation of nanosuspensions for enhancing the dissolution of poorly soluble drugs. Int J Pharm, 312: 179-186.

2. Cook, J., Addicks, W. and Wu, Y.H. (2008). Application of the biopharmaceutical

classification system in clinical drug development - an industrial view. AAPS J, 10: 306-310.

3. Hecq, J., Deleers, M., Fanara, D., Vranckx, H., Boulanger, P., Le Lamer, S. and Amighi, K. (2006). Preparation and in vitro/in vivo evaluation of nano-sized crystals for dissolution rate enhancement of ucb-35440-3, a highly dosed poorly water-soluble weak base. Eur J Pharm Biopharm, 64: 360-368.

4. Lobenberg, R. and Amidon, G.L. (2000). Modern bioavailability, bioequivalence and biopharmaceutics classification system. New scientific approaches to international regulatory standards. Eur J Pharm Biopharm, 50: 3-12.

5. Fakes, M.G., Vakkalagadda, B.J., Qian, F., Desikan, S., Gandhi, R.B., Lai, C., Hsieh, A., Franchini, M.K., Toale, H. and Brown, J. (2009). Enhancement of oral bioavailability of an HIV-attachment inhibitor by nanosizing and amorphous formulation approaches. Int J Pharm, 370: 167-174.

6. Abdelbary, A.A., El-Nabarawi, M., Elassasy, A., Li, X. and Jasti, B. (Submitted for publication). Enhancement of intrinsic dissolution rate of poorly water soluble drug, aripiprazole by nanomilling and comparison to coprecipitation. Int J Pharm, IJP D-11-00989.

7. Rabinow, B. (2005). Pharmacokinetics of drugs administered in nanosuspension. Discovery Med, 5: 74–79.

8. Craig, D.Q. (2002). The mechanisms of drug release from solid dispersions in water-soluble polymers. Int J Pharm, 231: 131-144.

9. Waghmare, A., Pore, Y. and Kuchekar, B. (2008). Development and characterization of zaleplon solid dispersion systems: a technical note. AAPS PharmSciTech, 9: 536-543.

10. Ghosh, I., Bose, S., Vippagunta, R. and Harmon, F. (2011). Nanosuspension for improving the bioavailability of a poorly soluble drug and screening of stabilizing agents to inhibit crystal growth. Int J Pharm, 409: 260-268.

11. Wu, Y., Loper, A., Landis, E., Hettrick, L., Novak, L., Lynn, K., Chen, C., Thompson, K., Higgins, R., Batra, U., Shelukar, S., Kwei, G. and Storey, D. (2004). The role of biopharmaceutics in the development of a clinical nanoparticle formulation of MK-0869: a Beagle dog model predicts improved bioavailability and diminished food effect on absorption in human. Int J Pharm, 285: 135-146.

12. Jinno, J., Kamada, N., Miyake, M., Yamada, K., Mukai, T., Odomi, M., Toguchi, H., Liversidge, G.G., Higaki, K. and Kimura, T. (2006). Effect of particle size reduction on dissolution and oral absorption of a poorly water-soluble drug, cilostazol, in beagle dogs. J Control Release, 111: 56-64.

13. Matsunaga, N., Nakamura, K., Yamamoto, A., Taguchi, E., Tsunoda, H. and Takahashi, K. (2006). Improvement by solid dispersion of the bioavailability of KRN633, a selective inhibitor of VEGF receptor-2 tyrosine kinase, and identification of its potential therapeutic window. Mol Cancer Ther, 5: 80-88.

14. Kushida, I., Ichikawa, M. and Asakawa, N. (2002). Improvement of dissolution and

oral absorption of ER-34122, a poorly water-soluble dual 5-lipoxygenase/ cyclooxygenase inhibitor with anti-inflammatory activity by preparing solid dispersion. J Pharm Sci, 91: 258-266.

15. Sinha, S., Ali, M., Baboota, S., Ahuja, A., Kumar, A. and Ali, J. (2010). Solid dispersion as an approach for bioavailability enhancement of poorly water-soluble drug ritonavir. AAPS PharmSciTech, 11: 518-527.

16. Kohri, N., Yamayoshi, Y., Xin, H., Iseki, K., Sato, N., Todo, S. and Miyazaki, K. (1999). Improving the oral bioavailability of albendazole in rabbits by the solid dispersion technique. J Pharm Pharmacol, 51: 159-164.

17. Burris, K.D., Molski, T.F., Xu, C., Ryan, E., Tottori, K., Kikuchi, T., Yocca, F.D. and Molinoff, P.B. (2002). Aripiprazole, a novel antipsychotic, is a high-affinity partial agonist at human dopamine D2 receptors. J Pharmacol Exp Ther, 302: 381-389.

18. Naber, D. and Lambert, M. (2004). Aripiprazole: a new atypical antipsychotic with a different pharmacological mechanism. Prog Neuropsychopharmacol Biol Psychiatry, 28: 1213-1219.

19. Katzman, M.A. (2011). Aripiprazole: a clinical review of its use for the treatment of anxiety disorders and anxiety as a comorbidity in mental illness. J Affect Disord, 128 Suppl 1: S11-20.

20. Lentz, K.A., Quitko, M., Morgan, D.G., Grace, J.E., Jr., Gleason, C. and Marathe, P.H. (2007). Development and validation of a preclinical food effect model. J Pharm Sci, 96: 459-472.

21. Amidon, G.L., Lennernas, H., Shah, V.P. and Crison, J.R. (1995). A theoretical basis for a biopharmaceutic drug classification: the correlation of in vitro drug product dissolution and in vivo bioavailability. Pharm Res, 12: 413-420.

22. Cardot, J.M. and Beyssac, E. (1993). In vitro/in vivo correlations: scientific implications and standardisation. Eur J Drug Metab Pharmacokinet, 18: 113-120.

23. Emami, J. (2006). In vitro - in vivo correlation: from theory to applications. J Pharm Pharm Sci, 9: 169-189.

24. Cardot, J.M., Beyssac, E. and Alric, M. (2007). In vitro-in vivo correlation: Importance of dissolution in IVIVC. Dissolution Technologies, 2: 15-19.

25. Vangani, S., Li, X., Zhou, P., Del-Barrio, M.-A., Chiu, R., Cauchon, N., Gao, P., Medina, C. and Jasti, B. (2009). Dissolution of poorly water-soluble drugs in biphasic media using USP 4 and fiber optic system. Clin Res Regul Aff, 26: 8–19.

26. Narang, A.S. and Srivastava, A.K. (2002). Evaluation of solid dispersions of clofazimine. Drug Dev Ind Pharm, 28: 1001-1013.

27. Tantishaiyakul, V., Kaewnopparat, N. and Ingkatawornwong, S. (1999). Properties of solid dispersions of piroxicam in polyvinylpyrrolidone. Int J Pharm, 181: 143-151.

28. Dai, W.G., Dong, L.C. and Song, Y.Q. (2007). Nanosizing of a drug/carrageenan complex to increase solubility and dissolution rate. Int J Pharm, 342: 201-207.

29. Jong, L. (2006). Effect of soy protein concentrate in elastomer composites.

Composites: Part A, 37: 438–446.

30. Lake, O.A., Olling, M. and Barends, D.M. (1999). In vitro/in vivo correlations of dissolution data of carbamazepine immediate release tablets with pharmacokinetic data obtained in healthy volunteers. Eur J Pharm Biopharm, 48: 13-19.

31. Lancelin, F., Djebrani, K., Tabaouti, K., Kraoul, L., Brovedani, S., Paubel, P. and Piketty, M.L. (2008). Development and validation of a high-performance liquid chromatography method using diode array detection for the simultaneous quantification of aripiprazole and dehydro-aripiprazole in human plasma. J Chromatogr B Analyt Technol Biomed Life Sci, 867: 15-19.

32. Shah, V.P., Midha, K.K., Dighe, S., McGilveray, I.J., Skelly, J.P., Yacobi, A., Layloff, T., Viswanathan, C.T., Cook, C.E., McDowall, R.D., et al. (1991). Analytical methods validation: bioavailability, bioequivalence and pharmacokinetic studies. Conference report. Eur J Drug Metab Pharmacokinet, 16: 249-255.

33. Volpato, N.M., Silva, R.L., Brito, A.P., Goncalves, J.C., Vaisman, M. and Noel, F. (2004). Multiple level C in vitro/in vivo correlation of dissolution profiles of two L-thyroxine tablets with pharmacokinetics data obtained from patients treated for hypothyroidism. Eur J Pharm Sci, 21: 655-660.

34. Kesisoglou, F., Panmai, S. and Wu, Y. (2007). Nanosizing-oral formulation development and biopharmaceutical evaluation. Adv Drug Deliv Rev, 59: 631-644.

35. Junghanns, J.U., Müller, R.H. (2008). Nanocrystal technology, drug delivery and clinical applications. Int J Nanomedicine, 3: 295-309.

36. Gao, L., Zhang, D., Chen, M., Zheng, T. and Wang, S. (2007). Preparation and characterization of an oridonin nanosuspension for solubility and dissolution velocity enhancement. Drug Dev Ind Pharm, 33: 1332-1339.

37. Ravichandran, R. (2009). Nanotechnology-based drug delivery systems. Nanobiotechnol, 5: 17-33.

38. Noyes, A. and Whitney, W. (1897). The rate of solution of solid substances in their own solutions. J Am Chem Soc, 19: 930-934.

39. Dolenc, A., Kristl, J., Baumgartner, S. and Planinsek, O. (2009). Advantages of celecoxib nanosuspension formulation and transformation into tablets. Int J Pharm, 376: 204-212.

40. Mosharraf, M. and Nyström, C. (1995). The effect of particle size and shape on the surface specific dissolution rate of microsized practically insoluble drugs. Int J Pharm, 122: 35-47.

41. Elshafeey, A.H., Kamel, A.O. and Fathallah, M.M. (2009). Utility of nanosized microemulsion for transdermal delivery of tolterodine tartrate: ex-vivo permeation and in-vivo pharmacokinetic studies. Pharm Res, 26: 2446-2453.

42. Mou, D., Chen, H., Wan, J., Xu, H. and Yang, X. (2011). Potent dried drug nanosuspensions for oral bioavailability enhancement of poorly soluble drugs with pH-dependent solubility. Int J Pharm, 413: 237-244.

43. Kortejarvi, H., Mikkola, J., Backman, M., Antila, S. and Marvola, M. (2002). Development of level A, B and C in vitro-in vivo correlations for modified-release levosimendan capsules. Int J Pharm, 241: 87-95.

44. Uppoor, V.R. (2001). Regulatory perspectives on in vitro (dissolution)/in vivo (bioavailability) correlations. J Control Release, 72: 127-132.

45. Olling, M., Mensinga, T.T., Barends, D.M., Groen, C., Lake, O.A. and Meulenbelt, J. (1999). Bioavailability of carbamazepine from four different products and the occurrence of side effects. Biopharm Drug Dispos, 20: 19-28.

46. Ammar, H.O., Khalil, R.M. and Omar, S.M. (1993). Discrepancy among dissolution rates of commercial tablets as a function of dissolution method. Part 5: In vitro/in vivo correlation for chlorpromazine hydrochloride tablets. Pharmazie, 48: 932-935.

47. El-Yazigi, A. and Sawchuk, R.J. (1985). In vitro-in vivo correlation and dissolution studies with oral theophylline dosage forms. J Pharm Sci, 74: 161-164.

48. Meyer, M.C., Straughn, A.B., Jarvi, E.J., Wood, G.C., Pelsor, F.R. and Shah, V.P. (1992). The bioinequivalence of carbamazepine tablets with a history of clinical failures. Pharm Res, 9: 1612-1616.

49. Brockmeier, D., Voegele, D. and von Hattingberg, H.M. (1983). In vitro—in vivo correlation, a time scaling problem? Basic techniques for testing equivalence. Arzneimittelforschung, 33: 598-601.

Current Trends in Biotechnology and Pharmacy
Vol. 5 (4) 1410-1413 October 2011, ISSN 0973-8916 (Print), 2230-7303 (Online)

Analysis of Ricin Subunits by High-Resolution Acidic Native Gel Electrophoresis

Payal Puri, Om Kumar*, Krishna Chaturvedi and Ramesh Kaul
Division of Pharmacology and Toxicology, Defence Research and Development Establishment
Jhansi Road, Gwalior-474002, India
*For Correspondence - omkumar63@rediffmail.com

Abstract

Ricin is a potent toxic castor bean glycoprotein comprising of two subunits, A chain and B chain. We studied ricin subunits in an acidic electrophoresis system followed by electro blotting. To the best of our knowledge, there is no study reported for characterization of ricin subunits using acidic native PAGE. Sample preparation steps for acidic native PAGE were optimized and adequate electrophoretic conditions were developed for achieving a complete separation of ricin subunits. Ricin subunits were separated and characterized at acidic pH (2.9 and 4.3) and their immunological detection was made using polyclonal antibodies. Our findings showed that this method results in sharper band and therefore high resolution than SDS-PAGE and also the following protein transfer is highly efficient and rapid.

Keywords: Ricin, Acidic non-denaturing PAGE, Electro blotting, Resolution.

Introduction

Ricin is a 64 kDa a glycoprotein belonging to the type II group of ribosome activating protein (1, 2). It is a two chain variant protein that exists in slightly different isoforms in beans of different origin with differences in their biochemical properties (3). Ricin and it's A chain has got therapeutic value as immunotoxins (4). Ricin has been extensively characterized using electrophoretic methods including SDS-PAGE and high resolution two-dimensional electrophoresis (2-DE) (5). In contrast, ricin subunits are poorly characterized in their native form by conventional electrophoresis. Ricin having molecular weight from 60 kDa to 65 kDa by SDS-PAGE technique has been reported under non-reduced conditions (6). Under reducing condition, ricin shows the presence of two subunits, corresponding to 30 kDa and 32 kDa (7).

In this study, we describe an additional electrophoretic method for rapid analysis of purity and homogeneity of the ricin subunits. The electrophoretic characterization of ricin has been done earlier at acidic pH 2.9 (8). To the best of our knowledge, there is no study reported for characterization of ricin subunits using acidic native PAGE. The aim of the present study was to optimize protocols for acidic non-denaturing PAGE of ricin subunits and their identification by blotting. We tested buffers of different pH for getting the best electrophoretic resolution. It was done at pH 2.9 and 4.3 with a gel concentration of 15% acrylamide.

Acidic native PAGE system without SDS enables the separation of proteins and peptides as a function of their combined charge and size. In particular acetic acid/KOH-PAGE system as described in the study provides excellent

Vol. 5 (4) 1410-1413 October 2011, ISSN 0973-8916 (Print), 2230-7303 (Online)

resolution of many proteins and peptides that might not be resolved using SDS- PAGE. The method uses an acidic buffer to retain protein solubility and gives uniform gels to allow migration of proteins. The electrophoretic run is much shorter (90 min) than conventional SDS-PAGE.

Materials and Methods

***SDS-PAGE*:** SDS-PAGE was performed under reduced and non-reduced conditions to assess the purity of ricin, and its subunits using Bio-RAD, USA electrophoretic apparatus. The SDS-PAGE was performed according to Laemmli (9).

***Acidic Native PAGE*:** Acidic non-denaturing gel electrophoresis of all the above mentioned samples was performed according to Hames (10) with slight modifications. The 5% stacking gel was prepared in 120 mM KOH and 0.75% acetic acid (pH-5.9). Ammonium per sulfate (APS) and TEMED concentration was 0.7% and 0.06% respectively. 15% resolving gel was prepared in 30 mM KOH and 13.25% acetic acid (pH-2.9). The concentration of APS was similar to that of stacking gel. TEMED concentration was increased to 0.6%. Electrode buffer was 0.16% acetic acid containing 0.65% b-alanine, pH-2.9. Loading buffer contained 0.8% glycerol, 2% methylene blue, 120 mM KOH and 0.75% acetic acid (5.9). The acidic PAGE at pH 4.3 was carried out in a similar fashion but pH of all the buffers was kept 4.3. Samples were mixed with equal volumes of loading buffer for application onto the gel. Electrophoresis was performed in the cold (4°C) at 200V for 75 min. Gel was stained in coomassie blue stain (0.4% dye made in 50% methanol/10% acetic acid). Destaining was carried out in 30% methanol/10% acetic acid solution.

***Electro blotting*:** Western blot analysis was performed as described by Caponi and Migliorini (11). After separation by acidic non-denaturing PAGE, proteins were transferred to PVDF membrane, (0.45 µm, pore size, Pierce Biotechnology, USA) using 0.7% acetic acid. Blotting was performed at constant voltage (80 V) for 2 h in Bio-Rad Trans- Blot apparatus. Temperature was kept low by using ice block supplied with the system.

For immunodetection, the blots were blocked overnight with 5% low fat milk powder in blocking buffer (5% milk powder, 0.05% Tween-20 in PBS) at 4°C. Blots were washed 3 x for 15 min each with PBST (PBS containing 0.05% Tween-20) and then incubated with primary antibody at 1:5000 dilution for 90 min at 37°C. The blots were incubated with a secondary antibody, goat anti-rabbit IgG-HRP conjugate (1:50,000) for 90 min at 37°C after washing thrice with PBST. After another three washes, the blots were developed using an enhanced chemiluminescent detection system (Super Signal West Pico Chemiluminescent Substrate, Pierce) according to manufacturer's protocol and the images were taken on Pierce CL-XPosure TM X-ray film.

Results and Discussion

***Electrophoretic characterization of Ricin subunits*:** The results of SDS–PAGE of ricin under non-reduced and reduced conditions are shown in Fig. 1A. Under non-reducing condition, ricin gave a single band in 60-65 kDa region. When ricin was treated with -mercaptoethanol, it gave two bands in the region of 30-34 kDa region which represent A and B subunits of the ricin. Ricin A subunit showed one major and one minor band in 30-34 kDa region. Ricin B subunit revealed one band (M_r » 33-34 kDa) compared to the molecular weight markers separated on the same gel.

The electrophoretic mobility of ricin and its subunits varied with pH of the buffer used in

Vol. 5 (4) 1410-1413 October 2011, ISSN 0973-8916 (Print), 2230-7303 (Online)

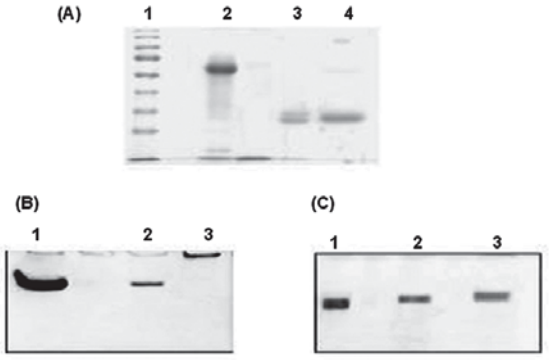

Fig. 1. (A) SDS-PAGE of purified subunits. Lanes: (1) Standard Marker; (2) Non-reduced ricin (20 µg); (3) A subunit (12µg); (4) B subunit (12µg). **(B)** Acidic non-denaturing PAGE of ricin and its subunits at pH-2.9 Lanes: (1) Standard Ricin; (2) Ricin A-chain; (3) Ricin B-chain**. (C)** Acidic non-denaturing PAGE of ricin and its subunits at pH 4.3 Lanes: (1) Standard Ricin; (2) Ricin A subunit; (3) Ricin B subunit.

native gel electrophoresis. We observed ricin and its A chain are highly charged at acidic pH 2.9 and moves faster in the gel. B chain carries insufficient charge at an acidic pH 2.9 and therefore is completely stacked in the gel (Fig. 1B). Both the chains of ricin have similar electrophoretic mobility and can be easily separated at pH 4.3 (Fig.1C). The electrophoretic mobility of ricin is higher than its subunits at pH 4.3. Ricin, ricin B chain as well as A chain can be resolved at pH 4.3, so this pH is taken as reference standard for their characterization.

Immunological characterization of Ricin subunits **:** We also demonstrated electrophoretic transfer of acidic native PAGE separated proteins using acetic acid as transfer buffer onto a PVDF membrane for immunodetection. Transfer of acidic native PAGE separated proteins onto a PVDF membrane occurred with high efficiency (12). The western blot study demonstrated that this system of electrophoresis of ricin subunits is very useful for the identification of antibody specificities. We observed that the anti ricin A chain antibody is highly specific to A chain but anti ricin B chain antibody is cross reactive to A chain upon blotting (Fig. 2A and 2B).

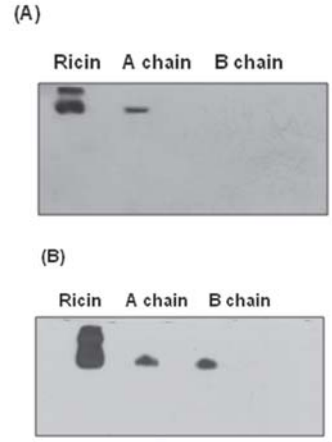

Fig. 2. Immunological reaction between Ricin, Ricin subunits and **(A)** anti rabbit IgG antiricin A-chain antibody, **(B)** anti rabbit IgG antiricin B-chain antibody.

Conclusion

Sodium dodecyl sulfate polyacrylamide gel electrophoresis (SDS-PAGE) is a common method for the separation and characterization of proteins. Electrophoretic separation of glycoproteins like ricin results in broad and fuzzy bands in SDS PAGE. Here, we report a modified acidic non-denaturing PAGE for the study of ricin and its subunits. This system of acidic non-denaturing PAGE gives greater resolution for separation of ricin subunits than SDS-PAGE. In addition, protein transfer following acidic PAGE is also rapid and efficient. Compared to western blotting after SDS PAGE, for which a higher concentration of Tris/glycine buffer is used, the method employing a dilute acetic acid as transfer buffer is more economical.

In conclusion our results indicates that the high resolution acidic native PAGE followed by electro blotting may prove to be a valuable tool for biochemical characterization and

development of standard methods for identification and detection of ricin and its subunits.

Acknowledgements

The authors thank Director, DRDE, Gwalior, for providing the necessary facilities and encouragement. Authors also thank Dr. S.J.S. Flora Head, Division of Pharmacology and Toxicology for extensive review of the manuscript. Payal Puri is thankful to Defence Research and Development Establishment for the award of research fellowship. This work was supported by institutional funding of Defence R&D Organization, Ministry of Defence, Government of India.

References

1. Audi, J.M., Belson, M., Patel, M., Schier, J. and Osterloh, J. (2005) Ricin poisoning: a comprehensive review. J. Am. Med. Assoc., 294: 2342–2351.
2. Doan, L.G. (2004). Ricin, mechanism of toxicity, clinical manifestations, and vaccine development. A review. Clin. Toxicol., 42: 201–208.
3. Sehgal, P., Khan, M., Kumar, O. and Vijayaraghavan, R. (2010). Purification, characterization and toxicity profile of ricin isoforms from castor beans. Food Chem. Toxicol., 48: 3171-3176.
4. Schnell, R., Vietta, E., Schindler, J., Barth, S., Winkler, U., Borchmann, P., Hansmann, M.L., Diehl, V., Ghetie, V. and Engert, A. (1998). Clinical Trial with an Anti-CD25 Ricin A-Chain Experimental and Immunotoxin (RFT5-SMPT-dgA) in Hodgkin's Lymphoma. Leuk Lymphoma, 30: 525-537.
5. Sehgal, P**.,** Rao, M.K., Kumar, O. and Vijayaraghavan R. Characterization of native and denatured ricin using MALDI-TOF/MS. Cell. Mol. Biol., 56: 1385-1399 (2010).
6. Nicolson, G.L., Blaustein, J and Etzler, M.E. (1974). Characterization of two plant lectins from Ricinus communis and their quantitative interaction with a murine lymphoma. Biochemistry, 13: 197–204.
7. Woo, B.H. and Lee, K.C. (1998). Purification of sepharose unbinding ricin from castor beans by hydroxyapatite chromatography. Protein Expression Purif., 13: 154-164.
8. Lugnier, A. and Dirheimer, G. (1973). Differences between ricin and phytohemagglutinins from Ricinus communis seeds. FEBS Lett.**,** 35: 117–120.
9. Laemmli, U.K. (1970). Clevage of structure proteins during the assembly of the head of the bacteriophage T_4. Nature, 227: 680-687.
10. Hames, B.D. (1990) In: Hames, B.D., Rickwood, D. (Eds.), Gel electrophoresis of protein: a practical approach. One dimensional polyacrylamide gel electrophoresis, Oxford University Press, New York, pp.1–147.
11. Caponi, L and Migliorini, P. (2005). Antibody usage in the lab: immunoblotting. Springer-Verlag Press, New York, pp. 32-46.
12. Mclellan, T. and Ramshaw, J.A.M. (1981). Serial electrophoretic transfers: a technique for the identification of numerous enzymes from single polyacrylamide gel. Biochem. Genet., 19: 647–654.

Current Trends in Biotechnology and Pharmacy
Vol. 5 (4) 1414-1423 October 2011, ISSN 0973-8916 (Print), 2230-7303 (Online)

In silico Modeling of Coat Protein of Cucumber Mosaic Virus Strain Banana and Building its Virion from the Modeled Polypeptide Chain

Anthony Johnson A.M. and Sai Gopal D.V.R.*
Department of Virology, Sri Venkateswara University, Tirupati -517502, A.P., India
*For Correspondence - dvrsaigopal@gmail.com

Abstract

Protein homology modeling was applied in understanding the architecture of Cucumber mosaic virus strain banana. Cucumber mosaic virus is a causative for infectious chlorosis disease on banana. The 3-dimensional structure for the 218 amino acid residue coat protein of this virus strain was predicted by homology modeling approach. Structural templates for the 218 residue amino acid strain were searched using PDBBLAST tool. The template was confirmed by detecting the template with fold recognition tools like FUGUE. Sequence to structure alignment was achieved using JOY server. PDB structure 1F15 was used as template for modeling and the structure was modeled using Modeller v 6.0. Loops were built by using SPDBV software v. 4.0.1. Modeled structure was validated by using PROCHECK and Verify 3D. Energy minimization was done using Tripos Sybyl v 6.7. Structural polymer, a trimer similar to that of the template was modeled using magic fit algorithm of SPDBV software. Further, a tricky step was performed for building the virion structure by applying the biomolecular rotational symmetries of the template (CMV strain_FNY). Here, we describe a largely automated procedure for modeling protein structure from sequence alignments with homologous structures. The advanced step in viral protein modeling, we have used is to build the complete virion. Structure was deposited into theoretical model archive of PDB with identification code 2IKA.

Keywords: Viral Coat protein, Polymer building, Virion symmetry, Virus architecture.

Introduction

In the present era of research, Macromolecular modeling/homology modeling of biomolecules is a powerful tool in understanding the structural aspects and biomolecular interactions. This technique is also highly applied in the field of Virology for better understanding of the Virion architecture and coat protein subunit interactions. In the current study, homology modeling technique was applied for *Cucumber mosaic virus* Banana coat protein to predict its 3D structure (2, 3). *Cucumber mosaic virus* (CMV) Banana is causative of heart rot or infectious chlorosis disease of banana (1, 10, 12). Virus disease is characterized by discontinuous leaf chlorotic streaks symptoms followed by necrosis. CMV is a RNA virus comprising of three species of RNA among which RNA-3 encodes the coat protein. CMV is an isometric virus with icosahedral symmetry. Coat protein polypeptide of this virus is organized into homotrimer polymer subunit that is known as capsomere which upon regular symmetrical arrangement forms the virion particle/capsid with

triangulation number T=3. In the present study, we have defined a largely automated procedure for modeling protein structure from sequence alignments with homologous structures. The advanced step in viral protein modeling, we have used is to build the capsomere subunit and also the complete virion to define the virus architecture for strain banana from the sequence from TrEMBL database Q66135, an amino acid sequence derived from the translation of corresponding gene CDS and annotated in the database.

Materials and Methods

***Template identification and fold recognition*:** The target considered for homology modeling was used for finding the corresponding template for homology modeling approach based 3D structure prediction. Initially, the template was searched by using PDB BLAST tool. Then the templates obtained were confirmed at the fold level by using fold recognition server Fugue that detects the template at fold level (6).

***3D Model building* :** The initial model of virus coat protein of CMV strain banana was built by using homology-modeling methods and the MODELLER 6V2 software; a program for comparative protein structure modeling optimally satisfying spatial restraints derived from the alignment and expressed as probability density functions (pdfs) for the features restrained (13, 4). The pdfs restrain C^{α}–C^{α} distances, main-chain N–O distances, main-chain and side-chain dihedral angles. The 3D model of a protein is obtained by optimization of the molecular pdf such that the model violates the input restraints as little as possible. The molecular pdf is derived as a combination of pdfs restraining individual spatial features of the whole molecule. The optimization procedure is a variable target function method that applies the conjugate gradients algorithm to positions of all non hydrogen atoms. Alignment between the target sequence and the template sequence was used for modeling the structurally conserved regions (SCR) of the target. The coordinates for the structurally conserved regions (SCRs) for CMV coat protein were assigned from the template using pair wise sequence alignment between the template and the target and also obtained sequence to structure alignment from joy server (**9**). The modeler commands used are represented in (Table-2). The structure having the least modeler objective function obtained from the modeler was used for further refinement by loop modeling and energy minimization.

***Model structure refinement*:** Loops were modeled for the regions that have bad conformations by using SPDBV software v 4.0.1 (5). After loop modeling, geometric optimizations were carried out using the standard Tripos force field with 0.05 kcal/mol energy convergence criteria and a distant dependent dielectric constant of 4.0 R to take into account the dielectric shielding in proteins employing Gasteiger-Marshilli charges with non-bonding interaction cut off as 15. All hydrogen atoms were included during the calculation. After undertaking 100 steps of Powell minimization method initially, a conjugate gradient energy minimization of the full protein was carried out until the root mean-square (r.m.s) gradient was lower than 0.05 kcal mol^{-1}.All calculations are performed on SGI 2000 workstation using the SYBYL software suite implemented on a Silicon Graphics O2+ workstation, operating under IRIX (SYBYL 6.7, Tripos Inc., 1699, South Hanley Rd., St. Louis, Missouri, 63144, USA) (11).

***Model validation and Ca Trace Superimposition*:** The final structure obtained, was analyzed by Ramachandran's map drawn using PROCHECK v.3.0 (7) (a program to check the stereo chemical quality of protein structures),

protein environment profile graph drawn by VERIFY-3D server (8) (structure evaluation server). The model satisfying all the parameters after evaluation was considered for the further process. The Ca trace structures of the target model and the template were then superimposed to identify the fold level conservation using the Ca trace overlap module of the SYBYL software suite.

***Capsomere subunit construction and virion building*:** A tricky method or approach was used in obtaining the viral capsomere subunit in order to generate the virion particle and also to describe the viral architecture. The iterative magic fit algorithm of the SPBDV software v. 4.0.1 was used to construct the capsomere. The resultant capsomere was used for the building of virion by applying the crystallographic symmetries of the template PDB as the template used also belongs to a strain of CMV.

Results

***Template identification and fold recognition*:** A high level of sequence identity should guarantee a more accurate alignment between the target sequence and template structure. In the results of PDB BLAST, a search against PDB and also fold level recognition by Fugue, only one reference protein 1F15 had high level of sequence identity (89%) that was marked as Certain by Fugue server prediction results and one more protein that was showing comparatively less identity that was marked as Marginal by Fugue server prediction results (Table-1). When the template was verified, we found that the template is a homo trimer with three chains a,b,c having 62-218, 29-218, 28-218 residues respectively. Remaining other residues were not located in the experiment (information extracted from PDB annotation). Finally the template chain c was chosen as a reference structure for modeling of CMV strain banana coat protein as it had maximum number of residues.

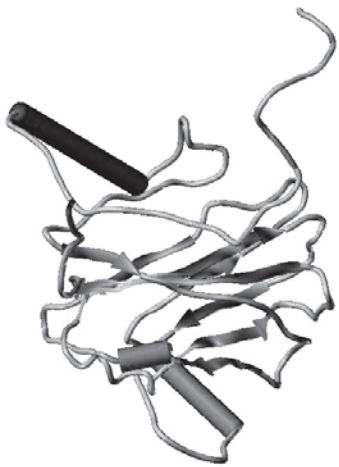

Fig. 1. Target model generated in the study

***Model building*:** Structurally conserved regions (SCRs) for the model and the template were determined by sequence alignment. Coordinates from the reference protein (1F15c) to the SCRs, structurally variable regions (SVRs), N-termini and C-termini were assigned to the target sequence based on the satisfaction of spatial restraints. All side chains of the model protein were set by rotamers. The initial model was generated from above defined procedure.

***Model structure refinement, Model Validation and Molecular Dynamics*:** The final model was further checked by VERIFY-3D graph and the results are shown in Fig.2. The compatibility score above zero in the VERIFY-3D graph (Fig.2) corresponded to acceptable side chain environments and the validation of the initial model was also carried out using Ramachandran plot calculations computed with the PROCHECK tool v.3.0. Analysis of the generated model indicated presence of unfavoured Ö and Ø distributions for four residues (Ala 30, Ser131, Val 136, Ser 213) in the protein structure which were not satisfactory

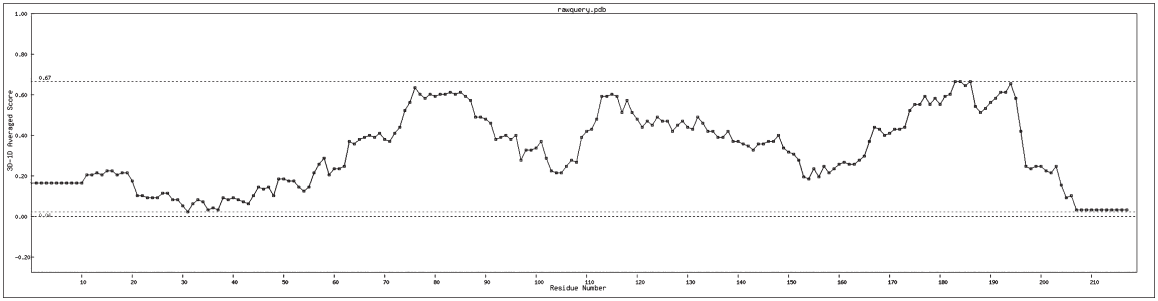

Fig. 2. VERIFY-3D graph for the target model before refinement

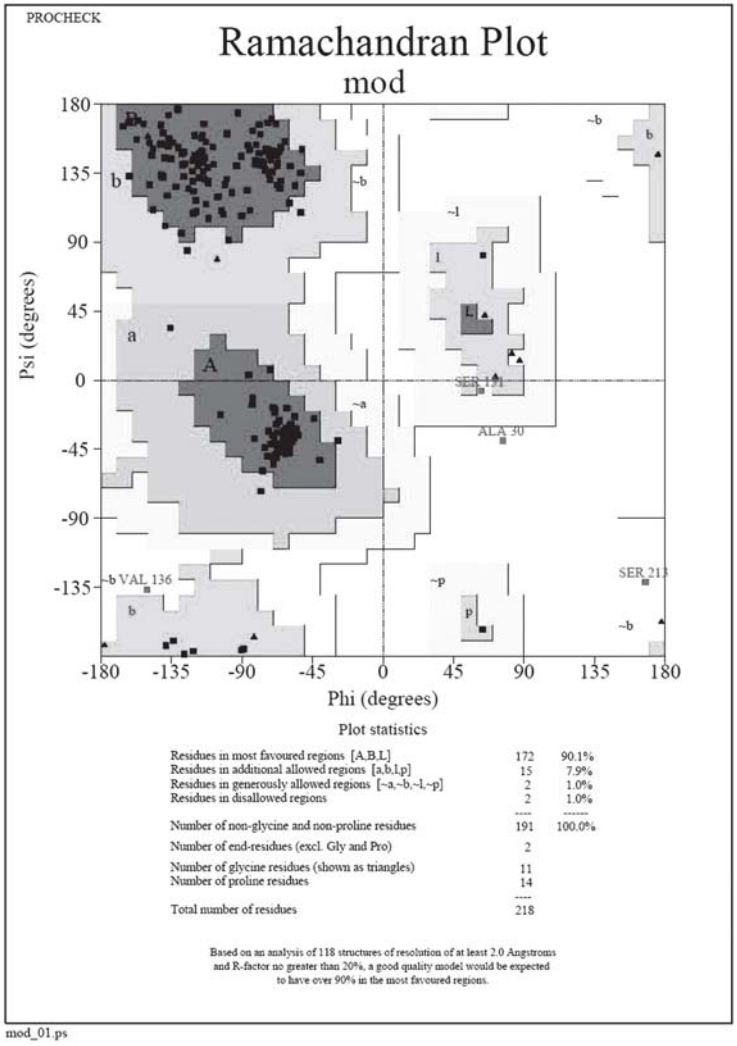

Fig. 3. Ramachandran Plot for the target model before refinement

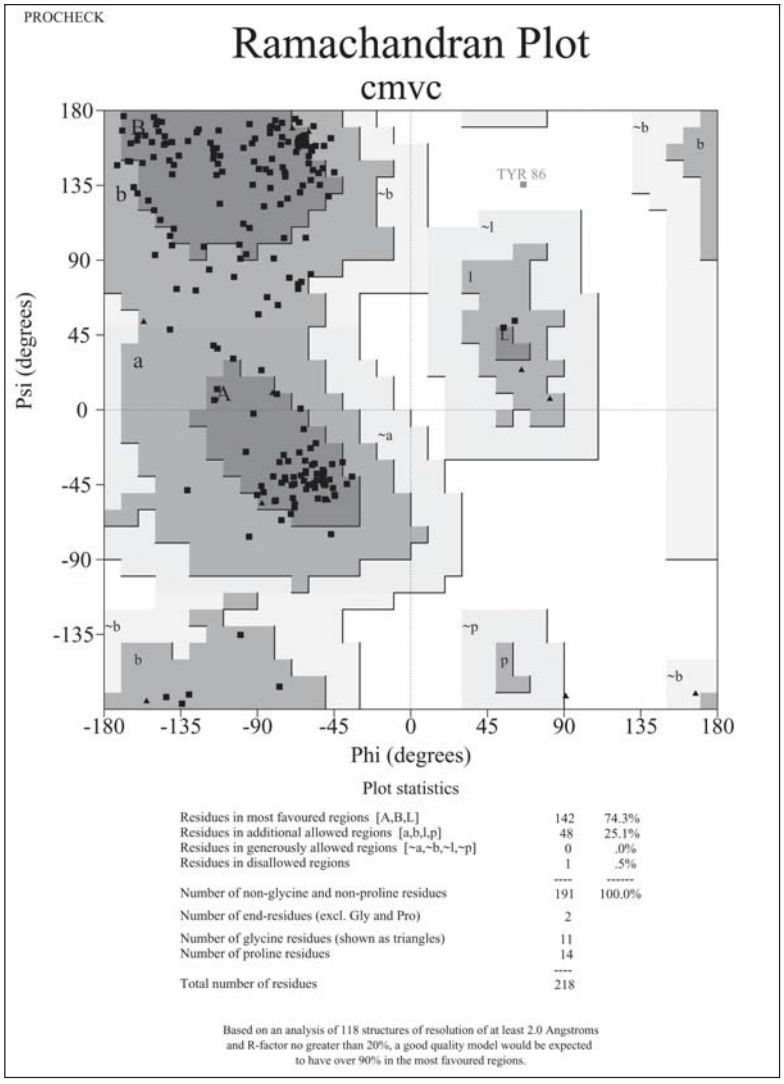

Fig. 4. Ramachandran Plot for the target model after refinement

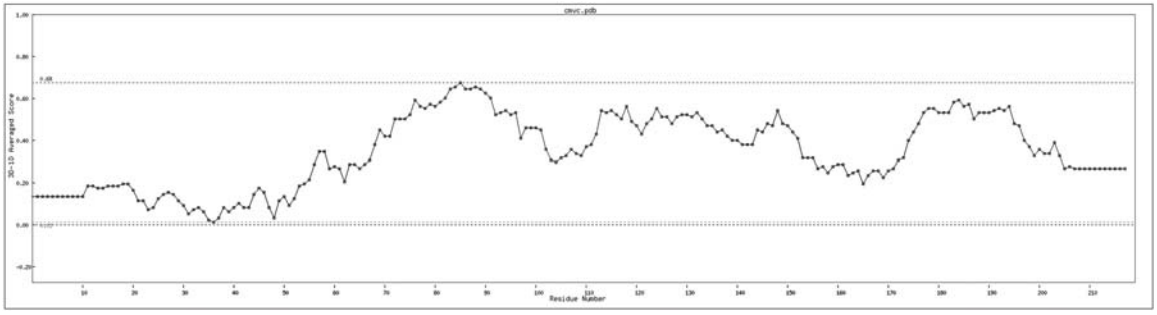

Fig. 5. VERIFY-3D graph for the target model after refinement

and hence considered for loop modeling Fig.3. When the modeled loop was inserted, it affected the complete structure and conformation of the molecule. Further, no suitable structural fragment was available to model these residue regions from the viral coat proteins. Therefore, a fragment outside the family was explored. The search was made using LOOP DATA BASE option in the SWISS PROTEIN DATABANK VIEWER software suite; http://www.expasy.org/spdbv. This database has been built by a large set of high-resolution protein structural fragments and one best segment was chosen. This model was again subjected to energy minimization described above. After refinement, the model was again validated by submitting to Verify3D, PROCHECK and Rampage as described above. The Ö and Ø distributions of the Ramachandran plots of non-glycine, non-proline residues after refinement are summarized

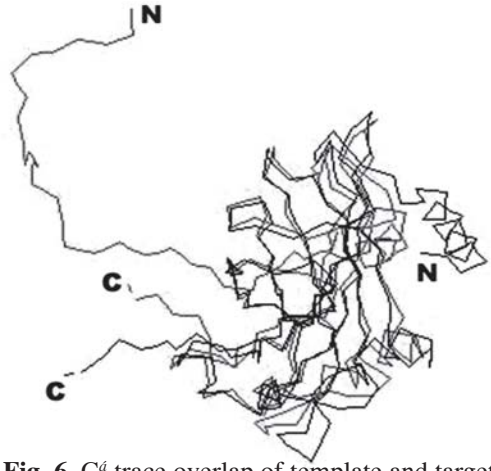

Fig. 6. C$^{\alpha}$ trace overlap of template and target protein using SPDBV software

Fig. 7. Joy alignment of the template structure and the target model

in Fig.4. Altogether 99.5% of the residues was in favored and allowed regions. The overall PROCHECK G-factor was - 0.35 and VERIFY-3D environment profile was good Fig.5. By the validation of the template, it was found that the template itself had 10 bad contacts in PROCHECK analysis and the environment profile in the Verify 3D was below the compatible score for the residues 1-10 and 16 which we have refined in our modeling experiment. Only one residue Tyr 86 showed deviation from Ramachandran plot in the refined model due to change in the angle of side chain planar group that is negligible. The molecular dynamics simulation was run using the standard NVT ensemble and NPE algorithm of MOE package V 2008.10, saving position velocity and acceleration every 0.5 picoseconds and 200 iterations every time. To attain stability of the protein 200 X 10 iterations were essential.

***Superimposition of 1f15 c with target model*:** The structural superimposition of C^{α} trace of template and target protein is shown in Fig.6. The weighted root mean square deviation of C^{α} trace between the template and final refined model was 1.16 Å with a significance score of 27.2. The RMS deviation between the modeled structure and the template was a little bit high because the template itself was analyzed to have 10 bad contacts in PROCHECK analysis which were refined in the modeled structure. This model was used for the construction of empty virion and also for the further process.

***Secondary structure prediction*:** The amino acid sequences of template and final modeled structures are generated using JOY server (protein sequence-structure representation and analysis (9), were aligned using CLUSTALW (not shown here). Given their PDB files, secondary structures were also analyzed and compared by the JOY program. The secondary structures of template and final modeled structures are highly conserved except in region between 1-28 (due to lack of residues in the structure which showed that final structure is highly reliable as shown in Fig.7).

***Capsomere subunit construction and virion building*:** Since the target model was also a strain of *Cucumber mosaic virus*, that was a trimer, the present modeled structure also being a strain of *Cucumber mosaic virus*, we tried to generate the homotrimer as that of the target structure. This trimer is the basic unit of generating the virion. Homotrimer was generated using the iterative magic fit algorithm of the SPDBV V4.0.1. The modeled polypeptide was used to generate the chains a,b,c of the homotrimer as that of the template chain a 62-218, chain b 29-218, chain c 28-218 residues respectively. The unwanted residues were excised out using the template as the reference. These three polypeptide chains prepared were individually fit on the template using iterative magic fit algorithm of the SPDBV

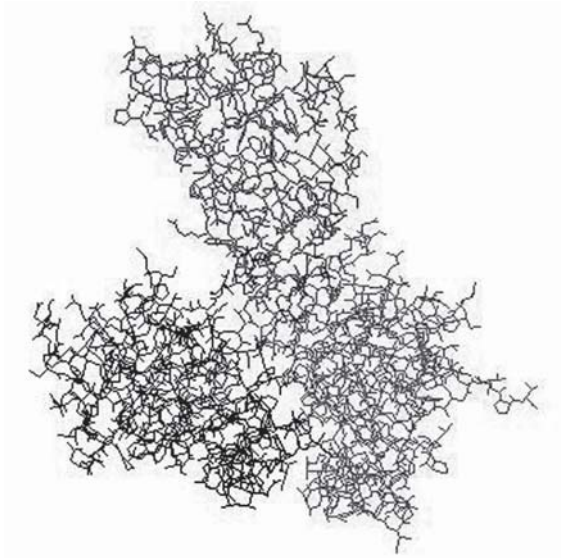

Fig. 8. Homo Trimer generated from the modeled structure

software suite. The three polypeptide chains fitted resembled as that of the template trimer. Later, the background template was removed and the three chains were merged into a homotrimer subunit Fig.8. This subunit was used to generate the empty virion molecule by applying the crystallographic rotational symmetries as that of the template molecule Fig.9. This method is rather tricky and worked with our target protein. After this, the model along with all the architectural features was submitted to the PDB theoretical model archive with identification code 2IKA.

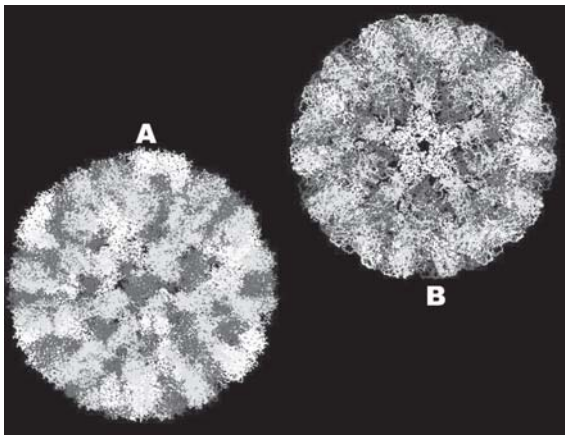

Fig. 9. Virion structure generated from the homotrimer a) Virion without side chains b) Virion with side chains

Discussion

Understanding of the Virion architecture and coat protein subunit interactions is a core area in the field of Virological research (3), the virion are built from protein subunits in a definite architectural manner which gives an important example for protein-protein interactions. Using the MODELLER software we tried to build a model and obtained a refined model after loop modeling and energy minimization. The final refined model was further assessed by VERIFY-3D and PROCHECK program, and the results show that this model is reliable. The stable structure is further used for empty virion particle generation to understand the arrangement of the protein subunits in the virion particle. Even though there are many servers available over internet that will perform the protein modeling

Table 1. Results from the Fugue sever confirming the template 1F15

Profile Hit	PLEN	RVN	RAWS	ZSCORE	ZORI	AL
Cucumo_coat	176	745	847	48.72	49.69	00 CERTAIN
hs1f15a	157	697	803	40.61	41.57	00 CERTAIN
hs1pi1a	185	-90	89	3.82	5.45	00 MARGINAL

Recommended cutoff : ZSCORE >= 6.0 (CERTAIN 99% confidence)
Other cutoff : ZSCORE >= 4.0 (LIKELY 95% confidence)
Other cutoff : ZSCORE >= 3.5 (MARGINAL 90% confidence)
Other cutoff : ZSCORE >= 2.0 (GUESS 50% confidence)
Other cutoff : ZSCORE < 2.0 (UNCERTAIN)
PLEN : Profile length
RAWS : Raw alignment score
RVN : (Raw score)-(Raw score for NULL model)
ZSCORE : Z-score normalized by sequence divergence
ZORI : Original Z-score (before normalization)
AL : Alignment algorithm used for Zscore/Alignment calculation

Table 2. Options used in Modeller program

INCLUDE	#	Include the predefined TOP routines
SET OUTPUT_CONTROL	=	1 1 1 1 1
SET MAXRES	=	300
SET ALNFILE	=	'query'
SET KNOWNS	=	'cmv'
SET SEQUENCE	=	'query'
SET ATOM_FILES_DIRECTORY	=	'./:../atom_files'
SET HETATM_IO	=	Off
SET STARTING_MODEL	=	1
SET ENDING_MODEL	=	20
CALL ROUTINE	=	'model'

such as Phyre, Swiss model server etc., the procedure defined here could of use to take care of each and every residue in the target protein structure to be modeled. Further the technique used to generate the homotrimer subunit proved to be advantageous in generating the biomolecular structures with distinct chains and single template structure. However, the chance of success of this technique depends on the modeling target and its template molecule.

Conclusions

Structure of coat protein of *Cucumber mosaic virus* infecting banana is modeled. A largely defined manual procedure for protein modeling is defined that can be made to use for other structures. Additionally, the complete virion structure is generated from the modeled structure. This principle of generation of trimer from modeled monomer and also generation of the virion molecule could also be used in generating the biomolecular structures with distinct chains and single template structure. The chance of success of this technique depends on the modeling target and its template molecule.

References

1. Avgelis, A. (1987). Cucumber mosaic virus on banana in crete.J. *Phytopathology*, 120: 20-24.

2. Ákos Gellért, Katalin Salánki, Gábor Náray-Szabó and Ervin Balázs. (2006). Homology modeling and protein structure based functional analysis of five cucumovirus coat proteins, 24: 319-327.

3. Baker, T. S., Drak, J. and Bina, M. (1988). "Reconstruction of the three-dimensional structure of simian virus 40 and visualization of chromatin core", Proc. Natl. Acad. Sci. USA, 85:422-426.

4. Eswar, N., Marti-Renom, M. A., Webb, B., Madhusudhan, M. S., Eramian, D., Shen, M., Pieper, U. and Sali, A. (2006). Comparative Protein Structure Modeling With MODELLER. Current Protocols in Bioinformatics, John Wiley & Sons, Inc., Supplement 15, 5.6.1-5.6.30.

5. Guex, N. and Peitsch, M. C. (1997). SWISS-MODEL and the Swiss-PdbViewer: an environment for comparative protein modeling. Electrophoresis 18: 2714-2723.

6. J. Shi, Blundell, T.L. and Mizuguchi, K. (2001) Fugue: Sequence-structure Homology Recognition using Environment-specific substitution Tables and structure-dependent Gap penalities. Journal of Molecular biology. 310:243-257.

7. Laskoswki, R. A., MacArthur, M. W., Moss, D. S. and Thornton, J. M. (1993). PROCHECK: a program to check the stereochemical quality of protein structures. J. Appl. Cryst. 26: 283-291.

8. Lüthy, R., Bowie, J. U. and Eisenberg, D. (1992). Assessment of protein models with three-dimensional profiles. Nature 356: 83-85.

9. Mizuguchi, K., Deane, C. M., Blundell, T. L., Johnson, M. S. and Overington, J. P. (1998). JOY: protein sequence-structure representation and analysis. Bioinformatics 14: 617-623.

10. Naydu M.V. (2007). Plant Virology, First Edition. Tata McGraw-Hill Publishers. pp 89.

11. Powell, M. J. D. (1977). Restart procedures for the conjugate gradient method. Math. Program. 12: 241-254.

12. Roger Hull (2000). Matthews Plant Virology, Fourth edition. Academic press. pp 109 – 169.

13. Sali, A. and Blundell, T. L. (1993). Comparative protein modelling by satisfaction of spatial restraints. J. Mol. Biol. 234: 779-81.

Current Trends in Biotechnology and Pharmacy
Vol. 5 (4) 1424-1433 October 2011, ISSN 0973-8916 (Print), 2230-7303 (Online)

Culture Conditions for the Production of Cellulase from Novel Fungus *Gliomastix indicus*

Richa Tyagi, Swati Allen and Ashima Kapoor*
Department of Biotechnology
Meerut Institute of Engineering & Technology, Meerut, India
*For Correspondence - ashimakapoor28@rediffmail.com

Abstract

Gliomastix indicus MTCC 3869, a novel fungus, isolated from wasteland soil sample and has never been exploited for production of industrial enzyme. Therefore in the present study, we have exploited the potential of *G. indicus* for cellulase production and optimize the physiochemical and nutritional parameters to maximize the cellulase production from the *G. indicus* under submerged fermentation conditions. The culture medium A was found to produce maximum cellulase activity (20.6 U/ml) among the four (A,B,C,D) tested media. The suitable temperature and pH of the production medium was found to be 30°C and 7.0 respectively. Among the various carbon tested, rice bran (1%) was proved to be the best carbon source. Among organic nitrogen sources, malt extract yielded maximum enzyme production whereas, inorganic nitrogenous sources did not support enzyme production. The metal ions such as Ca^{+2} increased the enzyme production. The crude cellulase was found to be optimally active at pH 6.0, exhibiting pH stability at pH 6.0 for 60 min. The optimum temperature for cellulase was found to be 30°C retaining 90% activity for 60 min. Among the additives, $CaCl_2$ had stimulating effect on cellulase activity while heavy metals were inhibitory. Tween-80, TritonX-100, β-mercaptoethanol, SDS and EDTA increased the enzyme activity whereas Tween-20 had inhibitory effect.

Key Words : Cellulase, *Gliomastix indicus,* Rice bran.

Introduction

Cellulase (a complex multienzyme system) acts collectively to hydrolyze cellulose from agricultural wastes to produce simple glucose units (1). Cellulolytic activity consists of three major components; Endo β-glucanase (E.C:3.2.1.4), Exo β-glucanase (E.C:3.2.1.91) and β-glucosidase (E.C:3.2.1.21) (2). The products are cellodextrins, cellobiose and glucose. Cellulase production has attracted a worldwide attention due to the possibility of using this enzyme complex for conversion of abundantly available renewable lignocellulose biomass for production of carbohydrates which has numerous industrial applications including bioethanol (3,4). The most promising technology for the conversion of the lignocellulosic biomass to fuel ethanol is based on the enzymatic breakdown of cellulose using cellulose enzymes (5). Cellulose microfibril fragments can be used as no calorie food additives. Hyper absorbent cellulose fibers from fragmented cellulose micro fibrils are used in biomedical and household absorbent material (6). Cellulases are also used

Vol. 5 (4) 1424-1433 October 2011, ISSN 0973-8916 (Print), 2230-7303 (Online)

in pulp and paper industry (7). They are widely applied in textile propelling to improve fabric appearance by reducing fuzz, piling and enhancing the softness, luster and color brightening of cotton fabrics (8).

Although a large number of microorganisms, including few bacteria and actinomycetes, are capable of degrading cellulose, fungi are the main cellulase producing microorganisms (9). The most common and well-studied fungal species are *Trichoderma sp., Aspergillus sp., Penicillium sp. and Humicola sp.* The major factors to exploit the commercial potential of cellulases are the yield, stability and cost of cellulase production. For above reasons, agricultural residues are used in cellulase production. Several studies have been carried out to produce cellulolytic enzymes from biowaste degradation by many micro-organisms (1,2,9).

The present study was carried out with the aim to produce cellulase from *Gliomastix indicus* MTCC 3869. The culture conditions were optimized for maximum cellulase production and some biochemical properties of cellulase were also characterized. This is the first report of enzyme production from *Gliomastix indicus.* However, it is earlier reported to be useful in bioremediation (10).

Materials and methods

Organism and Culture medium *:* The fungal culture *Gliomastix indicus* MTCC 3869 was isolated from a wasteland soil sample collected at Tiruchengode, Tamilnadu (11). The fungus was maintained on malt extract medium which consists of malt extract (2%), K_2HPO_4 (0.1%), NH_4Cl (0.1%) and agar (2%). For enzyme production, this medium was supplemented with 1% cellulose.

Inoculum preparation : To prepare the inoculum the fungus was grown on malt extract medium plates for 48 hr at 30°C. The hyphal discs of 0.8cm diameter from the freshly grown culture were cut (12). Each disc was used to inoculate 30ml medium.

Cellulase production : Cellulolytic nature of *Gliomastix indicus* was confirmed by observing the zone of hydrolysis around the growth of the culture on malt extract agar plates (malt extract medium supplemented with 1% cellulose). To determine extracellular cellulase production the culture was inoculated in production medium and grown at 30°C for 4 days in stationary condition. After incubation the culture was centrifuged at 8,000xg for 10 min at 4°C. The culture supernatant was used as crude enzyme and the cellulase activity was determined by performing cellulase assay.

Estimation of cellulase activity : Cellulase activity was determined using cellulose (1% w/v) as the substrate. The reaction mixture containing 1 ml substrate prepared in 0.1 M acetate buffer (pH 5.5) and 10 µl of enzyme solution was incubated for 20 minutes at 30°C in a water bath. The reaction was terminated by adding 1.0 ml 3, 5-dinitrosalicylic acid (DNSA) reagent (13). This was followed by boiling the reaction mixture for 10 min in a boiling water bath and thereafter, allowing it to cool to room temperature. The colour of the resultant mixture was detected at 550 nm against the reagent blank (reaction mixture without enzyme) and enzyme control (reaction mixture with boiled enzyme) under similar conditions.

One unit (U) of cellulase activity was defined as the amount of enzyme required to release 1µmole of glucose per ml per min under the assay conditions.

Biomass determination : To determine the fungal biomass the culture was centrifuged at 8,000xg for 10 min at 4°C and the pellet was

washed twice with distilled water. The washed mycelium was dried at 60°C for 24 hr in a pre weighed dry petridish to constant weight and expressed as g dry weight /30 ml medium.

Optimization of culture conditions for cellulase production : The following culture conditions were optimized to obtain maximum yield of cellulase from *Gliomastix indicus*.

Medium for enzyme production : To screen the medium for maximum cellulase production various production medium viz. medium A, B, C and D were tested. The composition of different medium were as follows: Medium A: Malt extract medium supplemented with 1% cellulose; Medium B: $NaNO_3$ (0.2%), K_2HPO_4 (0.1%), $MgSO_4.7H_2O$ (0.05%), KCl (0.05%), $FeSO_4.7H_2O$ (0.01%), cellulose (1.0%) (14); Medium C: NH_4NO_3 (0.14%), KH_2PO_4 (0.2%), $CaCl_2$ (0.03%), $MgSO_4$ (0.03%), protease peptone (0.75%), $FeSO_4$ (0.05%), $MnSO_4$ (0.16%), $ZnSO_4$ (0.14%), Tween-80 (2ml), cellulose (1.0%) (9); Medium D: CMC (1.0%), $NaNO_3$ (0.65%), K_2HPO_4 (0.65%), yeast extract (0.03%), KCl (0.65%), $MgSO_4.7H_2O$ (0.30%) (15).

Incubation period : To study the effect of incubation period, the fungal culture was inoculated in medium A and incubated at 30°C for 5 days in stationary condition. The samples were harvested at regular intervals of 24 hour and cell growth (biomass) as well as enzyme activity was measured.

Temperature and pH for enzyme production : The effect of incubation temperature on cellulase production was studied by growing the culture at temperatures 30° to 50°C. The effect of initial pH of the medium was studied by inoculating the inoculum of *Gliomastix indicus* in medium A of different pH ranging from 5.0-8.0 and incubated at 30°C for 3 days. After incubation in these conditions cellulase activity was determined from the culture filtrate.

Carbon source : The different carbon sources (1% w/v) viz. cellulose and lignocellulosic agro-residues like wheat straw, rice straw, corn cob, sugarcane bagasse, rice bran and sugars such as lactose, glucose and sucrose were tested. The production medium supplemented with these carbon sources was inoculated with the culture and incubated at 30°C. Cellulase activity and biomass was estimated after 72 hours. The lignocellulosic substrates were washed with distilled water to remove dust and solubles, dried at 60°C to remove moisture for 24 hour and then finely ground.

Nitrogen source : Different organic and inorganic nitrogen supplements such as malt extract, peptone, beef extract, yeast extract, tryptone, urea, $(NH_4)_2SO_4$, NH_4NO_3, NH_4Cl, were tested to achieve enhanced cellulase production.

Effect of metal ions : The effect of metal ions on enzyme production was studied by adding different salts (0.1% w/v) viz. Na^+, K^+, Ca^{+2} Mg^{+2}, Hg^{+2} and Fe^{+3} in the production medium. After incubation of the culture in these conditions, cellulase activity was determined from the culture filterate.

Biochemical characterization of enzyme

Determination of end product : The end product of cellulose hydrolysis by cellulase from *Gliomastix indicus* was analyzed by thin layer chromatography (TLC) on silica gel G, using the solvent system composed of ethyl acetate, acetic acid, formic acid and water (9:3:1:4 v/v), according to Goulart *et al.* (16). The hydrolytic product was detected with 0.2% orcinol (w/v) in sulfuric acid and methanol (10:90 v/v). Glucose was used as standard.

***Temperature optima and thermal stability*:** The temperature optima of crude cellulase produced by *G. indicus* was determined by incubating the enzyme with substrate for 20 min at various temperatures ranging from 25°C to 55°C. To determine the thermal stability, the enzyme was incubated in the standard buffer at 30°C and the enzyme activity was determined upto 90 min.

***pH optima and pH stability*:** To determine the pH optima, the enzyme was incubated with substrate in the buffers of different pH ranging from 5.5 to 8.0. Further, the enzyme was incubated in the buffer of pH 6.0 at 30°C and the activity was determined at regular intervals upto 120 min.

***Effect of metal ions and detergents*:** The effect of different additives on cellulase activity was determined by incubating the enzyme with substrate and additives (1mM) viz. NaCl, KCl, $CaCl_2$, $HgCl_2$, $MgCl_2$, $FeCl_3$, SDS (sodium dodecyl sulphate), EDTA, Tween-20, Tween-80, Triton X-100 and β-mercaptoethanol.

All the fermentations and assays were carried out in triplicate and the mean value was presented.

Results and discussion

***Cellulolytic potential of Gliomastix indicus*:** The cellulolytic capability of the fungus *G. indicus* was assessed on malt extract agar plate containing 1% cellulose where a clear zone of cellulose hydrolysis around the colony was observed. Further cellulase activity of the culture was estimated in malt extract liquid medium (medium A) supplemented with 1% cellulose at 30°C for 5 days and it was estimated to be 20.6 U/ml.

Optimization of culture conditions for cellulase production

***Screening of medium for maximum cellulase production by Gliomastix indicus* :** We have observed about 2.7 fold differences in cellulase activity when various production medium were used for cellulase production. Among the different medium tested viz. medium A, B, C and D, growth as well as enzyme production was found to be maximum in medium A (20.6 U/ml), followed by medium D and C (Table 1) and the minimum enzyme production was observed in medium B. The differential cellulase activity in different medium showed the dependence of the fungus on nitrogen sources like malt extract, yeast extract etc. These results were in accordance to the observations reported in Table 5.

***Effect of incubation period* :** Enzyme activity and cell growth of *Gliomastix indicus* on medium A was measured periodically, over a period of 5 days. Maximum cellulase production of 25.6 U/ml and growth was recorded at 72 h of incubation (Fig 1). Thereafter, both enzyme activity and cell growth started declining. The optimum incubation period of 72h for production of fungal cellulases has been reported by many workers (14, 17, 18, 20).

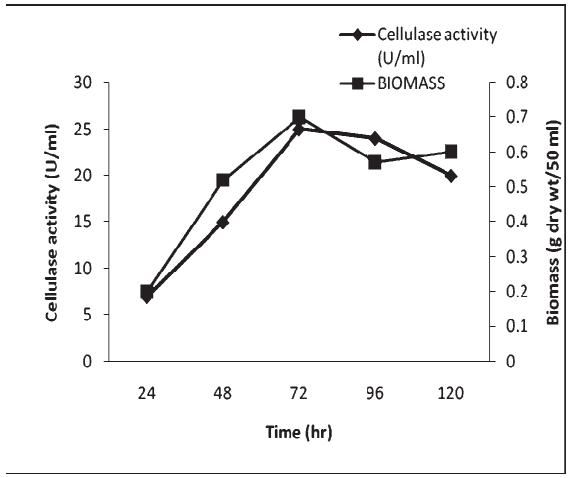

Fig 1. Effect of incubation period on growth and enzyme production

Vol. 5 (4) 1424-1433 October 2011, ISSN 0973-8916 (Print), 2230-7303 (Online)

***Effect of pH and incubation temperature*:** The growth as well as cellulase production was found to be maximum in the production medium of pH 7.0, indicating the culture is active at neutral pH (Table 2). Cellulase activity was significantly decreased in acidic and basic medium. Cellulase production by *G. indicus* was compared under various temperatures. Incubation temperature above or below 30°C was unfavourable for enzyme production (Table 3). The optimum temperature for fungal cellulases ranges from species to species, however in most cases the incubation temperature ranges from 28° to 35°C (17, 19, 21, 22).

***Effect of different carbon sources on cellulase production*:** Cellulase production by utilizing cheap lignocellulosic waste is a cost effective strategy. With this view, different agro residues (1%) such as wheat straw, rice straw, corn cob, sugarcane bagasse and rice bran were tested as carbon source with cellulose as control. The growth as well as cellulase production increased markedly using rice bran as carbon source (Table 4). Other agro-residues also induced appreciable amount of cellulase production. Milala et al. reported rice husk to be a good carbon source for production of cellulase by Aspergillus niger (1). Rice straw and wheat bran were reported to be better carbon source by Trichoderma viride ZY-01 for cellulase production (18). Similarly, Chandra et al. reported wheat bran to act as maximum cellulolytic enzyme producing carbon source (14). Pea peel waste, whey and wheat starch hydrolysates were also reported as potential substrate for cellulase production by Trichoderma reesei (22). The use of agro residues as a substrate makes the process of enzyme production economic as well as provides an alternative for the utilization of large amount of agro residues produced per year.

Sugars like lactose, glucose, sucrose were also tested as carbon source. However, sugars do not support the growth as well as enzyme production.

***Effect of nitrogen source*:** The effect of nitrogen source on microbial growth and release of hydrolytic enzymes is well established. Hence, various organic and inorganic nitrogenous source were supplemented in medium A to study the effect of nitrogen source on cellulolytic enzyme production by *G. indicus*. As shown in Table 5, malt extract at 1% concentration exhibited marked increase in cellulase production. Further, the effectiveness of nitrogen source in supporting cellulase production decreased in the following order: tryptone> yeast extract> malt extract (2%)> peptone. Inorganic salts including $(NH_4)_2SO_4$, NH_4NO_3, NH_4Cl, and organic sources namely beef extract and urea were the poor nitrogen sources. The dependence of the fungus on organic nitrogenous sources for growth and enzyme production was also observed in Table 1.

Cellulase production by *Aspergillus niger* was found to be maximum using urea and peptone as nitrogen source (23). Sun *et al.* (21) observed corn steep solid followed with peptone as the best nitrogen source for cellulase production by *Trichoderma* sp., inorganic nitrogenous salts did not support enzyme production.

***Effect of metal ions*:** The effect of different metal ions on production of cellulase enzyme was studied by adding different salts such as NaCl, KCl, $CaCl_2$, $MgCl_2$, $HgCl_2$, $FeCl_3$ in the production medium. The maximum yield of cellulase was found with Ca^{+2} (Table 6).

Biochemical properties of cellulase

***Analysis of hydrolytic product by TLC*:** The hydrolytic product from the action of cellulase on cellulose was analyzed by thin layer chromatography and the result was shown in Fig

Table 1. Screening of media for maximum production of cellulase by *Gliomastix indicus*

Media	Cellulase activity (U/ ml)
Medium A	20.6 (0.75)
Medium B	7.6 (0.18)
Medium C	10.2 (0.68)
Medium D	15.3 (0.55)

Values in parenthesis represents biomass (g dry wt./30 ml)

Table 2. Effect of pH on cellulase production

pH	Cellulase activity(U/ml)
5.0	18.0 (0.40)
6.0	22.1 (0.58)
7.0	30.1 (0.72)
8.0	18.0 (0.46)

Values in parenthesis represents biomass (g dry wt./30ml)

Table 3. Effect of temperature on enzyme production

Temperature (^oC)	Cellulase activity(U/ml)
30	28.0 (0.69)
35	18.0 (0.35)
40	10.0 (0.22)
45	N.D. (0.0)
50	N.D. (0.0)

N.D. = Not Detectable

Values in parenthesis represents biomass (g dry wt./30ml)

Table 4. Effect of carbon source

Carbon Source	Cellulase activity(U/ml)
Cellulose (control)	27.8 (0.66)
Wheat straw	30.0 (1.18)
Rice straw	26.3 (1.29)
Corn cob	30.8 (1.28)
Sugarcane bagasse	31.2 (1.65)
Rice bran	39.8 (1.32)
Lactose	6.2 (0.16)
Glucose	-- (0.0)
Sucrose	2.3 (0.11)

Values in parenthesis represents biomass (g dry wt./30ml)

Table 5. Effect of nitrogen source

Nitrogen Source (1%)	Cellulase activity(U/ml)
Malt extract (control) (2%)	36.6 (1.86)
Malt extract	44.3 (1.08)
Peptone	30.0 (1.24)
Tryptone	38.6 (2.32)
Yeast extract	36.3 (1.28)
Beef extract	25.6 (1.96)
Urea	26.6 (1.06)
NH_4Cl (0.1%)	15.6 (0.96)
$(NH_4)_2SO_4$ (0.1%)	20.8 (0.83)
NH_4NO_3 (0.1%)	16.3 (0.83)

Values in parenthesis represents biomass (g dry wt./30ml)

2. The incubation of enzyme with cellulose for 2 hr produced mainly glucose as end product. The results were in accordance to that reported by Allardyce and Linton (24) and Karnchanatat *et al.* (25).

***Temperature optima and thermal stability*:** The optimum temperature for crude cellulase was found to be 30°C (Fig 3). Further, The thermostability of the enzyme was studied by incubating the enzyme at 30°C for 2 hr. As a result, the enzyme retained 90% of its original activity upto 1 hr of incubation (Fig 4). Thereafter, the stability of the enzyme decreased sharply with total loss after 90 min.

***pH optima and pH stability* :** The pH optima of crude cellulase was 6.0. However, it was found to be active in the pH range of 5.5 to 7.0 (Fig 5). Karnchanatat *et al.* also reported similar pH optima for cellulase produced by the fungus wood-decaying fungus *Daldinia eschscholzii* (25).

For the application of cellulase in industries, screening criteria for cellulases from diverse microbial strains involves better thermostability and higher pH stability. The cellulase from *G. indicus* was stable at pH 6.0 for 60 min retaining 85% activity (Fig 6). Similarly, cellulase from

Fig 2. Analysis of hydrolytic product by TLC

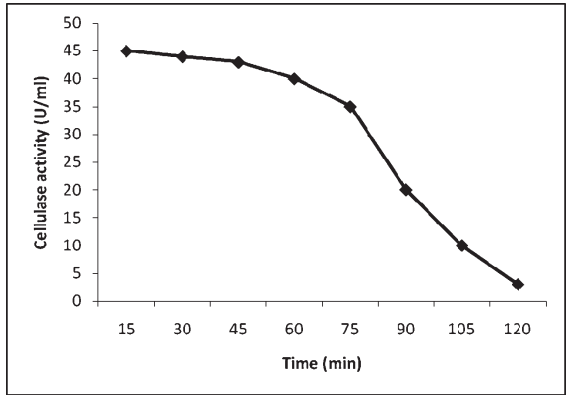

Fig 4. Temperature stability of crude cellulase by *G. indicus* at 30°C

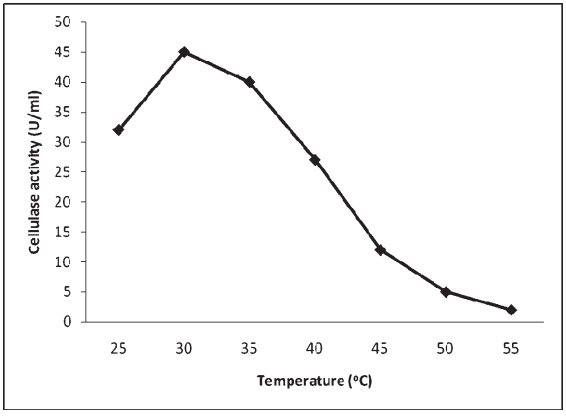

Fig 3. Temperature optima of crude cellulase from *G. indicus*

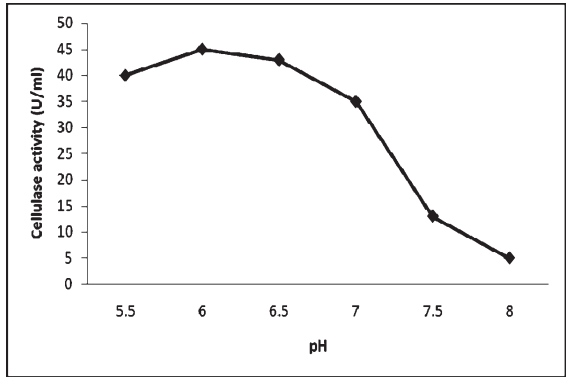

Fig 5. pH optima of crude cellulase

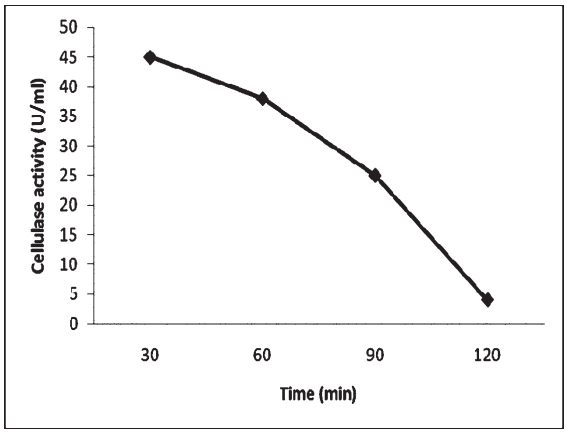

Fig 6. pH Stability of crude cellulase by *G. indicus* at pH 6.0

the yeast *Rhodotorula glutinis* was found to be stable in acidic pH range at 30°C when incubated for 60 min (26).

***Effect of additives*:** The effect of different salts, detergents and chelators was seen on cellulase activity. It was observed that $CaCl_2$ had stimulatory effect while $HgCl_2$ and $FeCl_3$ were inhibitory for cellulase activity. Similarly, Tween-80, TritonX-100, β-mercaptoethanol, SDS and EDTA increased the enzyme activity whereas Tween-20 had inhibitory effect (Table 7). The cellulase from *Daldinia eschscholzii* was significantly inhibited by Hg^{2+}, Cu^{2+}, and Fe^{2+}, and stimulated by Ca^{2+}, Mg^{2+} and EDTA (25, 27). In contrast, SDS was found to inhibit the activity of cellulase by *Aspergillus awamorii* VTCC-F099 (27) and *Aspergillus oryzae* (28).

Conclusion

The optimization of the culture conditions enhanced the level of cellulase production from *Gliomastix indicus* to about two-fold. Further, the results of the investigation highlight the industrial potential of the extracellular cellulase from *G. indicus* because of its yield, economic production using agro-residue and biochemical properties which are suitable for its use in food industry.

Acknowledgement

The authors express sincere gratitude to Prof. A. Subrahmanyam, Head, Department of Biotechnology, Meerut Institute of Engineering and Technology (MIET), Meerut, for providing the fungal culture of *Gliomastix indicus.*

Table 6. Effect of metal ions on enzyme production

Metal ions (0.1%)	Cellulase activity (U/ml)
Control	45.3
Na^+	44.3
K^+	42.8
Ca^{+2}	50.0
Mg^{+2}	30.3
Hg^{+2}	10.0
Fe^{+3}	36.0

Table 7. Effect of additives on cellulase activity

Additives (1mM)	**Cellulase activity (U/ml)**	**Relative activity (%)**
Control (0.1%)	44.8	100
NaCl	42.0	93.74
KCl	41.0	91.43
$CaCl_2$	50.0	111.5
$HgCl_2$	9.2	20.51
$MgCl_2$	41.0	91.43
$FeCl_3$	35.6	79.38
SDS	48.8	107.26
EDTA	47.3	105.47
Tween-20	16.7	37.24
Tween-80	49.2	109.71
Triton X- 100	53.1	118.41
β-mercaptoethanol	46.3	103.24

Vol. 5 (4) 1424-1433 October 2011, ISSN 0973-8916 (Print), 2230-7303 (Online)

References

1. Milala, M.A., Shugaba, A., Gidado, A., Ene, A.C. and Wafer J.A. (2005). Studies on the use of agriculture wastes for celluase enzyme production by *Aspergillus niger*. Res. J. Agri. Biol. Sci. 1(4): 325-328.

2. Beguin, P. and Aubert, J.P. (1994). The biological degradation of cellulose. FEMS Microbiol. Rev. 13: 25-58.

3. Gadgil, N.J., Daginawala, H.F., Chakarbarti, T. and Khanna, P. (1995). Enhanced cellulase production by a mutant of *Trichoderma reesei*. Enz. Microb. Technol. 17(10): 942-946.

4. Hayward, T.K., Hamilton, J., Tholudur, A. and McMillan, J.D. (2000). Improvements in titre, productivity and yield using solka-floc for cellulase production. Appl. Biochem. Biotechnol. 84-86(1-9): 859-874.

5. Ahmed, S., Bashir A., Saleem H., Saadia M., and Jamil A. (2009). Production and purification of cellulose degrading enzymes from a filamentous fungus *Tricoderma harzianum.* Pakistan J. Bot. 41(3): 1411-1419.

6. Winkelmann, G. (1992). Degradation of Natural Products .VCH Verlagsgesellschaft mbH, Weinheim, Germany.

7. Yinbo, Q., Peiji G., Dong, W., Xi, Z. and Xiao, Z. (1996). Production, characterization and application of cellulase-free xylanase from *Aspergillus niger*. Appl. Biochem. Biotechnol. 58: 375-381.

8. Ohmiya, K., Sakka, K., Karita, S. and Kimura, T. (1997). Structure of cellulases and their applications. Biotechnol. Genet. Eng. Rev. 14: 365-413.

9. Immanuel, G., Akila Bhagavath, C.M., Iyappa Raj, P., Esakkiraj, P. and Palavesam, A. (2007). Production and partial purification of cellulase by *Aspergillus niger* and *A. fumigatus* fermented in coir waste and sawdust. The Internet Journal of Microbiology. 3(1).

10. Singh, R.K., Kumar, S., Kumar, S. and Kumar, A. (2008). Biodegradation kinetic studies for removal of p-cresol from waste water using *Gliomastix indicus* MTCC 3869. Biochem Engg. J. 40: 293-303.

11. Nagalakshmi, S., Vijayalakshmi, M. and Subrahmanyam, A. (2009). *Gliomastix indicus sp. nov.* Curr. Trends Biotechnol. Pharm. 3(1): 111-112.

12. Ray, R.R. and Chkraverty, R. (1998). Extracellular α - amylase from *Syncephalastrum racemosum*. Mycol. Res. 102: 1563-1567

13. Miller, G.L. (1959). Use of dinitrosalicylic acid for determination of reducing sugar. Anal. Chem. 31: 426-429.

14. Chandra, S.M., Viswanath, B. and Reddy, B.R. (2007). Cellulolytic enzymes on lignocelluloses substrate in solid state fermentation by *A. niger*. Indian J. Microbiol. 47: 322-328.

15. Peciulyte, D. (2007). Isolation of cellulolytic fungi from waste paper gradual recycling materials. Ekolo-gija 53(4): 11-18.

16. Goulart, A.J., Carmona, E.C. and Rubens, M. (2005). Partial purification and properties of cellulase free alkaline xylanase produced by *Rhizopus stolonifer* in solid state fermentation. Brazilian Arch. Biol. Technol. 48: 327-333.

17. Singhania, R.R., Sukumaran, R., Pillai, A., Prema, P., Szakacs, G. and Panday, A. (2006). Solid state fermentation of lignocelluloses substrates for cellulase production by *Trichoderma reesei* NRRL 11460. Indian J. Biotechnol. 5: 337-345.

18. Benkun, Q., Risheng, Y., Ying, Y. and Yuan, C. (2007). Influence of different ratios of rice straw to wheat bran on production of cellulolytic enzymes by *Trichoderma viride* ZY-01 in solid state fermentation. Electronic J. Environ. Agri. Food Chem. 6(9): 2341-2349.

19. Sohail, M., Siddiqui, R., Ahmed, A. and Khan, S.A. (2009). Cellulase production from *Aspergillus niger* MS82: effect of temperature and pH. New Biotechnol. 25(6): 437-441.

20. Chinedu, S.N., Eni, A.O., Adeniyi, A.I. and Ayangbemi, J.A. (2010). Assessment of growth and cellulase production of wild-type microfungi isolated from Ota, Nigeria. Asian J. Plant Sci. 9: 118-125.

21. Sun, H., Ge, X., Hao, Z. and Peng, M. (2010). Cellulase production by *Trichoderma* sp. on apple pomace under solid state fermentation. African J. Biotechnol. 9(2): 163-166.

22. Verma, N., Bansal, M.C. and Kumar, V. (2011). Pea peel waste: a lignocellulosic waste and its utility in cellulase production by *Trichoderma reesei* under solid state cultivation. Bioresources 6(2): 1505-1519.

23. Narasimha, G., Sridevi, A., Viswanath, B., Subhash, C.M. and Reddy, R.B. (2006). Nutrient effects on production of cellulolytic enzymes by *Aspergillus niger*. African J. Biotechnol. 5(5): 472-476.

24. Allardyce, B. J. and Linton, S.M. (2008). Purification and characterisation of endo -1,4-glucanase and laminarinase enzymes from the gecarcinid land crab *Gecarcoidea natalis* and the aquatic crayfish *Cherax destructor*. The J. Exptl. Biol. 211: 2275-2287.

25. Karnchanatat, A., Petsom, A., Sangvanich, P., Piapukiewb, J., Whalley, A.J.S., Reynolds, C.D., Gaddd, G.M. and Sihanonth, P. (2008). A novel thermostable endoglucanase from the wood-decaying fungus *Daldinia eschscholzii* (Ehrenb.:Fr.) Rehm., Enz. Microb. Technol. 42: 404–413.

26. Oikawa, T., Tsukagawa, Y. and Soda, K. (1998). Endo-ß-glucanase secreted by a psychrotrophic yeast: purification and characterization. Biotechnol. Biochem. 62: 1751-1756.

27. Nguyen, V.T. and Quyen, D.T. (2010). Purification and properties of a novel thermoactive endoglucanase from *Aspergillus awamori* VTCC-F099. Australian J. Basic Appl. Sci. 4(12): 6211-6216.

28. Riou, C., Salmon, J., Valier, M., Günata, Z. and Barre, P. (1998). Purification, characterization and substrate specificity of a novel highly glucose-tolerant ß-glucosidase from *Aspergillus oryzae*. Appl. Environ. Microbiol. 64: 3607-3614.

Current Trends in Biotechnology and Pharmacy
Vol. 5 (4) 1434-1444 October 2011, ISSN 0973-8916 (Print), 2230-7303 (Online)

Sustainable Bioprocess Evaluation for Xylanase Production by Isolated *Aspergillus terreus* and *Aspergillus fumigatus* Under Solid - State Fermentation Using Oil Palm Empty Fruit Bunch Fiber

G. Suvarna Lakshmi, P. Lakshmi Bhargavi and R. S. Prakasham*
Bioengineering and Environmental Centre, Indian Institute of Chemical Technology
Hyderabad – 500 607, India
*For Correspondence - prakasam@iict.res.in

Abstract

Xylanase bioprocess by isolated *Aspergillus terreus* and *Aspergillus fumigatus* strains under solid-state fermentation using oil palm empty fruit bunch fiber as substrate was investigated. The productions of xylanase enzyme in these fungal strains were influenced by bioprocess parameters. Though enzyme production was noticed in the wide range of pH (3.0 – 8.0), effective xylanase production observed at pH 6.0 and 7.0 by *A. terreus* and *A. fumigatus* respectively. Similarly, enzyme titer values improved with increase in moisture content (70%) and inoculum concentration of 2.0 and 1.5 ml (1 x 10^6 spore solution per ml) for *A. terreus* and *A. fumigatus* respectively. Particle size mediated variation also noticed where 2.0 - 0.7 and 2.8- 2.0 mm (15,990 and 14,563 U/g) was effective for xylanase production by *A. terreus* and *A. fumigatus*, respectively. Whereas, supplementation of xylose and fructose to *A. terreus* and *A. fumigatus* were enhanced the xylanase production to 32,074 and 25,038 U/g, respectively. Furthermore, addition of 0.6 g of sodium nitrate and 0.4 g of ammonium chloride had resulted 39,136 and 35,380 U/g of xylanase titers by using *A. terreus* and *A. fumigatus* respectively. Over all xylanase enzyme productivity was improved to the tune of 3.0 and 2.8 folds with *A. terreus* and *A. fumigatus* after bioprocess optimization, respectively.

Keywords: *Aspergillus,* Bioprocess, Palm fiber, Solid state fermentation, Xylanase.

Introduction

Aspergillus sp are one of the most important group of filamentous fungi capable of degrading cellulosic and hemicellulosic part of the plant cell wall due to their capability to synthesize hydrolytic enzymes (cellulases and xylanases). These enzymes are responsible to degrade complex substrate molecules into low molecular weight compounds which are used by fungi for their nutrition (1). Among different hydrolytic enzymes, xylanases are mainly responsible for the hydrolysis of the main chain of xylan which has potential applications in many industries. Hence, many researchers focused their attention on production of xylanases using different fermentation strategies. Since, biotechnological applications require large amounts of low cost enzymes, which can be achieved by utilization of lignocellulosic waste or by products as substrates (2). From the literature reports it was revealed that, various lignocellulosic substrates and *Aspergillus* sp have

Vol. 5 (4) 1434-1444 October 2011, ISSN 0973-8916 (Print), 2230-7303 (Online)

been used for the xylanase production under submerged and solid state fermentations. Though xylanase production is reported by different strategies, enzyme production by solid-state fermentation (SSF) is an attractive one because it presents many advantages, especially for fungal cultivation. Xylanase production from *Aspergillus niger* and *Aspergillus ochraceus* was improved by the combination of corn cobs and wheat bran as substrate (3). Whereas, similar strain *A. niger* has shown maximum xylanase production (3099 U/g) using 10 g of sugar cane bagasse and soybean meal in the ratio of 65 and 35%, respectively (4). Grape pomace is a suitable substrate for xylanase production (60U/g) by *A. awamori* (5). All the above reports have indicated that, each microbial strain has different profile in terms of enzyme productivity and utilization of different substrates as carbon sources.

Hence, in the present study, an attempt has been made for xylanase production using isolated fungal strains, *A. terreus* and *A. fumigatus* under solid state fermentation. Here, oil palm empty fruit bunch fiber is selected as substrate based on the earlier studies performed under submerged fermentation (6). Furthermore, in this study, different physiological (pH, moisture content and particle size) and nutritional parameters (carbon and nitrogen sources) were optimized for effective xylanase e production using these strains.

Materials and Methods

***Microorganisms and cultural conditions*:** *A. terreus* and *A. fumigatus* were isolated in our laboratory from soil samples collected from Rajahmundry and in our laboratory premises. These isolates were identified and deposited as *A. terreus* and *A. fumigatus* at Institute of Microbial Technology (IMTECH), Chandigarh, India. The cultures were maintained regularly on potato dextrose agar slants and stored at 4° C.

***Xylanase production by solid state fermentation and enzyme extraction*:** Solid state fermentation experiments were performed using OPEFB fiber as solid material. This material was collected from palm oil industry and processed using USA standard sieve set Nos. 7, 10, 25, 50 and 70 to obtain mean particle sizes of 2.8 - 2.0; 2.0 - 0.7; 0.7 - 0.3 and 0.3 - 0.2 mm and used for bioprocess experiments. Five grams of substrate was used in 250 ml Erlenmeyer flasks and moistened to 70% with pH 7.0 supplemented with (for 5.0 g solid material) yeast extract - 0.2 g; peptone - 0.2 g; KH_2PO_4 - 0.05 g; K_2HPO_4- 0.05 g; NaCl- 0.05 g and $MgSO_4$ - 0.05 g unless otherwise stated. The contents of the flasks were mixed thoroughly and autoclaved at 121° C for 15 min. After cooling to room temperature, the flasks were inoculated with 1 ml of *A. terreus* and *A. fumigatus* spore suspensions (1.0 x 10^6 spores per ml) and incubated at 30 p C. After suitable time of incubation, the flasks were removed and the fermented media was extracted using 100 ml of 50 mM citrate buffer pH 5.0 under shaking at 150 rpm and 30° C for 30 min for three times. Then the pooled contents were centrifuged and the supernatant was collected and used as source of xylanase enzyme.

***Measurement of xylanase activity*:** Xylanase activity was determined using DNS method (7). Enzyme assay was performed at 50° C for 30 min using 1.0% (w/v) oat spelt xylan as substrate. One unit (U) of xylanase activity was defined as the amount of enzyme that releases 1µmol of xylose per min under the standard assay conditions. Xylanase production was expressed as U/g dry substrate. Enzyme assays were performed in triplicate with analytical grade reagents and average values were represented.

***Evaluation of different fermentation factors for xylanase production using one variable at a time approach*:** To investigate the optimum

physical and nutritional parameters for xylanase production the following conditions were optimized. The moisture content was optimized by moistening the solid substrate to 60, 65, 70 and 75% moisture level. The particle size of the substrate was optimized by using 2.8 to 2.0, 2.0 to 0.7, 0.7 to 0.3 and 0.3 to 0.1 mm particle size. The effect of medium pH and inoculum level were optimized in the pH range from 3.0 to 8.0 and 0.25 to 2.5 ml inoculum ($1x10^6$ spores per ml) respectively. Moreover, effect of metabolizable sugars and different nitrogen sources on xylanase production was investigated by using 0.2 g per 5 g of OPEFB fiber.

Results and Discussion

***Time course of xylanase production by A. terreus and A. fumigatus*:** To investigate the suitable fermentation time for xylanase production using *A. terreus* and *A. fumigatus,* bioprocess was carried out over a period of 96 h. The data revealed that xylanase titer values of *A. terreus* and *A. fumigatus* were improved with increase in incubation time up to 60 h and 72 h, respectively. Further increase in incubation time resulted in decreased xylanase production in both strains. At 60 h of incubation time *A. terreus* produced 13,370 U/g whereas *A. fumigatus* produced 12,898 U/g xylanase (Fig.1). Xylanase production values noticed at 24, 36 and 48 h of incubation time with *A. terreus* were 59%, 74% and 91%, respectively when compared to xylanase production at 60 h of incubation time. After 72, 84 and 96 h of incubation time, xylanase production was gradually decreased to 17, 25 and 27% respectively. In case of *A. fumigatus* after 24, 36, 48 and 60 h of incubation time 48, 50, 58 and 78% of xylanase production was measured. After 72 h of incubation time xylanase production was decreased to 11 and 13% at 84 and 96 h respectively. These variations in xylanase enzyme production values over incubation time may be attributed to insufficient growth of the microorganism, loss of moisture, inhibition of the enzyme by end products, depletion of macro-and micronutrients in the fermentation medium, alteration in the medium pH, etc (8). This data indicated that biocatalyst production by these fungal strains is growth associated and produced xylanase helps in increasing the availability of carbon source for their growth by hydrolyzing the xylan portion of the OPEFB. Similar trend was reported in other extracellular enzyme production by other microbial strains: *Penicillium canescens* and *Paecilomyces thermophila* J18 produced maximum xylanase after 7 and 8 days of incubation time (9, 10). Ghanem *et al.,* (11) and Nogueira *et al.,* (12) reported that *A. terreus* produced maximum xylanase (922 U/ml) after 4 days of incubation whereas *A. fumigatus* and *A. niveus* showed maximum activity (370 and 180 U/g, respectively) after 96 h and 120 h of incubation time. From all these literature reports, it is evident that among fungal xylanase producers the isolated *Aspergillus* species of this study produced maximum xylanase in shorter incubation periods. However, isolated *A. terreus* produced maximum xylanase titers in lesser incubation period (60 h) when compared to *A. fumigatus* (72 h) which is advantageous for industrial application. In addition, the presented

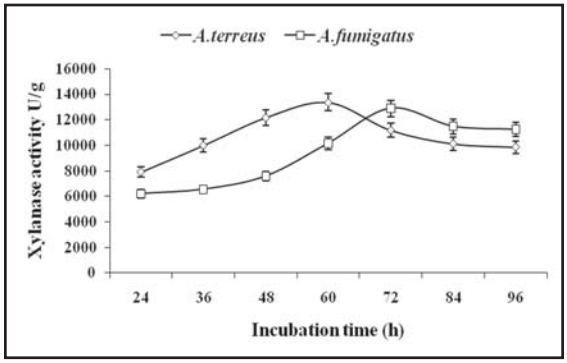

Fig 1. Effect of incubation time on xylanase production by *A. terreus and fumigatus*

data denoted that both these strains differ in their metabolic pathways involved in xylanase production and utilization of OPEFB as substrate material.

***Effect of moisture content on xylanase production by A. terreus and A. fumigatus*:** Solid-state fermentation unlike submerged one occurs at near absence or free flow of water in the fermentation vessel. Hence, supplementation of appropriate quantity of moisture plays critical role for microbial growth and xylanase production in solid-state fermentation (13, 14). So in the present study to evaluate the xylanase production by *A. terreus* and *A. fumigatus,* OPEFB fiber was moistened with different moisture levels. The data revealed that the maximum xylanase production by *A. terreus* and *A. fumigatus* (13,565 and 13,248 U/g) was noticed at 70% moisture content (Fig. 2). At 60 and 65% of moisture content, xylanase production by *A. terreus* and *A. fumigatus* were 9855, 11458 and 9129, 10892 U/g, respectively. Further varying the moisture content to 70%, little variation in xylanase production was noticed. This may be due to the fact that, low moisture content decreases the metabolic and enzymatic activities owing to the reduction of the solubility of nutrients. Whereas, a level of moisture content higher than the optimum causes a decrease in porosity, an alteration in substrate particle structure, a gummy texture, and a lower oxygen transfer is influencing the mass transfer, thus, limiting the nutrients utilization level (15, 16). Authors working with *Penicillium canescens* and *Paecilomyces themophila* J18 reported that 80% and 83% of initial moisture level was the most suitable environment for optimum xylanase production using soya oil cake and wheat straw as substrates (9, 10). In another study, 75% moisture level was noticed effective for maximum xylanase production by *A. terreus* with wheat straw as carbon source (11). These reports supported that moisture content in solid-state fermentation plays an important role on xylanase production. In the present study both *Aspergillus* strains showed maximum xylanase activity at 70% moisture content. This similarity may be due to the same substrate (OPEFB) fiber was used for the production of xylanase enzyme by these strains. So level of moisture content is mainly dependent on the type of substrate used for the enzyme production (15).

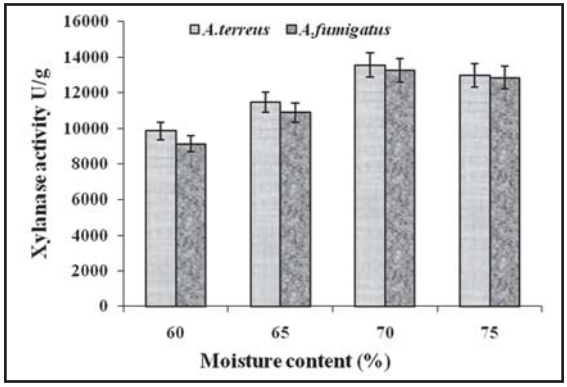

Fig 2. Effect of moisture content on xylanase production

***Influence of particle size on xylanase production by A. terreus* and *A. fumigatus*:** Particle sizes of the substrate during solid-state fermentation influence the microbial growth and allowed heat and mass transfer (13, 15, and 17). From literature, it was reported that *Trichoderma reesei* showed highest xylanase and cellulase activities using small particle size of horticultural waste (15). But *A. terreus* and *A. fumigatus* showed high xylanase titers when used large particle size of palm fiber. In view of the above, different particle sizes of palm fiber tested in order to determine their effects on xylanase production by these two *Aspergillus* sp. It was apparent from the experimental data that particle size affected the enzyme production (Fig. 3). The highest titers of xylanase (15,990 and 14,563 U/g) produced by *A. terreus* and *A. fumigatus* using 2.0 - 0.7 and 2.8 - 2.0 mm size of the OPEFB

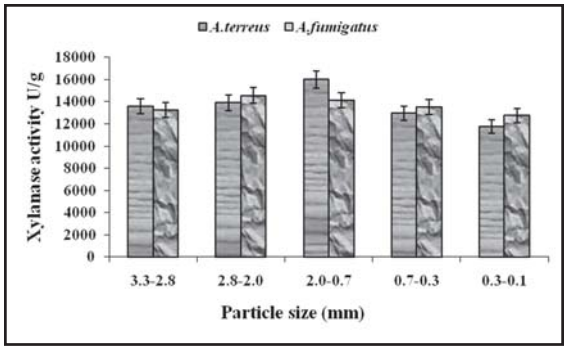

Fig 3. Effect of particle size of the substrate on xylanase production

fiber respectively. After screening of the particle size of the OPEFB fiber, xylanase production by *A. terreus* and *A. fumigatus* was improved to 17% and 9%, respectively and all other tested particle sizes revealed lower productivity values especially with smaller particle sizes. The observed variation in enzyme production values with particle size could be due to its impact on available surface area for microbial growth. This is because, use of smaller particles provide larger surface area for microbial adhesion thus making the environment advantageous for heat transfer and exchange of oxygen and carbon dioxide between the air and the solid surface. However, too small particles may result in substrate agglomeration, which may interfere with microbial respiration and thus result in the poor cell growth (15). However, even though large particle size provides better aeration to microbe may result in poor accessibility of nutrients which limits the microbial growth leads to decreased enzyme production. The literature reports revealed that influence of the particle size varied to the type of the substrate and microorganism used for the enzyme production. *Penicillium canescens* and *Paecilomyces thermophila* J18 produced maximum xylanase using 5.0 mm size of soya oil cake and 0.45 - 0.3 mm size of wheat straw as substrates (9, 10). Here, 2.0 to 0.7 mm and 2.8- 2.0 mm size of palm fiber were found to be suitable for higher titers of xylanase production by *A. terreus* and *A. fumigatus.*

***Effect of medium pH on xylanase production by A. terreus and A. fumigatus*:** pH is an important environmental factor, which significantly affects the production of microbial enzymes and microbial growth (6,18). Analysis on xylanase production by *A. terreus* and *A. fumigatus* at different pH environments ranging from pH 3.0 to 8.0 suggested that the xylanase production is regulated by medium pH. Maximum enzyme production by *A. terreus* and *A. fumigatus* (18,684 and 15,258 U/g, respectively) was noticed with pH 6.0 and 7.0 (Fig. 4). Altering of the pH on either sides of the optimum pH caused the decreased xylanase production. The data further confirmed that these two microbial strains has potential to grow in pH range of 3.0 to 8.0 and produces appreciable quantities of xylanase enzyme. When compared to pH 6.0, at pH 3.0, 4.0 and 5.0, *A. terreus* produced 77, 78 and 85% of xylanase respectively. But when compared to pH 6.0, at pH 7.0 and 8.0 xylanase production was decreased to 14 and 32%, respectively. While in case of *A. fumigatus*, the respective xylanase titers at pH 3.0, 4.0, 5.0, 6.0 and 8.0 were noticed

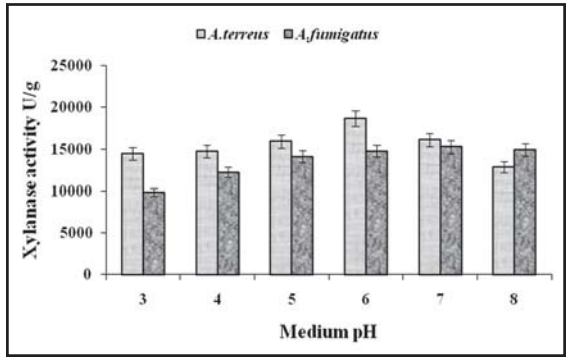

Fig 4. Role of medium pH on xylanase production

as 64, 80, 92, 96 and 97% when compared to xylanase activity at pH 7.0. From these results it was concluded that, pH 3.0 to 6.0 was favorable for xylanase production by *A. terreus.* While in the case of *A. fumigatus*, neutral and alkaline pH were favorable for xylanase production. Such pH dependent xylanase production in solid state fermentation was observed in other microbial strains. *Paecilomyces thermophila* J18 and *Fusarium oxysporum* produced maximum xylanase at pH 7.0 and *A. awamori* showed optimum xylanase production at pH 4.0 (10, 19, and 20). *A. fumigatus* and *A. niveus* produced maximum xylanase in the pH range of 5.0 to 5.5 and 4.5 to 5.0, respectively (12). From these reports it can be showed that fungal xylanases were produced in the pH range of 4.0 to 7.0.

Effect of inoculum concentration on xylanase production by A. terreus and A. fumigatus **:** All microbial growth associated enzymes production is directly proportional to microbial biomass (13). To optimize the initial inoculum concentration for xylanase production by *A. terreus* and *A. fumigatus*, different concentration of spore suspension (1 x 10^6 spores per ml) ranging from 0.25 to 2.5 ml (v / 5.0 g of substrate) were evaluated and xylanase production at 60 and 72 h of growth were measured. The data clearly indicated that enzyme productions by both these strains were influenced by inoculum concentration. Xylanase production by *A. terreus* and *A. fumigatus* was increased by using 2.0 ml and 1.5 ml of spore solutions respectively and further increase in inoculum level, decreased the enzyme production (Fig. 5). Similar effects of inoculum level on xylanase production are reported in the literature. Gaffney *et al*., (21) reported that *Thermomyces lanuginosus* produced higher titers of xylanase using higher inoculum level. Ghanem *et al*., (11) reported that maximum xylanase production was obtained by *Aspergillus terreus* using 1.2 x10^4 spores per 2.0 ml. These reports suggested that lower inoculum volumes in SSF might not accommodate mycelial expansion and subsequent product formation. Increased levels of inoculum typically improve growth- related activities, but after a certain point, they serve to restrict gaseous exchange, reduce heat removal, and increase the demand for nutrients from the substrate. Furthermore, a higher inoculum volume in SSF can increase the incidence of bacterial contamination (22). From this data it was concluded that inoculum level plays an important role on xylanase production. Lower or higher levels of inoculum level inhibit the xylanase production.

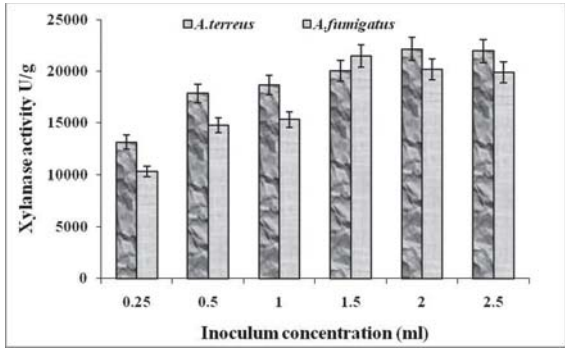

Fig 5. Effect of inoculum concentration on xylanase production

Effect of different easily metabolizable sugars on xylanase production by A. terreus and A. fumigatus**:** To evaluate the effect of easily metabolizable sugars, different sugars such as glucose, fructose, xylose, galactose, maltose, arabinose, mannose and lactose were taken at 0.2% level and sterilized separately from fermentation medium and used for the xylanase production. The data indicated that enzyme production differed with the type of carbon source used (Fig. 6). Maximum xylanase production by *A. terreus* and *A. fumigatus* (32,074 and 25,038 U/g) occurred in xylose and fructose supplemented conditions indicating an increase of 45% and 16%, respectively over

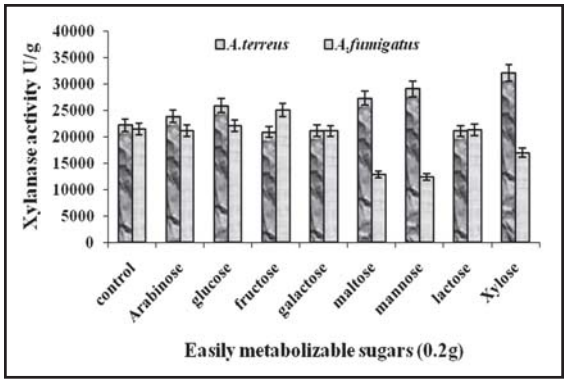

Fig 6. Effect of different easily metabolizable sugars on xylanase production

control (without any addition of carbon source). Not only xylose, other simple sugars glucose, maltose and mannose also increased (17, 23 and 31%, respectively) the xylanase production by *A. terreus* when compared to control. But xylanase production by *A. fumigatus* was only enhanced by fructose supplementation and all other sugars inhibited the xylanase production. This data suggested that utilization pattern of externally supplemented carbon sources by these two strains differ and only fructose is effective for xylanase production by *A. fumigatus* and not for *A. terreus*. Effect of simple sugars on xylanase production was studied by many other researchers. Shah and Madamwar (23) reported that fructose and lactose inhibited the xylanase production which was similar to xylanase production by *A. terreus* of this study. Xylanase production by *Thermomyces lanuginosus* was enhanced by the addition of glucose and cellulose whereas xylose and sucrose reduced the xylanase activity by 9 and 8% (21). Christakopoulos *et al*., (24) reported that xylanase production was repressed by the addition of simple sugars such as glucose, xylose and lactose. Smith and Wood (20) also reported the similar result about the effect of simple sugars on xylanase production. In this case, except xylose, all the sugars repressed the xylanase production. This data revealed that maximum number of tested simple sugars repressed the xylanase production. In addition, xylanase production by *A. terreus* and *A. fumigatus* was enhanced by the addition of low concentrations of xylose and fructose. Further increase in carbon source did not improve the enzyme production and showed catabolic repression (data not shown).

***Effect of different nitrogen sources on xylanase production by A. terreus and A. fumigatus*:** Nitrogen sources are known to regulate the production of extracellular enzymes in different microbial strains by altering the availability of precursors for protein synthesis (25). In the present study, to evaluate the effect of different nitrogen sources on xylanase production by *A. terreus* and *A. fumigatus*, various organic nitrogen sources such as yeast extract, peptone, beef extract, tryptone, soya bean meal, corn steep liquor, urea and casein (0.2 g per 5.0g of substrate) and inorganic nitrogen sources such as $(NH_4)_2SO_4$, NH_4Cl, NH_4NO_3, $NaNO_3$ and KNO_3 (0.2%) were added in the production media and checked for the xylanase production. As shown in Fig. 7, among all the organic nitrogen sources tested, urea and peptone were the best for achieving optimal xylanase production (37,799 and 28,520 U/g, respectively) by *A. terreus* and *A. fumigatus* and least xylanase production (13,462 and 15,180 U/g dry substrate, respectively) was obtained with corn steep liquor as nitrogen source by both strains. Other nitrogen sources have shown nearly similar effect on xylanase production by both strains. While, in the case of *A. terreus,* when compared to the xylanase production by using urea, addition of yeast extract, peptone, beef extract, tryptone, soybean meal and casein decreased the xylanase production to 35, 38, 30, 35, 33 and 38% respectively. While, in the case of xylanase production by *A. fumigatus*, the differences in

Vol. 5 (4) 1434-1444 October 2011, ISSN 0973-8916 (Print), 2230-7303 (Online)

xylanase production by using other nitrogen sources was less, when compared to the xylanase production by using peptone. Here, addition of casein and yeast extract have shown similar impact on xylanase production. When compared to the xylanase production by peptone, both of these nitrogen sources have shown 25% decrement in xylanase production followed by tryptone (22%). Whereas, supplementation of beef extract was caused 11% reduction in xylanase production and soybean meal has shown similar effect on xylanase production like as peptone. However, addition of corn steep liquor to the production media led to the 64% and 46% of reduction in xylanase production by *A. terreus* and *A. fumigatus* respectively. Even though, corn steep liquor is a rich nitrogen source, both of these fungal strains were unable to utilize this source properly due to its non synthetic and complex nature which led to the lower xylanase production. In this study, urea supplementation has given higher titers of xylanase production by *A. terreus* compared to other studied organic nitrogen sources. The results are in agreement with *Chaetomium cellulolyticum, Phanerocheate chrysosporium* and *Rhizopus stolonifer* (26, 27). In contrast to the above result, urea inhibited the xylanase production by using A. *niveus, A. ochraceus* and *A.niger* (3). *A.niger* showed maximum xylanase activity using peptone as nitrogen source which was similar to the xylanase production by *A. fumigatus* (3). The above data revealed that supplementation of the organic nitrogen sources greatly enhanced the xylanase titers in the present study by isolated fungal strains.

Among all the tested inorganic nitrogen sources, supplementation of $NaNO_3$ and NH_4Cl caused maximum and minimum xylanase production by *A. terreus* (39,136 and 23,545 U/g dry substrate) respectively (Fig.7). When compared to the organic nitrogen source (urea), addition of inorganic nitrogen source ($NaNO_3$) showed maximum influence on enzyme production (Fig 7). In contrast to the above result, *A. fumigatus* produced higher titers of xylanase using NH_4Cl (35,380 U/g) as nitrogen source which caused lower xylanase production using *A. terreus*. As per literature report, *Trichoderma harzianum* showed maximum xylanase activity by the addition of $NaNO_3$ which was similar to the xylanase production by *A. terreus* (28). Seyis and Aksoz (29) reported that addition of ammonium sulphate enhanced the xylanase production by *Trichoderma harzianum*. NH_4NO_3 and $(NH_4)_2HPO_4$ supplementation in *Schizophyllum commune* increased the xylanase production (30). By observing these literature reports, it was found that not only organic nitrogen sources but also inorganic nitrogen sources positively affected the xylanase production. In the present study among all the organic and inorganic nitrogen sources, addition of $NaNO_3$ and NH_4Cl enhanced the xylanase production by *A. terreus* and *A. fumigatus*. Hence, further optimization of xylanase production by *A. terreus* and *A. fumigatus* was done by supplementing different concentrations of $NaNO_3$ and NH_4Cl (0.2, 0.4, 0.6, 0.8 and 1g). The results revealed that 0.6 g of $NaNO_3$ showed maximum xylanase production by *A. terreus*,

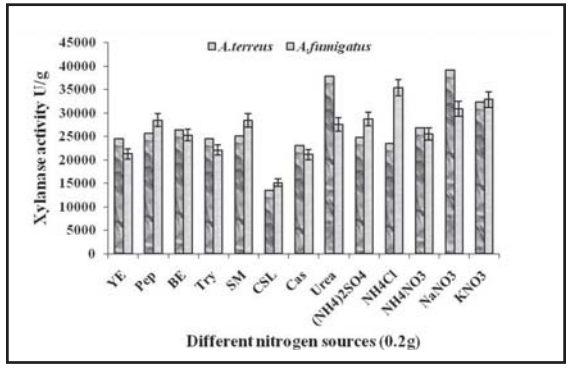

Fig. 7. Effect of different nitrogen sources on xylanase production

whereas 0.4 g of NH_4Cl has shown maximum xylanase production in the case of *A. fumigatus*. Overall, after optimization of the nitrogen source, xylanase production by *A. terreus* and *A. fumigatus* was improved by 5 and 4.5%, respectively.

Conclusion

Overall xylanase production pattern was investigated under solid state fermentation by isolated *A. terreus* and *A. fumigatus* strains using oil palm empty fruit bunch fiber as solid support material. Different fermentation parameters such as incubation period, moisture content, particle size, medium pH, inoculum concentration, carbon and nitrogen sources were optimized. These isolated strains showed effective enzyme production (*A. terreus*: 41,000 and *A. fumigatus*: 36,985 U/g) upon supplementation of sodium nitrate and ammonium chloride as nitrogen sources, xylose and fructose as inducers at the optimum pH of 6.0 and 7.0 with 70% moisture content in 60 and 72 h of incubation with an initial inoculum concentration of 2.0 ml and 1.5 ml (1 x 10^6 spore solution) respectively. The xylanase production by both these strains and was increased by 3.0 (*A. terreus*) and 2.8 (*A. fumigatus*) folds under optimized conditions. When compared to *A. fumigatus*, *A. terreus* showed higher xylanase production.

Acknowledgments

Authors are thankful to Council of Scientific and Industrial Research, New Delhi for financial support and Director, Indian Institute of Chemical Technology, Hyderabad for his encouragement.

References

1. Kachlishvili, E., Penninckx, M.J., Tsiklauri, N. and Elisashvili, V. (2005). Effect of nitrogen source on lignocellulolytic enzyme production by white-rot basidiomycetes under solid-state cultivation. World Journal of Microbiology and Biotechnology, 22(4): 391-397.

2. Haltrich, D., Nidetzky, B., Kulbe, K.D., Steiner, W. and Zupancic, S. (1996). Production of fungal xylanases. Bioresource Technology, 58: 137-161.

3. Betini, J.H.A., Michelin, M., Peixoto-Nogueira, S.C., Jorge, J.A., Terenzi, H.F. and Polizeli, M.L.T.M. (2009). Xylanases from *Aspergillus niger*, *Aspergillus niveus* and *Aspergillus ochraceus* produced under solid-state fermentation and their application in cellulose pulp bleaching. Bioprocess Biosyst Engineering, 32: 819 - 824.

4. Maciel, G.M., de Souza, L.P., Vandenberghe, Haminiuk, C.W.I., Fendrich, R.C., Bianca, B.E.D., Brandalize, T.Q.S., Pandey, A. and Soccol, C.R. (2008). Xylanase production by *Aspergillus niger* LPB 326 in solid-state fermentation using statistical experimental designs. Food Technology and Biotechnology, 46 (2): 181-187.

5. Botella, C., Diaz, A., Ory, I., Webb, C. and Blandino, A. (2007). Xylanase and pectinase production by *Aspergillus awamori* on grape pomace in solid state fermentation. Process Biochemistry, 42: 98-101.

6. Suvarna Laxmi, G., Sathish, T., Subba Rao, Ch., Brahmaiah, P., Hymavathi, M. and Prakasham, R.S. (2008). Palm fiber as novel substrate for enhanced xylanase production by isolated *Aspergillus* sp. RSP-6. Current Trends in Biotechnology and Pharmacy, 2(3): 447- 455.

7. Miller, G.L. (1959). Modified DNS method for reducing sugars. Analytical Chemistry, 31: 426 - 428.

8. Lucia, M., Simoes, G., Torniseilo, S.M.T. and Tapia, D.M.T. (2009). Screening of culture condition for xylanase production by filamentous fungi. African Journal of Biotechnology, 8 (22): 6317-6326.

9. Antoine, A.A., Jacqueline, D. and Thonart, P. (2010). Xylanase production by *Penicillium canescens* on soya oil cake in solid-state fermentation. Applied Biochemistry and Biotechnology, 160: 50 - 62.

10. Yang, S.Q., Yan, Q.J., Jiang, Z.Q., Li, L.T., Tian, H.M. and Wang, Y.Z. (2006). High-level of xylanase production by the thermophilic *Paecilomyces themophila* J18 on wheat straw in solid-state fermentation. Bioresource Technology, 97: 1794 -1800.

11. Ghanem, N.B., Yusef, H.H. and Mahrouse, H.K. (2000). Production of *Aspergillus terreus* xylanase in solid-state cultures: application of the Plackett - Burman experimental design to evaluate nutritional requirements. Bioresource Technology, 73: 113-121.

12. Nogueira, S.C.P., Michelin, M., Betini, J. H. A., Jorge, J.A., Terenzi, H.F. and Polizeli, M.L.T.M. (2009). . Production of xylanase by *Aspergilli* using alternative carbon sources: application of the crude extract on cellulose pulp biobleaching. Journal of Industrial Microbiology and Biotechnology, 36:149-155.

13. Prakasham, R.S., Subba Rao, Ch. and Sarma, P. N. (2006). Green gram husk—an inexpensive substrate for alkaline protease production by *Bacillus* sp. in solid-state fermentation. Bioresource Technology, 97: 1449-1454.

14. Prakasham, R. S., Subba Rao, Ch., Sreenivasa Rao, R. and Sarma, P. N. (2007). Enhancement of acid amylase production by an isolated *Aspergillus awamori*. Journal of Applied Microbiology, 102: 204–211.

15. Xin, F. and Geng, A. (2010). Horticultural waste as the substrate for cellulase and hemicellulase production by *Trichoderma reesei* under solid-state fermentation. Applied Biochemistry and Biotechnology, 162: 295-306.

16. Mahalaxmi, Y., Sathish, T., Subba Rao, Ch. and Prakasham, R.S. (2010). Corn husk as a novel substrate for the production of rifamycin B by isolated *Amycolatopsis* sp. RSP-3 under solid state fermentation. Process biochemistry, 45:47-53.

17. Prakasham, R. S., Sreenivasa Rao, R., Subba Rao, Ch. and Sarma, P. N. (2005). cyclodextringlycosyl transferase production using isolated *Bacillus* sp and *Bacillus circulance*. Indian Journal of Biotechnology, 4: 347-352.

18. Prakasham, R. S., Subba Rao, Ch., Sreenivasa Rao, R. and Sarma, P. N. (2005). Alkaline protease production by an isolated *Bacillus circulance* under solid-state fermentation using agro-industry waste: Process parameters optimization. Biotechnology Progress, 21: 1380-138.

19. Panagiotou, G., Kekos, D., Macris, B.J. and Christakopoulos, P. (2003). Production of cellulolytic and xylanolytic enzymes by *Fusarium oxysporum* grown on corn stover in solid state fermentation. Industrial crops and products, 18: 37- 45.

20. Smith, D. C. and Wood, T.M. (1991). Xylanase production by *Aspergillus awamori*. Development of a medium and optimization of the fermentation parameters for the production of extracellular xylanase and â-xylosidase while maintaining low protease production. Biotechnology and Bioengineering, 38: 883-890.

21. Gaffney, M.., Doyle, S. and Murphy, R. (2009). Optimization of xylanase production by *Thermomyces lanuginosus* in solid-state fermentation. Bioscience, Biotechnology and Biochemistry, 73 (12): 2640-2644.

22. Pandey, A., Socool, C.R. and Mitichell, D. (2000). New developments in solid-state fermentation. I. Bioprocess and products. Process Biochemistry, 35: 1153-1169.

23. Shah, A.R. and Madamwar, D. (2005). Xylanase production by a newly isolated *Aspergillus foetidus* strain and its characterization. Process Biochemistry, 40: 1763-1771.

24. Christakopoulos, P., Kekos, D., Macris, B.J., Claeyssens, M. and Bhat, M.K. (1996). Purification and characterization of a major xylanase with cellulose and transferase activities from *Fusarium oxysporum*. Carbohydrate Research, 289: 91-104.

25. Kulkarni, N., Shendye, A. and Rao, M. (1999). Molecular and biotechnological aspects of xylanases. FEMS Microbiology Reviews, 23: 411- 456.

26. Dubeau, H., Chahal, D.S. and Ishaque, M. (1987). Xylanase of *Chaetomium Cellulolyticum*: its nature of production and hydrolytic potential. Biotechnology letters 9 (4): 275-280.

27. Kanmani, P., Karuppasamy, P., Pothiraj, C. and Venkatesan, A. (2009). Studies on lignocellulose biodegradation of coir waste in solid state fermentation using *Phanerocheate chrysosporium* and *Rhizopus stolonifer*. African Journal of Biotechnology, 8 (24): 6880-6887.

28. Sater, M.A.A. and Said, A.H.M. (2001). Xylan-decomposing fungi and xylanolytic activity in agricultural and industrial wastes. International Biodeterioration and Biodegradation, 47: 15-21.

29. Seyis, I. and Aksoz, N. (2005). Effect of carbon and nitrogen sources on xylanase production by *Trichoderma harzianum* 1073 D3. International Biodeterioration and Biodegradation, 55(2)*:* 115-119.

30. Haltrich, D., Preiss, M. and Steiner, W. (1993). Optimization of a culture medium for increased xylanase production by a wild strain of *Schizophyllum commune*. Enzyme and Microbial Technology, 15: 854-860.

Vol. 5 (4) 1445-1453 October 2011, ISSN 0973-8916 (Print), 2230-7303 (Online)

UV Mutagenesis of *Leuconostoc mesenteroides* NRRL B-640 for Generation of a Mutant (B-640M) with Hyper-Producing Dextransucrase Activity

Mayur Agrawal, Rishikesh Shukla and Arun Goyal*
Department of Biotechnology
Indian Institute of Technology Guwahati
Guwahati 781 039, Assam, India
*For Correspondence - arungoyl@iitg.ernet.in

Abstract

This study reports the strain improvement of *Leuconostoc mesenteroides* NRRL B-640 by classical mutation technique using ultraviolet radiation to achieve the mutant strain with higher dextransucrase activity. A large number of mutants were generated, cultured and tested for dextransucrase activity. The selected mutant gave considerably higher (46%) dextransucrase activity (0.8 U/mg) as compared to the wild-type strain (0.55 U/mg). Interestingly, the selected mutant yielded 21% higher dextran concentration (8.2 mg/ml) as compared to wild type strain (6.8 mg/ml) in the broth. The selected mutant was characterized for antibiotic sensitivity, carbohydrate fermentation and dextran forming activity and compared with the wild-type strain. The antibiotic sensitivity test showed that, the mutant, unlike the wild-type strain was resistant to kanamycin, claxacin and amikacin. The mutant also showed resistance towards amoxyclav and tobramycin, unlike the wild-type strain which was moderately sensitive to these antibiotics. The carbohydrate fermentation profile showed that the mutant, unlike the wild-type, utilized lactose but did not show any activity towards cellobiose and rhamnose. Dextransucrase from the mutant was purified by PEG fractionation and its analysis by SDS-PAGE revealed the same molecular size of 180 kDa as that of wild-type strain. The analysis of dextransucrase from the mutant by activity staining using Periodic Acid Schiff's protocol also showed a single band and no change in dextran forming activity when compared to wild-type. ^{1}H NMR and ^{13}C NMR spectroscopic and Scanning Electron Microscopic (SEM) analysis of dextran produced by mutant strain B640M showed no difference from the wild type *Leuconostoc mesenteroides* NRRL B-640.

Key words: *Leuconostoc mesenteroides* NRRL B-640, UV mutagenesis, dextransucrase, dextran

Introduction

Dextran, a homopolysaccharide of D-glucose, is synthesized by dextransucrase (sucrose: 1,6-α-D-glucan 6-α-glucosyltransferase, EC 2.4.1.5), a glucosyltransferase produced, as an exo-cellular enzyme, by lactic acid bacteria viz., *Leuconostoc, Lactobacillus* and *Streptococcus* spp. Dextransucrase from *L. mesenteroides* is a sucrose inducible enzyme that catalyzes the polymerization of the glucopyranosyl moiety of sucrose to form linear chain dextran containing α(1→6) linkages with α(1→2), α(1→3) and α(1→4) branched linkages. Dextrans have various applications in food industry as viscosifying, stabilizing, emulsifying or gelling agents and as potential

Vol. 5 (4) 1445-1453 October 2011, ISSN 0973-8916 (Print), 2230-7303 (Online)

therapeutic agents and drug-delivery systems in medical sciences (1, 2). Dextran and its derivatives are used as blood plasma expander and blood flow improver, anti-ulcer agent, against iron-deficiency anemia and in open wound healing (1). Its derivative dextransulfate inhibits viral infections. It binds to the attenuated poliovirus and interferes with its initial adsorbtion to susceptible cells. Sodium salt of dextransulfate inhibits AIDS virus. The derivatives of dextran like Sephadex and DEAE-dextran serve as molecular sieves and are extensively used in the separation of biomolecules (1). Dextran hydrogels are used in various pharmaceutical and biomedical applications such as contact lenses, cell encapsulation for drug-delivery, burn dressing and in spinal cord regeneration (3, 4). There are several strains of *Leuconostoc mesenteroides* available and many of them have been extensively studied. One such strain is *Leuconostoc mesenteroides* NRRL B-640 which gives highly soluble dextran with 97% $\alpha(1\rightarrow6)$ glucosidic linkage. *Leuconostoc mesenteroides* NRRL B-640 has been well characterized based on antibiotic sensitivity, carbohydrate fermentation and dextran synthesizing activity. *Leuconostoc mesenteroides* NRRL B-640 showed resistance towards the antibiotics co-trimazine, norfloxacin, norflaxacin and vancomycin, strongly fermented cellobiose, dextrose, fructose, galactose, maltose, mannose, melibiose, sucrose and trehalose, produced single dextran synthesizing protein band of approximately 180 kDa on activity staining and possessed a single plasmid (5). The culture conditions for production of dextransucrase from *Leuconostoc mesenteroides* NRRL B-640 have been optimized (6). Under optimized conditions, *Leuconostoc mesenteroides* NRRL B-640 gave an enzyme activity of 4.8 U/ml and specific activity of 0.58 U/mg (JFB 2008). Further optimization of medium composition using Response surface methodology gave increased dextransucrase activity of 10.7 U/ml and specific activity of 0.68 U/mg (8). The current work focuses on strain improvement of *Leuconostoc mesenteroides* NRRL B-640 by classical mutation technique using ultraviolet radiation to achieve the mutant strains with higher dextransucrase activity. The dextran production of selected mutant with higher dextransucrase activity was estimated. The mutant with maximum dextran yield was characterized based on antibiotic sensitivity, carbohydrate fermentation and dextran producing activity and dextransucrase from the mutant was purified by PEG fractionation and analyzed using SDS-PAGE.

Materials and Methods

Generation of mutant **:** 1 ml of the 12h culture (cell OD at 600 nm = 2.41) of *Leuconostoc mesenteroides* NRRL B-640, grown in 10 ml MRS-S medium (8) at 25°C and 180 rpm, was serially diluted in 9 ml saline solutions (0.85%) up to dilution factor of 10^7. Then, 100 µl of cell broth at dilution factors 10^4, 10^5, 10^6 and 10^7 were spread-plated on MRS-S agar (1.7%, w/v) containing petri-plates. Then the petri-plates were exposed to UV radiation for different exposure time period of 15s to 180s. The plates were immediately kept in the dark to avoid photo-reactivation. Each set of dilution and exposure time was taken in duplicate. The UV exposed petri-plates were incubated at 25°C. After 36h of incubation, the colonies showing around 1% survival rates were picked and maintained as MRS-S agar (1.7%) stabs. The survival rate is defined as number of colonies obtained in petri-plate (with UV-exposure) percent colonies in the control plate (without UV-exposure). These colonies were analyzed for their enzyme activity. A loopful from each colony was grown using enzyme production medium (9). The cell free supernatants obtained by centrifugation at

Vol. 5 (4) 1445-1453 October 2011, ISSN 0973-8916 (Print), 2230-7303 (Online)

10,000g and 4°C for 10 min, were analyzed for enzyme activity using reducing sugar estimation (10, 11).

Analysis of mutant for dextransucrase activity : The mutant was grown in 50 ml liquid medium of Tsuchiya (9) at 25°C and 180 rpm. At various time intervals 1 ml sample was withdrawn, centrifuged and cell free supernatant was analysed for enzyme activity and protein concentration. For the assay of dextransucrase, 1 ml of reaction mixture contained 146 mM (5%) sucrose in 20 mM sodium acetate buffer (pH 5.4) and the cell free supernatant (20 µl) for the enzyme. The reaction mixture was incubated at 30°C for 15 min. The enzyme activity was measured by estimating the liberated reducing sugar (10, 11). The aliquot (0.1 ml) from the reaction mixture were analyzed for reducing sugar concentration. The absorbance was measured at 500 nm by UV-visible spectrophotometer (Cary100 Bio, Varian Inc., USA) using D-fructose as a standard. One unit (U) of dextransucrase activity is defined as the amount of enzyme that liberates 1 ìmole of reducing sugar per min at 30°C in 20 mM sodium acetate buffer (pH 5.4). The protein concentration of the cell free supernatant and purified enzyme was estimated by the method of Lowry *et al.* using BSA (25 µg/ml to 500 µg/ml) as a standard (12).

Antibiotic sensitivity of selected mutant : The mutant was tested for susceptibility to 29 antibiotics (Table 2) by agar diffusion test (13) using commercially available octodiscs containing different antibiotics. The culture grown in MRS medium (8) for 12h, were seeded in MRS agar (0.8%) medium and overlaid on the already prepared petri-plates with MRS agar (1.8%) medium. The petri-plates were allowed to dry for 2 min. The octodiscs were gently placed over seeded MRS (0.8% agar) surface and the plates were incubated at 28°C. The plates were observed for zone of inhibition around the discs after 24h.

Carbohydrate fermentation profile of selected mutant : The mutant was tested for its ability to ferment 13 carbohydrates (Table 3) using the method of Kandler and Weiss, 1986 (14). From culture grown in MRS medium for 12h, 50 µl was inoculated in 5 ml liquid MRS medium containing different carbohydrates and 0.001% (w/v) Phenol red dye and incubated at 28°C for 2 days without shaking. The acid production, indicated by a change of color of Phenol Red dye from red to yellow, was recorded.

Purification of dextransucrase of selected mutant by PEG fractionation : The mutant was grown in 100 ml liquid medium described by Tsuchiya *et al.*, 1952 (9) at 25°C and 180 rpm for 16h. To 100 ml of cell free extract obtained by centrifugation of the broth at 10,000g for 10 min at 4°C, ice-cold PEG-400 was added to obtain the final concentration of 25% (v/v). The mixture was incubated for 12h at 4°C to allow the dextransucrase to precipitate. It was centrifuged at 13,200g for 30 min at 4°C to separate the pellet. The enzyme pellet was dissolved in 20 mM sodium acetate buffer (pH 5.4) and subjected to dialysis using 5kDa cut off membrane. After dialysis, the dextransucrase was analyzed for enzyme activity and protein concentration as described earlier.

SDS-PAGE analysis and detection of dextran formation activity of dextransucrase : SDS-PAGE was performed following the method of Laemmli, 1970 (15) using 7.5% (w/v) acrylamide for resolving gel and 4% (w/v) acrylamide for stacking gel. The purified enzyme was loaded on gel under denaturing conditions. Electrophoresis was carried out at 2.5 mA current per lane. After the run, protein bands were fixed with 5% (v/v) acetic acid for 5 min, then stained with 0.25% (w/v) Coomassie Brilliant

Vol. 5 (4) 1445-1453 October 2011, ISSN 0973-8916 (Print), 2230-7303 (Online)

Blue (CBB) and destained by a solution of 20% (v/v) methanol and 10% (v/v) acetic acid. Molecular weight marker proteins (ranging from 205000- 29000) from Genei, India, were used.

Dextran formation activity of dextransucrase was detected on 7.5% acrylamide gel run under non-denaturing SDS-PAGE using the protocol described by Holt *et al*., 2001 (16) with some modification. The PEG-purified enzyme from the mutant was loaded on 7.5% polyacrylamide gel. After the run, the gel was incubated in sodium acetate buffer (20 mM sodium acetate, pH 5.4, 0.3 mM $CaCl_2$ and 0.1% Tween 80). Then, the gel was incubated in sodium acetate buffer (20 mM sodium acetate (pH 5.4), 0.3 mM $CaCl_2$) supplemented with 5% sucrose, for 48h at 30°C. Following incubation, the gel was washed once with a solution of methanol:acetic acid (50:10) in water for 30 min, then with water for 30 min, and incubated in periodic acid solution (1% periodic acid in 3% acetic acid) for 45 min at room temperature. Then the gel was washed with water for 2h with several changes. The gel was then stained with 15 ml Schiff reagent (0.5% w/v Fuchsin basic, 1% sodium bisulphate and 0.1 N HCl) until the discrete magenta bands appeared.

Purification, estimation and characterization of dextran produced by the mutant : The mutant was grown in 10 ml liquid Tsuchiya medium at 25°C and 180 rpm for 48h. The culture supernatant was obtained by centrifugation of the broth at 10,000g for 10 min at 4°C. The 9.0 ml supernatant was added with 3 volumes of pre-chilled 95% (v/v) ethanol and centrifuged at 13,000g for 30 min. The dextran pellet obtained was resuspended in 9 ml water. The process of precipitation with 3 volumes of ethanol was carried out 3 times to remove any trace impurities or free reducing sugars. The dextran content was determined by phenol-sulfuric acid method (17) in a micro titer plate (18). Dextran T-40 (10 kDa) in the range 0.1–1 mg/ml was used as the standard. The dextran pellet was resuspended in deionized water to ensure removal of any remaining sucrose and was frozen at -20°C. The solidified sample was then freeze dried using a lyophilizer (Christ GmbH, model ALPHA 1-4 LD) at -51°C at a vacuum pressure of 35×10^{-3} mbar for 24h. The purified dextran from mutant was subjected to NMR and SEM analysis and compared with dextran from wild-type strain.

Results and Discussion

Generation and selection of mutants based on dextransucrase activity : UV induced mutagenesis of *Leuconostoc mesenteroides* NRRL B-640 generated 188 colonies at various dilutions and exposure times. Only the plates having survival rates of nearly 1% were considered for selection of mutants. 35 colonies from such plates were visually selected based on their larger colony sizes. These colonies were grown in enzyme production medium and analyzed for dextransucrase activity. The conditions for growing the mutants used were same as that of wild type (6). From the results it was observed that out of 35 selected colonies, 15 showed considerably higher enzyme activity as compared to the wild-type *Leuconostoc mesenteroides* NRRL B-640, including 8 mutants with more than 20% increase. Table 1 shows 15 mutants with UV-mutagenesis conditions and their dextransucrase activity. Mutant numbers were randomly assigned to the selected colonies from petri-plates. The data from Table 1 clearly showed that the dilution factor 10^4 (initial cell density 5.6×10^8) and UV exposure time of 30s were optimum conditions for generation of mutants with higher dextransucrase activity. The percent increase in dextransucrase activity of mutants with respect to wild type was calculated. Interestingly, a consistent percent increase was observed both in enzyme activity and specific

Table 1. Mutagenesis conditions and dextransucrase activity of mutants

S.No.	Strains	Conditions		Enzyme Activity (U/ml)		Specific Activity (U/mg)	
	Wild-type B-640			4.12		0.55	
	Mutant No.	Dilution Factor	UV Exposure Time (s)		% Increase		% Increase
1.	14A	10^4	30	4.92	19.2	0.65	18.9
2.	B640M	10^4	30	5.96	44.7	0.8	45.5
3.	14D	10^4	30	5.52	33.9	0.7	27.1
4.	14E	10^4	30	5.3	28.7	0.72	30.8
5.	14F	10^4	30	5.29	28.4	0.69	26.2
6.	14I	10^4	30	5.63	36.6	0.77	39.3
7.	14J	10^4	30	4.96	20.4	0.68	23.8
8.	14K	10^4	30	5.05	22.4	0.66	19.6
9.	5A	10^4	60	4.32	5.0	0.57	4.5
10.	5B	10^4	60	5.36	30.0	0.69	26.2
11.	5C	10^4	60	5.37	30.3	0.71	29.4
12.	7A	10^4	75	4.35	5.5	0.61	11.9
13.	9A	10^5	30	4.17	1.2	0.56	2.4
14.	10A	10^4	30	4.75	14.6	0.63	14.2
15.	10B	10^4	30	4.26	3.5	0.57	3.5

activity for a particular mutant strain. The mutant was named B640M that showed highest dextransucrase activity (6.0 U/ml, 0.8 U/mg). The enzyme activity and the specific activity of dextransucrase from the mutant B640M were 45% higher than those of wild-type *Leuconostoc mesenteroides* NRRL B-640.

Antibiotic sensitivity of the selected mutant : The susceptibility of a microorganism to an antibiotic is determined by the size of the zone of inhibition. Based on comparison of measured size of the zone of inhibition with the standardized limits (Resistant (R): 0-2mm, Moderately sensitive (M): 3-6mm, Sensitive (S): 7-13mm), the test microorganism was determined to be resistance or susceptible to the antibiotic. Like the wild-type *Leuconostoc mesenteroides* NRRL B-640, mutant B640M was resistant to the antibiotics co-trimazine, norfloxacin and vancomycin, moderately sensitive to ampicilin, erythromycin, gentamycin, novobiocin and oxacillin and susceptible to amoxicillin, bacitracin, carbenicillin, cephalothin, caphatoxamine, chloramphenicol, clindamycin, linomycin, oxytetracyclin, penicillin-G and tetracycline (Table 2). Unlike the wild-type strain, the mutant was resistant to kanamycin, claxacin and amikacin. The mutant also showed resistance towards amoxyclav and tobramycin, unlike the wild-type strain which was moderately sensitive to these antibiotics (Table 2).

Vol. 5 (4) 1445-1453 October 2011, ISSN 0973-8916 (Print), 2230-7303 (Online)

Table 2. Antibiogram of the wild-type *Leuconostoc mesenteroides* NRRL B-640 and mutant B640M

S. No.	Antibiotic	Conc. (μg)	B-640	B640M
1	Amoxyclav (Ac)	10	M	R
2	Cephalexin (Cp)	10	R	M
3	Ciproflaxacin (Cf)	10	R	M
4	Clindamycin (Cd)	2	S	S
5	Claxacin (Cx)	1	M	R
6	Erythromycin (E)	15	M	M
7	Tetracyclin (T)	30	S	S
8	Ampicilin (A)	10	M	M
9	Carbenicillin (Cb)	100	S	S
10	Cephatoxamine (Ce)	30	S	S
11	Chloramphenicol (C)	30	S	S
12	Co-Trimazine (Cm)	25	R	R
13	Gentamycin (G)	10	M	M
14	Norfloxacin (Nx)	10	R	R
15	Oxacillin (Ox)	5	M	M
16	Amikacin (Ak)	10	M	R
17	Amoxycillin (Am)	10	S	S
18	Bacitracin (B)	10	S	S
19	Cephalothin (Ch)	30	S	S
20	Novobiocin (Nv)	30	M	M
21	Oxytetracyclin (O)	30	S	S
22	Vancomycin (Va)	30	R	R
23	Cephaloridin (Cr)	30	R	M
24	Kanamycin (K)	30	S	R
25	Linomycin (L)	2	S	S
26	Methicillin (M)	5	M	S
27	Oleandomycin (Ol)	15	S	M
28	Penicillin-G (P)	10	S	S
29	Tobramycin (Tb)	10	M	R

R – Resistant: 0-2mm, M – Moderately sensitive: 3-6mm, S – Sensitive: 7-13mm
(Note: Values in mm corresponds to the size of zone of inhibition)

Carbohydrate fermentation profile of the selected mutant : Like the wild-type *Leuconostoc mesenteroides* NRRL B-640, the mutant B640M strongly fermented dextrose, fructose, maltose, mellibiose, sucrose and trehalose, and did not show any activity towards raffinose (Table 3). Unlike the wild-type strain, the mutant utilized lactose but did not show any activity towards cellobiose and also did not utilize rhamnose, unlike the wild-type strain which actively utilized rhamnose (Table 3).

Purification of dextransucrase by PEG fractionation : The fractionation of dextransucrase present in cell free supernatant of mutant B640M by PEG-400 (25%, v/v) gave a specific activity of 10.5 U/mg (1.2 mg/ml) resulting in 13 fold purification. The wild-type *Leuconostoc mesenteroides* NRRL B-640 showed similar pattern of activity of dextransucrase purified under the same conditions (6).

Table 3. Carbohydrate fermentation profile of the wild-type *Leuconostoc mesenteroides* NRRL B-640 and mutant B640M after 48h.

S.No.	Carbohydrate	B640	B640M
1	Cellobiose	+++	--
2	Dextrose	+++	+++
3	Fructose	+++	+++
4	Galactose	+++	++
5	Lactose	--	++
6	Maltose	+++	+++
7	Mannitol	--	+
8	Melibiose	+++	+++
9	Raffinose	--	--
10	Rhamnose	++	--
11	Sucrose	+++	+++
12	Trehalose	+++	+++
13	Xylose	+	++

-- negative (red) + weakly positive (orange red) ++ fairly positive (orange) +++ strongly positive (yellow)

SDS-PAGE analysis and activity staining analysis of mutant dextransucrase : SDS-PAGE analysis of purified dextransucrase from the mutant B640M showed multiple bands after staining with CBB. There was a prominent band of approximately, 180 kDa molecular size (Fig. 1A, lane 1). The dextransucrase activity was confirmed by activity staining. The activity staining produced a single dextran-synthesizing band (Fig. 1B, lane 1) which corresponded to the band of approximately, 180 kDa molecular size that appeared with CBB staining (Fig. 1A, lane 1). This also confirmed the dextransucrase activity of the mutant. The molecular size of purified dextransucrase of mutant B640M was same as that of the wild-type *Leuconostoc mesenteroides* NRRL B-640, reported earlier (7).

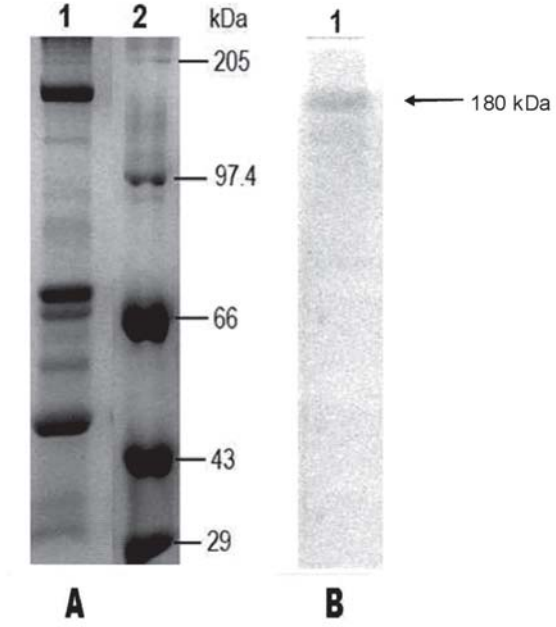

Fig. 1. Dextransucrase activity patterns by mutant; A: Coomassie Brilliant Blue staining, B: Activity staining using Schiff's reagent. Lanes: (1) Mutant B640M (2) Molecular Weight Marker

Analysis of dextran from selected mutant : On analysis of dextran from the mutant B640M, interestingly, it was found that the selected mutant gave higher dextran concentration than the wild-type strain. The mutant showed 21% higher dextran concentration (8.2 mg/ml) as compared with the wild-type *Leuconostoc mesenteroides* NRRL B-640 (6.8 mg/ml) (Table 4). The results of ^{13}C-NMR and ^{1}H-NMR spectra showed that purified dextran produced by dextransucrase of mutant contains linkages same as that of wild type strain (19). The SEM analysis of dextran from the mutant showed a porous or web like structure which also showed the similarity with wild-type strain (19). Owing to its small pore size distribution, the polymer can hold water and can be used as a texturing agent in food industry. Polysaccharides are widely used in foods as thickening, gelling, stabilizing, emulsifying and water-binding agents (20).

Conclusions

The optimized conditions to achieve the mutant with higher dextransucrase activity from *Leuconostoc mesenteroides* NRRL B-640 were found at 10^4 dilution factor (initial cell density 5.6 X 10^8) and UV exposure time of 30s. Eight mutants with 20% increase in dextransucrase activity were obtained. The mutant B640M showed maximum specific activity with an increase of 45.5% and increase of 20.5% in dextran production as compared to the wild-type *Leuconostoc mesenteroides* NRRL B-640. Unlike the wild-type strain, the mutant was resistant to kanamycin, claxacin and amikacin. The mutant utilized lactose but not the cellobiose unlike wild-type. The activity staining gave single band of 180 kDa molecular size, when compared to the gel with Coomassie Brilliant Blue staining. The ^{1}H-NMR, ^{13}C-NMR and SEM analysis of dextran from mutant B640M showed no difference from the wild-type. The dextrans are widely used in food, pharmaceutical and

cosmetics industries which require exploration of new species with higher enzyme or dextran production. The mutant B640M generated by UV-mutagenesis of *Leuconostoc mesenteroides* NRRL B-640 with enhanced dextransucrase activity and dextran production, thus may find their way for commercial applications.

Table 4. Comparison of dextran produced by wild type and mutant

Strains	Dextran conc. (mg/ml)	Increase %
Wild-type B-640	6.8	--
Mutant B640M	8.2	20.5

Acknowledgements

The research work was financially supported by a project grant from Council of Scientific and Industrial Research (CSIR), New Delhi, India to AG.

References

1. Robyt, J.F. (1986). Dextran. In: Encyclopedia of polymer science and technology Vol.4 (ed. Mark H.F., Bikales N.M., Overberger C.G. and Menges G.) John Wiley and Sons, pp. 752-767.
2. Purama, R.K. and Goyal, A. (2005). Dextransucrase production by *Leuconostoc mesenteroides*. Indian Journal of Microbiology, 2: 89-101.
3. Ferreira, L., Gil, M.H., Cabrita, A.M.S. and Dordick, J.S. (2005). Biocatalytic synthesis of highly ordered degradable dextran-based hydrogels. Biomaterials, 26: 4707-4716.
4. Aumelas, A., Serrero, A., Durand, A., Dellacherie, E. and Leonard, M. (2007). Nanoparticles of hydrophobically modified dextrans as potential drug carrier systems. Colloids and Surfaces B: Biointerfaces. 59: 74-80.
5. Purama, R.K., Agrawal, M., Majumder, A., Ahmed, S. and Goyal, A. (2008). Antibiotic sensitivity, carbohydrate fermentation and plasmid profiles of glucansucrase producing four *Leuconostoc* strains. Journal of Pure and Applied Microbiology, 2: 139-146.
6. Purama, R.K. and Goyal, A. (2009). Optimization of conditions of *Leuconostoc mesenteroides* NRRL B-640 for production of dextransucrase and its assay. Journal of Food Biochemistry, 33: 218-231.
7. Purama, R.K. and Goyal, A. (2008). Screening and optimization of nutritional factors for higher dextransucrase production by *Leuconostoc mesenteroides* NRRL B-640 using statistical approach. Bioresource Technology, 99: 7108-7114.
8. Goyal, A. and Katiyar, S.S. (1996). Regulation of dextransucrase productivity of *Leuconostoc mesenteroides* B-512F by the maintenance media. Journal of General and Applied Microbiology, 42: 81-85.
9. Tsuchiya, H.M., Koepsell, H.J., Corman, J., Bryant, G., Bogard, M.O., Feger, V.H. and Jackson, R.W. (1952). The effect of certain culture factors on production on dextransucrase by *Leuconostoc mesenteroides*. Journal of Bacteriology, 64: 521-526.
10. Nelson, N. (1944). A photometric adaptation of the Somoyogi method for the determination of glucose. Journal of Biological Chemistry, 153: 375-380.
11. Somoyogi, M. (1945). A new reagent for determination of sugars. Journal of Biological Chemistry, 160: 61-68.

12. Lowry, O.H., Rosebrough, N.J., Farr, A.L. and Randall, R.J. (1951). Protein measurement with the Folin phenol reagent. Journal of Biological Chemistry, 193: 265-275.

13. Barry, A.L. and Thornsberry, C. (1980). Susceptibility testing: diffusion procedures. In: Manual of Clinical Microbiology 3rd edn (ed. Lennette E.H., Balows A., Hausler W.J. Jr and Traunt J.P.) American Society for Microbiology, Washington D.C., pp. 463-474.

14. Kandler, O. and Weiss, N. (1986). Regular, non-sporing gram-positive rods. In: Bergey's Manual of Systematic Bacteriology Vol.2 (ed. Sneath P.H.A., Mair N.S., Sharpe M.E. and Holt J.G.) Williams and Wilkins, Baltimore, pp. 1208-1219.

15. Laemmli, U.K. (1970). Cleavage of structural proteins during the assembly of the head of bacteriophage T_4. Nature, 227: 680-685.

16. Holt, S.M., Al-Sheikh, H. and Shin, K.J. (2001). Characterization of dextran producing *Leuconostoc* strains. Letters in Applied Microbiology, 32: 185-189.

17. Dubois, M., Gilles, K.A., Hamilton, J.K., Rebers, P.A. and Smith, F. (1956). Colorimetric method for determination of sugars and related substances. Analytical Chemistry, 28: 350-356.

18. Fox, J.D. and Robyt, J.F. (1991). Miniaturization of three carbohydrate analyses using a micro-sample plate reader. Analytical Biochemistry, 195: 93-96.

19. Purama, R.K., Goswami, P., Khan, A.T. and Goyal, A. (2009). Structural analysis and properties of dextran produced by *Leuconostoc mesenteroides* NRRL B-640. Carbohydrate Polymers, 76: 30-35.

20. Khan, T., Park, J.K. and Kwon, J.H. (2007). Functional biopolymers produced by biochemical technology considering applications in food engineering. Korean Journal Chemical Engineering, 24: 816-826.

Current Trends in Biotechnology and Pharmacy
Vol. 5 (4) 1454-1461 October 2011, ISSN 0973-8916 (Print), 2230-7303 (Online)

A Preliminary Study on Bacteriological Infections of Surgical Wounds

K. Sobha[1*], P. Sarvani[1] and G. Krishna Murthy[2]
[1]Department of Biotechnology, RVR & JC College of Engineering
Guntur – 522 019, Andhra Pradesh, India
[2]Department of Microbiology, Guntur Medical College, Guntur – 522 004
Andhra Pradesh, India
[*] For Correspondence - sobhak66@gmail.com

Abstract

Surgical wound infections, better termed as Surgical Site Infections, are common and cannot be completely eliminated. But a reduction in the infection rate could have significant benefits like reduction in the postoperative morbidity and mortality, wastage of health care resources and finances. The general causes for increased predisposition to wound infections are pre-existing illness, prolonged operating time, the wound class and wound contamination. Technical problems with the operation, particularly bleeding, the amount of devitalized tissue generated, and the need for drains within the wound determine the risk of infection along with patient's general metabolic status which includes obesity and diabetes. Rigorous wound surveillance, a technically perfect operation along with the judicious use of prophylactic antibiotics would greatly aid in attaining minimum wound infection in any type of surgery.

Key Words: Surgery, Wound, Pus, Bacteria, Gram positive, Gram negative,Wound Surveillance, Morbidity, Mortality etc.

Introduction

One of the most common postoperative complications that results in significant morbidity and mortality, extended hospitalization and economic burden to the patients is the infection of surgical wounds. Efforts to minimize the rate of infection will definitely yield benefits in terms of both patient comfort and medical resources used (1). Any purulent discharge from a closed surgical incision, together with signs of inflammation of the surrounding tissue should be considered as wound infection, irrespective of whether micro-organisms can be cultured from the discharge (2). In 1992, the Surgical Wound Infection Task Force (SWITF) replaced the term "surgical wound infection" with "surgical site infection", to include infections of organs or spaces deep in the skin and soft tissues, such as peritoneum and bone. Surgical site infection is broadly classified into *incisional* (superficial) or *deep incisional* site infection and organ / space infection (3,4). Various independent and dependent factors that affect the susceptibility of any wound to infection include pre-existing illness, length of operation, wound class and contamination, extremes of age, malignancy, metabolic diseases, malnutrition, immunosuppression, cigarette smoking, remote site infection, emergency procedures and long duration of pre-operative hospitalization (5). Wound classification system divides the surgical patients into *clean, clean-contaminated*, *contaminated, and infected or dirty* as they enter

Vol. 5 (4) 1454-1461 October 2011, ISSN 0973-8916 (Print), 2230-7303 (Online)

the operating room. Within these categories, assessment of the following factors could be done: microbe-related risk factors, with *Staphylococcus aureus* and *Streptococcus pyogenes* (being particularly virulent); host-related factors with morbid obesity, protein-calorie malnutrition, diabetes, cancer and systemic infection; and operation - related risk factors including prolonged hospital stay before surgery, tissue trauma, poor hemostasis and foreign material in the wound (6). A report from the Scoliosis Research Society Morbidity and Mortality Committee on rates of infection after spine surgery based on 108, 419 procedures suggests that post surgical infection, even among skilled spine surgeons, is an inherent potential complication and recommends efforts to improve safety of care (7).

Studies on the effect of pre-existing illnesses on wound infection identified four independent risk factors viz., surgical procedures lasting more than 2 hours, wound contamination, three or more diagnoses at the time of discharge (excluding those related to surgical wound infections and their complications) and abdominal operations (8,9). Studies have repeatedly shown that the risk of wound infection is directly proportional to the duration of the operative procedure, risk reported to roughly double with every hour of the procedure (10,11). The judicious use of antibiotics and the use of an organized system of wound surveillance are the most effective means to reduce the wound infection rate (12). While procedures such as preoperative hair removal, use of adhesive drapes and wound irrigation are of small benefit, tissue level factors such as micro-environment and the presence of white cells and cellular products are important elements of the local immune response. Hence their manipulation would certainly be useful in planning wound management strategies.

It is a known fact that the postoperative surgical infection depends upon the type of operative approach: laparoscopy with low incisional infection but relatively higher degree of organ space infection (OSI) as compared to open surgery. The study on the risk of postoperative surgical infections using a multivariate analysis of factors associated with laparoscopic appendectomy from the NSQIP database suggested that the degree of risk of infection depends on the clinical profile of a surgical patient in addition to the operative procedure adopted (13). It is therefore important for the clinicians to recognize the differences in risk and choose an appropriate operative approach for the benefit of the patient.

Burke (1961), (14) demonstrated the importance of the timely use of prophylactic antibiotics in surgery. Haley et al. (1) reported that antibiotic prophylaxis can decrease post-operative morbidity, shorten hospital stay and reduce overall costs attributable to infection. The wound classification scheme devised by the National Research Council (1964) and the guidelines published (15,16) regarding the selection and use of prophylactic antibiotics to treat surgical wounds are to be followed for reducing the risk of infection. The dose of prophylactic antibiotics should not be smaller than the standard therapeutic dose of the drug and a single prophylactic dose is generally effective and preferred to multiple doses (17). However, inappropriate and indiscriminate use of prophylactic antibiotics may increase costs and the emergence of resistant organisms. Also, the potential toxicity of antibiotics is an important risk of antibiotic prophylaxis.

The rigorous surveillance and reporting of wound infection rates have been advocated as the best way to decrease wound infection rates (12, 18). The present study is aimed at

Vol. 5 (4) 1454-1461 October 2011, ISSN 0973-8916 (Print), 2230-7303 (Online)

understanding the bacteriological infections of surgical wounds in patients undergoing treatment in a Government General Hospital and the kind of antibiotics used to minimize the post-operative morbidity in these patients.

Materials and Methods

The current study collected 50 wound infections developed after clean elective or emergency surgery at Government General Hospital, Guntur. The processing of the collected wounds were done at Department of Microbiology, Guntur Medical College. Each patient's case history was collected in a standard format including the age, sex, diagnosis, nature of operation, post-operative period, nutritional status, diabetic and HIV status, past medical history, family history, socio-economic status of the person under study, pre-operative antibiotics used if any, antibiotic sensitivity etc. Swabs which were sterilized in hot air oven at 160^0C for 1 hour were used for collection of samples from the infected surgical wounds. The samples were then subjected to different tests like Gram's staining, cultured on different types of media like basal, enriched and differential media and were then tested for biochemical constituents to identify the bacterial infection. Biochemical tests included IMVIC, catalase, oxidase, urease and coagulase tests and simultaneously the culture was spread on agar plates and incubated overnight to know the antibiotic sensitivity by Kirby-Bauer disc diffusion method. The commonly administered antibiotics which were used in our study included Tetracycline, Gentamycin, Ciprofloxane, Impenem, Amikacin, Metrogyl, Monocef, Amoxycillin, Methicilin, Azithromycin, Magenx and Cefoperazone.

Results and Discussion

Samples selected, screened and included in the present study are fifty only (n=50) although hundreds of samples were collected from patients of different wards. Although both blood and pus samples were collected from patients with and without surgical site infections, only surgical site infections are discussed in this study. The data pertaining to the samples collected are presented in Tables 1 to 7. Results of the biochemical tests performed are presented in Figs. 3 to 8.

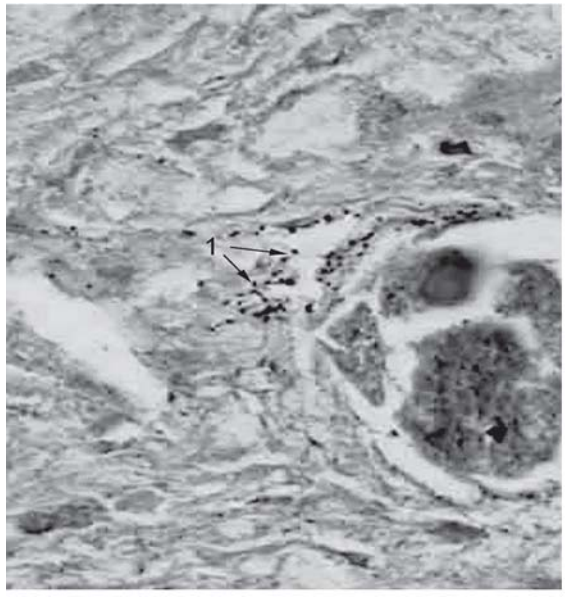

Fig. 1. Gram Positive Organism

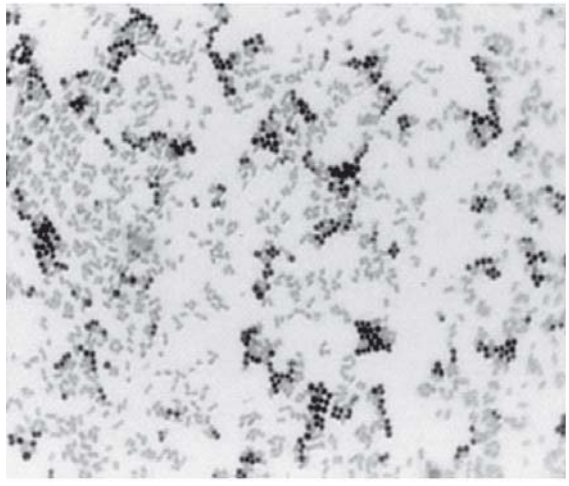

Fig. 2. Gram Negative Organism

Table 1. Type of Surgical wound samples collected for the present study

S.No	Type of Surgery	Number	Percentage%
1	Major	34	68
2	Minor	16	32

Table 2. Surgical wound samples classified based on the type of surgery performed

S.No	Type of Surgery Performed	Number	Percentage%
1	Elective	20	40
2	Emergency	30	60

Table 3. Medical status of the patients from whom surgical wound samples were collected

S.No	Medical Status	Number	Percentage%
1	Diabetic	33	66
2	Non Diabetic	17	34

Table 4. Social Status of the patients from whom surgical wound samples were collected

S.No	Social Status	Number	Percentage%
1	Poor	42	84
2	Middle/upper middle class	8	16

Table 5. Analysis of the collected surgical wound samples based on the type of organism obtained on culture

S.No	Type of Organism	Number	Percentage%
1	Single Pathogen	9	18
2	Mixed Pathogen	41	82

Table 6. Type of organisms most commonly found in surgical wound infections

S.No	Common Organism	Number	Percentage%
1	*Staphylococcus*	33	66
2	Gram Negative bacteria	44	88

The most common single pathogen accounting for 66% of the isolates was *Staphylococcus sp*., mostly *aureus* (Gram +ve; Fig. 1). Our observations are in compliance with the results of the recent studies reported (19,20). Among gram –ve bacteria (Fig. 2), *Escherichia coli*, *Klebsiella sp*. and atypical coliforms accounted for 88% of the isolates. Mixed infections were noticed in 41 wound samples accounting for about 82% of the wound infections studied and single pathogen infections were found in 9 samples accounting for the remaining 18%. It is also observed that the infection rate is high in major surgeries (34) and

Table 7. Sensitivity of the isolates to various commonly used antibiotics

S. No	Common Antibiotics used for different organisms	Number	Percentage%
1	Gentamycin	21	42
2	Tetracyclin	13	26
3	Amikacin	16	32
4	Co-trimoxazole	8	17.1
5	Ampicillin	11	22
6	Ciprofloxacin	13	26
7	Ceftriaxone	21	42
8	Imipenem	10	20
9	Azithromycin	10	20
10	Cefoperazone	11	22
11	Ceftazidime	2	4

contributed 68% of the observed infections while minor surgeries for 32%. As expected, we observed high infection rates in emergency surgeries (60%) while in elective surgeries, the infection rate is only 40%. It is also evident from the data that the infection rate is high in the low socio-economic strata of the people and accounted for 84% of the infection and in comparison, in the middle/upper middle class, the infection rate is 16%, the difference could be well attributed to the hygiene and nutritional status of the individuals. Diabetics had an infection rate of 66% and non-diabetics had an infection rate of only 34%.

The most common antibiotics for which the majority of the isolates were sensitive were found to be Gentamycin (42%) and Ceftriaxone (42%) followed by Amikacin (32%), Ciprofloxacin (26%), Tetracycline (26%), Cefoperazone (22%) and others as shown in Table 7. A primary strategy for preventing and treating wound infection in chronic wounds is the use of topical antiseptics and wound irrigating agents. A study was conducted with five clinically used antiseptics and wound irrigating agents (Prontosan, Lavasept, Braunol, Octenisept, and Betaisodona) in the presence or absence of 42 wound dressings against *Staphylococcus aureus* and antibacterial activity was assessed by disc diffusion assay. Analysis of the antimicrobial activity of antiseptics and wound irrigating agents used with commercially

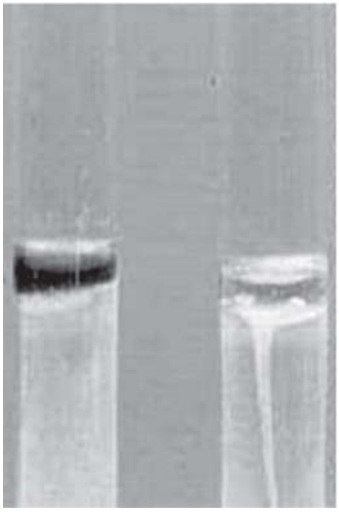

Fig. 3. Indole test

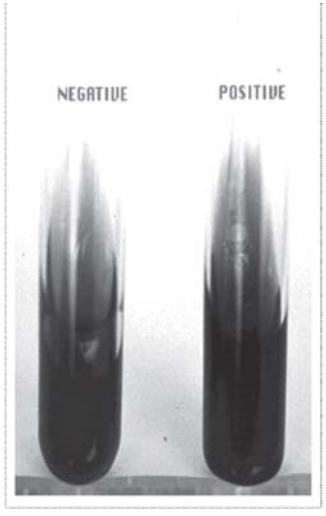

Fig. 4. Citrate utilization test

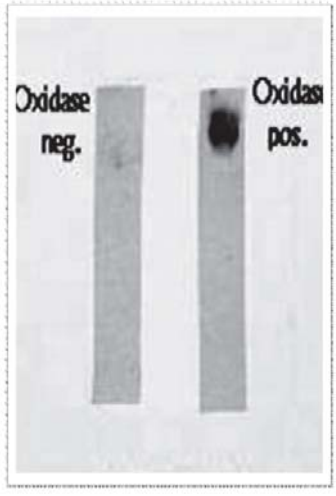

Fig. 5. Oxidase Test

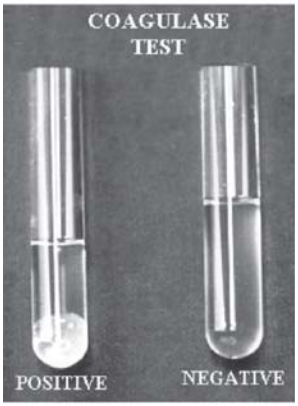

Fig. 6. Coagulase Test

Fig. 7. Spread Plate Technique

Fig. 8. Antibiotic Sensitivity Pattern

available wound dressings revealed that commonly used wound dressings dramatically reduce antibacterial activity of clinically used antiseptics and wound irrigating agents in vitro (21). The results of this study could be verified by clinicians for effective wound management in their patients.

The various factors that contribute to the wound infections in a tertiary care hospital like Government General Hospital, Guntur include the host factors, the hospital factors and the environmental factors. The observance of *Staphylococcus aureus* as the most common single pathogen isolate indicates that this organism is still the common inhabitant of human skin and the hospital environment. In mixed infections, gram –ve bacilli are very common as compared to others (22). A study on treatment regimen with vancomycin in 309 pediatric patients with post-operative infections including wound-related (37.2%), localized infection (12.9%), catheter-related infections (9.4%), meningitis (8.7%) or endocarditis (6.8%) confirmed pathogens in 79 cases: 28 cases of methicillin-resistant *Staphylococcus epidermidis* (35.4%) and 25 of methicillin resistant *Staphycococcus aureus* (31.6%) (19). The study concluded that a common vancomycin dosing regimen, 40 mg/kg/day, was not high enough to achieve trough levels of over 10 mg/L in pediatric patients and that an increase in initial dose of vancomycin be considered in pediatric patients. Results of the French OPIDIA study on Management of patients hospitalized for diabetic foot infection (20) indicated that Gram-positive cocci, and *Staphylococcus aureus*, in particular, were by far the most frequently isolated microorganisms from the wounds mostly located on the toes and forefoot.

Infection rate in major surgeries is higher than in minor surgeries and this can be due to factors like involvement of more personnel during surgical procedure, long duration of exposure and more handling of tissues and blood. Similarly, the infection rate is higher in emergency procedures than in elective owing to inadequate pre-operative preparation of the patient and absence of prophylactic antibiotic treatment. Nutritional and general health status of the patient is another significantly influencing factor in determining the occurrence of wound infections. Even in otherwise normal individuals with metabolic diseases like *Diabetes mellitus*, the infection rates would be high. Also, stress in patients undergoing surgeries is another causative factor for increased rate of wound

Vol. 5 (4) 1454-1461 October 2011, ISSN 0973-8916 (Print), 2230-7303 (Online)

infections as stress is well known to increase blood glucose levels and thus increase susceptibility to infection. Although several antibiotics are available in the market, the drugs of choice for pre and post surgical procedures are Gentamycin, Ceftraxone and Amikacin.

In recent years, intensive studies are being carried out for identifying potential biomedical applications of nanoparticles. One such investigation suggested that cationic fullerenes (BF6) have clinical potential as antimicrobial photosensitizer for superficial infections where red light is not needed to penetrate tissue (23). In the study, two stable bioluminescent gram negative bacteria viz., *Proteus mirabilis* and *Pseudomonas aeruginosa* and a low light imaging system were employed to follow the progress of the infection noninvasively in real time using mouse models. Results of the study suggested that there was a light-dose-dependent reduction of bioluminescence from the wound not observed in control groups (light alone or BF6 alone). Further investigations need to be carried out to explore the clinical potential of cationic fullerenes as antimicrobial photosensitizers and if proven, could be used for superficial infections where red light is not needed to penetrate tissue.

Acknowledgements

The authors express their sincere thanks to the Principals of the Guntur Medical College and the RVR & JC College of Engineering for granting permission to collect the patients' samples and use the laboratory facilities for this study. Also, the second author expresses her sincere thanks to the Head of the Department of Biotechnology, RVR & JC College of Engineering for the encouragement and support.

References

1. Haley, R.W., Schaberg, D.R., Crossley, K.B., Von Allmen, S.D. and McGowan JE Jr. (1981). Extra charges and prolongation of stay attributable to nosocomial infections: a prospective interhospital comparison. Am. J. Med., 70: 51-58.

2. Nandi, P.L., Soundara Rajan, S., Mak, K.C., Chan, S.C. and So, Y.P. (1999). Surgical Wound Infection. HKMJ, 5: 82-86.

3. Garner, J.S., Jarvis, W.R., Emori, T.G., Horan, T.C. and Hughes, J.M. (1988). CDC definitions of nosocomial infections. Am. J. Infect. Control, 16: 128-140.

4. Horan, T.C., Gaynes, R.P., Martone, W.J., Jarvis, W.R., Emori, T.G. (1992). CDC definitions of nosocomial surgical site infections 1992: a modification of CDC definitions of surgical wound infections. Am. J. Infect. Control, 20: 271-274.

5. Sawyer, R.G. and Pruett, T.L. (1994). Wound infections. Surg. Clin. North Am., 74: 519-536.

6. Rubin, R.H. (2006). Surgical Wound Infection: epidemiology, pathogenesis, diagnosis and management. BMC infectious diseases, 6: 171-172.

7. Smith, J.S., Shaffrey, C.I., Sansur, C.A., Berven, S.H., Fu, K.M., Broadstone, P.A., Choma, T.J., Goytan, M.J., Noordeen, H.H., Knapp, D.R. Jr., Hart, R.A., Donaldson, W.F., 3rd, Polly, D.W. Jr., Perra, J.H., Boachie-Adjei, O. (2011). Retrospective review of a prospectively collected database. Spine (Phila Pa 1976), 36(7): 556-63.

8. Haley, R.W, Culver, D.H., Morgan, W.M., White, J.W., Emori, T.G. and Hooton, T.M. (1985). Identifying patients at high risk of surgical wound infection. A simple multivariate index of patient susceptibility and wound contamination. Am. J Epidemiol., 121: 206-215.

9. Garibaldi, R.A., Cushing, D. and Lerer, T. (1991). Risk factors for post-operative infection. Am. J. Med. , 19 (Suppl 3B): 125S-157S.

10. Cruse, P.J. and Foord, R. (1973). A five-year prospective study of 23, 649 surgical wounds. Arch. Surg., 107: 206-210.

11. Cruse, P.J. and Foord, R. (1980). The epidemiology of wound infection: a 10-year prospective study of 62,939 wounds. Surg. Clin. North Am., 60: 27-40.

12. Olson, M.M. and Lee, J.T. Jr. Continuous, 10 year wound infection surveillance. Results, advantages, and unanswered questions. Arch. Surg., 125: 794-803.

13. Fleming, F.J., Kim, M.J., Messing, S., Gunzler, D., Salloum, R. and Monson, J.R. (2010). Balancing the risk of postoperative surgical infections: a multivariate analysis of factors associated with laparoscopic appendectomy from the NSQIP database. Ann Surg., 252(6): 895-900.

14. Burke, J.F. (1961). The effective period of preventive antibiotic action in experimental incisions and dermal lesions. Surgery, 50: 161-168.

15. Page, C.P., Bohnen, J.M., Fletcher, J.R., Mc Manus, A.T., Solomkin, J.S. and Wittmann, D.H. (1993). Antimicrobial prophylaxis for surgical wounds. Guidelines for clinical care. Arch. Surg., 128: 79-88.

16. Yuen, K.Y. (1994). Prophylactic antibiotics in surgery. The College of Surgeons of Hong Kong Newsletter. Aug: 11-14.

17. Mc Donald, M., Grabsch, E., Marshall, C. and Forbes, A. (1998). Single-versus multiple-dose antimicrobial prophylaxis for major surgery: a systematic review. Aust. NZ J. Surg., 68: 388-396.

18. Delgado-Rodriguez, M., Sillero-Arenas, M., Medina-Cuadros, M. and Martinez-Gallego, G. (1997). Nosocomial infection in surgical patients: comparison of two measures of intrinsic patient risk. Infect. Control Hosp. Epidemiol., 18: 19-23.

19. Kim, D.I., Im, M.S., Choi, J.H., Lee, J., Choi, E.H. and Lee, H.J. (2010). Therapeutic monitoring of vancomycin according to initial dosing regimen in pediatric patients. Korean J Pediatr, 53(12): 1000-5.

20. Richard, J.L., Lavigne, J.P., Got, I., Hartemann, A., Malgrange, D., Tsirtsikolou, D., Baleydier A. and Senneville E. (2010). Management of patients hospitalized for diabetic foot infection: Results of the French OPIDIA study. Diabetes Metab. (In press)

21. Hirsch, T., Limoochi-Deli, S., Lahmer, A., Jacobsen, F., Goertz, O., Steinau, H.U., Seipp, H.M. and Steinstraesser, L. (2011). Antimicrobial activity of clinically used antiseptics and wound irrigating agents in combination with wound dressings. Plast Reconstri Surg., 127(4): 1539-45.

22. Shaw, E.J., Datta, N., Jones, G., Marr, F.M. and Froud, W.J.B. (1973). Effect of stay in hospital and oral chemotherapy on the antibiotic sensitivity of bowel coliforms. J. Hyg. Camb., 71: 529.

23. Lu, Z., Dai, T., Huang, L., Kurup, D.B., Tegos, G.P., Jahnke, A., Wharton, T. and Hamblin, M.R. (2010). Photodynamic therapy with a cationic functionalized fullerene rescues mice from fatal wound infections. Nanomedicine (Lond.), 5(10): 1525-33.

Current Trends in Biotechnology and Pharmacy
Vol. 5 (4) 1462-1468 October 2011, ISSN 0973-8916 (Print), 2230-7303 (Online)

Callus Induction and Organogenesis in *Sesamum indicum* L. CV. E 8

Srinath Rao* and Havgeppa N. Honnale
Plant Tissue Culture and Genetic Engineering Laboratory
Department of Post-Graduate Studies and Research in Botany, Gulbarga University
Gulbarga - 585 106, Karnataka, India
*For Correspondence - srinathraom@rediffmail.com

Abstract

Hypocotyl and cotyledon explants excised from 5-7 days old in vitro grown seedlings of sesame were inoculated for callus induction and direct regeneration on MS medium supplemented with different concentrations(1-4mg/l) and combinations of auxins viz., NAA, 2, 4-D, 2, 4, 5-T, IAA and IBA. Hypocotyl and cotyledon explants were found suitable for induction of callus on MS medium supplemented with NAA at 2.0mg/l. Hypocotyl was found to be a better explant for the induction of maximum callus. Cytokinins like BAP, Kn and TDZ were used for regeneration from callus. Regeneration from callus was not obtained on any of the cytokinins supplemented media. Direct regeneration from hypocotyl (40%) explant was obtained on MS medium supplemented with 1.0 mg/l Kn compared to other cytokinins. The plant-lets were subsequently rooted on MS medium supplemented with IBA (3.0 mg/l).

Keywords: *Sesamum indicum,* Callus induction, organogenesis, NAA, Kn, IBA

Introduction

Sesamum indicum L. is commonly known as sesame or the 'Queen of oil seeds' belongs to the family Pedaliaceae, consists of 40 species, of these 7 are distributed in India (1) and has been cultivated in both tropical and temperate areas from ancient times (2). Geographically they are distributed in Tropical Africa, Madagascar, Tropical Australia and Eastern Islands of Malaysian Archipelago. India ranks first, both in the area and production of *Sesamum* in the world.

The seeds contain powerful antioxidants called lignans (sesamins), sesamolin and phytosterol which impart a high degree of resistance against oxidative rancidity (3, 4) They also contain lecithin which has antioxidant and hepatoprotective activity, it has cancer preventive capability (5) and oil is used in pharmaceutical aid as a solvent for intramuscular injections. It has nutritive, demulcent and emollient properties (6) and also has been used as a laxative (7) In India; Sesame oil is used as an antibacterial mouthwash, to relieve anxiety and insomnia (8) and also used for treating nasal mucosa dryness (9)

In general the productivity of sesame is relatively low as compared to that of other oil crops because the cultivation of sesame is restricted by poor soil (10, 11) recently cell culture techniques have been successfully utilized to obtain useful variants such as high lysine mutants, salts, aluminum and herbicide

Vol. 5 (4) 1462-1468 October 2011, ISSN 0973-8916 (Print), 2230-7303 (Online)

tolerant cell lines which may represent a new and useful source of genetic variations (2).

Keeping this background in view, the present investigation was taken up to develop protocols for induction of callus and regeneration of plantlets from various seedling explants. These techniques along with genetic engineering can be used for the improvement of this species. In the present investigation *in vitro* raised explants were tried for the induction of callus its further growth and their efficiency for direct regeneration. Effects of different auxins on callus initiation from different explants on MS-medium and efficient reproducible protocol has been given for plant regeneration from hypocotyl explants of *Sesamum indicum*.

Material and Methods

Seeds of *Sesamum indicum* L. genotype E-8 were obtained from Agriculture Research Station, Raichur. The seeds were soaked in solution containing Bavistin (1.0%) a fungicide and dilute detergent (Teepol) for 10-15 min, and then the seeds were washed thoroughly in running tap water, followed by surface sterilization with 0.1% mercuric chloride for 45-50 seconds under sterile conditions and subsequently the seeds were rinsed thoroughly in sterile distilled water for 3-4 times to remove the traces of mercuric chloride. They were then germinated on pre-sterilized culture tubes on Filter Paper Bridge, cotyledons and hypocotyls were excised from 5-7 days old *in vitro* raised seedlings, and used as explants for callus induction and regeneration.

They were then inoculated on to MS medium (12) supplemented with various auxins viz., 2,4-Dichloro phenoxy acetic acid (2,4-D) 2, 4, 5-Trichloro phenoxy acetic acid (2,4,5-T) a-Naphthalene acetic acid (NAA) Indole acetic acid (IAA) and Indole butyric acid (IBA) and cytokinins 6-Benzyl amino purine (BAP) and 6-Furfurilaminopurine (Kn) alone or in combination. The pH of the medium was adjusted to 5.6 – 5.8 prior to autoclaving at 121 ºC for 20 min.. The cultures were maintained at 25 ± 2 ºC under a light intensity of 3000 lux provided by cool-white fluorescent lamps. The callus was maintained by regular sub-culture at 4 weeks interval on fresh medium with the same composition or on regeneration media. The data obtained was subjected to statistical analysis.

Results and Discussion

Different explants were cultured on MS medium supplemented with various auxins and cytokinins in varied combinations to assess the morphogenetic potential of the explant. In the present investigations it was noticed that callus induction could be obtained from both cotyledon and hypocotyl explants however it was possible to obtain shoot regeneration only from hypocotyl explants. Both the explants cotyledons and hypocotyls showed excellent response for callus induction. However, hypocotyls were found superior over cotyledons. Callus induction occurred within 15-20 days on MS medium containing different concentrations of auxins (2, 4-D, 2, 4, 5-T, NAA, IAA and IBA) and cytokinins (BAP & Kn).

Callus induction was observed in cultures on MS-medium supplemented with auxins viz., NAA and IAA at different concentration (1.0 - 5.0 mg/l). From the results, it is clear that among the other auxins used NAA was found more effective for callus induction followed by IAA however medium supplemented with 2,4-D and 2,4,5-T even at all the concentrations used (1.0 - 3.0mg/l) was not suitable for the induction of callus. However, somatic embryo like structures were initiated which ultimately turned brown and died.

At 2.0 mg/l NAA maximum amount of callus (4580 ± 0.12 mg) was formed (Plate-I a)

when hypocotyls were used as explants followed by cotyledon explants at 4.0 mg/l NAA (4100 ± 0.11 mg; Plate-I b). As the concentration of NAA increased the amount of callus formation decreased (Table - 1). However, other auxins 2,4,5-T and IAA showed very poor response with respect to induction and further growth of the callus. Further enhancement of callus formation was observed when MS-medium was supplemented with NAA + BAP.

In the present studies hypocotyl explants responded well producing high amount of callus on medium supplemented with NAA (2.0 mg/l) + BAP (1.0 mg/l) (Table-2; Plate-I c&d). In earlier reports (13-15) the same combination of growth regulators and explant proved to be efficient for callogenesis in this species. However, in another report (16) on this species var. Mtwara-2 it has been observed that the same combination was unsuccessful in induction of callus. The diverse results reported shows that response to callogenesis and organogenesis is highly genotype dependent in *S. indicum*. Callus induction has been reported from hypocotyl explants in other oil seed plants *viz.,* Mustard (17-20) Sunflower (21, 22) Groundnut (23) and Soybean (24-26)

Regeneration Studies

In order to achieve the regeneration from callus, hypocotyls and cotyledon derived calli pieces (~ 200mg) were transferred to MS-medium supplemented with BAP, Kn and TDZ (1.0 - 3.0 mg/l) along with $AgNO_3$ (1.0 - 3.0mg/l). In all the combinations callus did not responded for the regeneration (data not shown) however, farther enhancement of callus was noticed in all the cultures with negligible numbers of roots. In earlier reports (14, 26) it has been observed that regeneration from callus was not induced.

Table 1. Effect of auxins on induction of callus in *Sesamum indicum*

Growth Hormone	Conc mg/l	Hypocotyl			Cotyledon		
		Fresh wt. (mg/g)	Drywt. (mg/g)	Frequency (%)	Fresh wt. (mg/g)	Dry wt. (mg/g)	Frequency (%)
NAA	1	3230 ± 1.55	308.66 ± 4.48	80	3060 ± 0.00	312.66 ± 1.76	80
	2	4580 ± 0.12	488.00 ± 1.76	90	2490 ± 0.00	254.66 ± 2.02	70
	3	4140 ± 0.00	434.66 ± 2.40	70	3700 ± 0.11	383.00 ± 1.15	70
	4	3100 ± 0.00	274.33 ± 3.38	90	4100 ± 0.11	432.66 ± 1.76	82
	5	1940 ± 0.00	114.66 ± 2.02	85	3120 ± 0.00	318.66 ± 1.85	90
IAA	1	2230 ± 1.00	273.00 ± 1.73	91	1810 ± 0.00	174.66 ± 2.02	89
	2	2110 ± 1.20	245.66 ± 1.85	86	1920 ± 0.00	252.66 ± 1.76	86
	3	1950 ± 1.15	212.66 ± 1.45	92	1610 ± 0.00	167.00 ± 2.08	90
	4	1860 ± 0.00	194.00 ± 2.64	80	1500 ± 0.00	174.33 ± 2.33	70
	5	1570 ± 0.00	182.66 ± 1.76	80	1310 ± 0.00	151.66 ± 0.88	75

Data represents average of three replicates each replicate consists of 25 cultures. Mean ± SE

Hypocotyl and cotyledon explants were used to induce direct regeneration on MS medium supplemented with BAP and Kn (1.0 - 3.0 mg/l), from the observations it is clear that hypocotyl explants proved to be better explants for the induction of multiple shoots and cotyledon explants resulted in inducing callus. Only KN at 1.0 mg/l induced multiple shoots

Table 2. Effect of NAA (2.0 mg/l) in combination with cytokinins on induction and growth of callus in *Sesamum indicum*

Auxin + Cytokinin	Conc. (mg/l)(mg/l)	Fresh wt. (mg/g)	Hypocotyl Dry wt. (mg/g)	Frequency (%)
NAA + BAP	2.0 + 0.5	5160 ± 0.00	616 ± 3.05	89
	2.0 + 1.0	5690 ± 0.00	635 ± 2.02	92
	2.0 + 1.5	5580 ± 0.00	627 ± 1.45	86
NAA + Kn	2.0 + 0.5	4890 ± 0.00	512 ± 1.45	91
	2.0 + 1.0	4870 ± 0.00	502 ± 1.76	90
	2.0 + 1.5	4690 ± 0.00	494 ± 2.40	87

Data represents average of three replicates each replicate consists of 25 cultures. Mean ± SE

Table 3. Effect of Kn on Direct regeneration of multiple shoots in *Sesamum indicum*

Cytokinin	Conc. mg/l	Hypocotyl	
		No. of multiple shoots (SE±)	Frequency (%)
Kn	1.0	5.26 ± 0.60	40
	2.0	3.40 ± 0.25	40
	3.0	2.80 ± 0.17	40

Data represents average of three replicates each replicate consists of 25 cultures. Mean ± SE

Table 4. Effect of IBA on induction of roots in *Sesamum indicum*

Growth Hormone	Conc. mg/l	No. of multiple roots (SE±)	Frequency (%)
IBA	1.0	06.50 ± 0.66	70
	2.0	10.00 ± 0.37	80
	3.0	15.50 ± 0.46	90
	4.0	05.30 ± 0.68	80

Data represents average of three replicates each replicate consists of 25 cultures. Mean ± SE

(5.26 ± 0.60) with 40% frequency (Table-3; Plate-I e, f) after 20 days of growth period, multiple shoots were green elongated and healthy. However, with an increase in the concentration of KN a gradual decrease in number of shoots (2.80 ± 0.17) per explant was observed. The shoots produced at higher concentration of Kinetin were very weak, however on BAP supplemented medium only induction of callus was noticed from both the explants.

It has been reported earlier (15,28)that callus derived from hypocotyls and cotyledon explants when cultured on MS medium fortified with BAP, NAA, IAA and IBA induction of green shoot buds were noticed, which failed to grow further.

Investigations were also carried out to study the effect of cytokinins BAP and KN for induction of shoots directly from hypocotyl and cotyledon explants. Regeneration was achieved only from the hypocotyl explant on KN at lower concentrations, on the other hand cotyledon explant completely failed to regenerate in all the combinations & concentration of cytokinins tested. From the literature it is very clear that no reports are available on direct regeneration from hypocotyls as an explant. There are reports that only cotyledon explants were responsive to organogenesis in variety Mtwara-2 (16,28) in other 10varieties (14) (variety not mentioned). Our results are in agreement with earlier work (15) that BAP supplemented media did not support organogenesis in cv. VRI-1 of this species.

This shows that organogenesis as callogenesis is also highly dependent on genotype. In our investigation organogenesis was not obtained on BAP supplemented media however earlier reports mentioned above have reported BAP as suitable cytokinin for induction of shoots. For the induction of roots, 25-30 days old elongated (4-5cm) shoots were separated carefully and were transferred to medium supplemented with IBA and IAA at 1.0 - 3.0 mg/l. It was noticed that only IBA at 3.0 mg/l induced maximum number of roots (15.50 ± 0.46) from the cut ends of plants which are thick and elongated (Table-4; Plate-I g, h) with 90% frequency recorded. Rooted plantlets were transferred on half strength media for two weeks for hardening. The roots become strong and thick on this medium. After hardening the shoots were transferred to pots containing sterile vermiculate and later established in soil in the glasshouse, where 50% of them survived and resumed growth (Plate-1).

References

1. Subramanian, M. (2003). Wide crosses and chromosome behavior in *Sesamum, Madras Agric. J.,* 90(1-3): 1-15.

2. Tae Ho Kwon., Toshinori A. B. E. and Takeo Sasahara., (1993). Efficient Callus Induction and Plant Regeneration in *Sesamum* species, Plant tissue Culture Letters, 10(3): 260-266.

3. Kato, M. J., Chu, A., Davin, L. B. and Lewis, N. G. (1998). Biosynthesis of antioxidant lignans in *Sesamum indicum* seeds. Phytochemistry, 47**:** 583-591.

4. Sirato-Yasumoto, S., Katsuta, M., Okuyama, Y., Takahashi, Y. and Ide T. (2003). Effect of Sesame seeds rich in sesamin and sesamolin on fatty acid oxidation in liver, J. Agr. Food Chem, 49: 2647-2651.

5. Beckstrom-Sternberg, S. M. and Duke, J. A. (1994a). "The Phytochemical database", ars-genome. cornell.edu/cgi bin/WebAce/ webac?db=phyochemdb

6. Tyler, V. E., Brady L. R. and Robbers J. E. Lipids. (1976). In:Pharmacogonosy, Lea & Febiger, Philadelphia, PA. p:121-122.

7. Dark Graham., On-line medical dictionary, (1998). www.grylab.ac.uk/cgi-bin/omd?sesame+oil

8. Annussek, G. (2001). Sesame oil. In: Gale encyclopedia of alternative medicine, Gale group.

9. Johnson, J., Bratt, B. M., Michel-Barron, Glennow, C. and Peruson B. (2001). Pure sesame oil vs isotonic sodium chloride solution as treatment for dry nasal mucosa. Arch. Otolaryngol Head Neck Surg, 127: 1353-1356.

10. Evans, D. A., Sharp, W. R. and Bravo, J. E. (1984). Cell culture methods for crop improvement. In: In Handbook of plant cell culture: crop species. Eds. W. R. Sharp, D. A. Evans, P. V. Ammirato and Yamada, Y. Macmillan Publishing Co, New York. 47-68.

11. George, L., Bapat, V. A. and Rao, P. S. (1987). *In vitro* multiplication of sesame (Sesamum indicum) through tissue culture. Ann. Bot., 60:17-21.

12. Murashige, T. and Skoog, F. (1962). A revised medium for rapid growth and bioassay with tobacco tissue cultures, Physiol. Plantatrum, 15: 473-497.

13. Shoji, K., Masuda, K., Sugai, M. and Kobayashi, T. (1988). Cytologia, 53: 205-211.

14. Taskin, K. M. and Turgut, K., (1997). *In vitro* regeneration of Sesame (*S. indicum* L.). Tr. J. Bot., 21: 15-18.

15. Baskaarana, P. and Jayabalan, N. (2006). *In vitro* mass propagation and diverse callus orientation on *Sesamum indicum* L. – an important oil plant, Journal of Agricultural Technology, 2(2):259-269.

16. Beatrice, W. A., Samuel Gudu., Augustino, O., Onkware., Anders Carlsson, A. and Margareta Welander. (2006). *In vitro* regeneration of Sesame (*Sesamum indicum* L.) from seedling cotyledon and hypocotyl explants, Plant Cell, Tissue and Organ Culture, 85(2): 235-239.

17. Yuxiu Zhang., Jin Xu., Lu Han., Wei Wei., Ziqiu Guan., Lin Cong. and Tuanyao Chai. (2006). Efficient shoot regeneration and *Agrobacterium* mediated transformation of Brassica juncea, Plant Molecular Biology Reporter, 24: 255a-255.

18. Sethi, U., Basu, A., Guha-Mukherjee, S. (1990). Control of cell proliferation and differentiation by modulators of ethylene biosynthesis and action in *Brassica* hypocotyl explants, *Plant Sci.,* 69. 225-229.

19. Radke, S. E., Turner, J. C. and Facciotti , D. (1992). Plant Cell Rep., 11: 499-505.

20. Gupta, V., Agnihotri, A., Jagannathan, V. (1990). Plant regeneration from callus and protoplasts of *Brassica nigra* (IC 217) through somatic embryogenesis, Plant Cell Reports, 9: 427-430.

21. Paterson, K. E. and Everett, N. P. (1985). Regeneration of *Helianthus annuus* inbreeds plants from callus, Plant Science, 42: 125-132.

22. Piubello, S. M. and Caso, O. H. (1986). *In vitro* culture of sunflower (*Helianthus annuus* L.) tissues, Phyton. Int. J. Exp. Bot., 46(2): 131-137.

23. Venkatachalam, P., Kavikishor, P. B. and Jayabalan, N. (1997). High frequency

somatic embryogenesis and efficient plant regeneration from hypocotyl explants of groundnut (*Arachis hypogia* L.), Current Science, 72(4): 271-275.

24. Hammatt, N. and Davey, M. R. (1988). Isolation and culture of Soyabean hypocotyl protoplast, In Vitro Cell Dev. Biol. J. Tissue Cult. Assoc., 24(6): 601-604.

25. Horn, M. E., Martin, B. A. and Widholm, J. M. (1992). Phototrophic growth of soyabean in suspension culture Z. optimization culture medium and conditions, Plant Cell Tissue and Organ Culture, 30(2): 85-91.

26. Horn, M. E. and Widholm, J. M. (1994). Photoautotrophic growth of soybean cells in suspension culture 4 free amino acid pools and the effect of nitrogen on chlorophyll leaves, Plant Cell Tissue and Organ Culture, 39(3): 245-250.

26. Chae, Y. A., Park, S. K. and Anand I. J. (1987). Selection *in vitro* for herbicide tolerant cell lines of *Sesamum indicum* 2: Selection of herbicide tolerant calli and plant regeneration, Korean Journal of Plant Breeding, 19: 5-80.

27. Rajender Rao, K. and Vaidyanath, K. (1997). Callus induction and morphogenesis in sesame (*Sesamum indicum* L.), Advances in Plant Sciences, 10: 21-26.

28. Seo , H. Y., Kim, Y. J., Park, T. I., Kim, H. S., Yun, S. J., Park, K. H., Oh M. K., Choi, M. Y., Paik, C. H., Lee Y. S. and Choi Y. E. (2007). High- frequency plant regeneration via adventitious shoot formation from dembryonated cotyledon explants of *Seseamum indicum* L, In Vitro Cell Dev. Biol-Plant, 43: 209-214.

Current Trends in Biotechnology and Pharmacy
Vol. 5 (4) 1469-1472 October 2011, ISSN 0973-8916 (Print), 2230-7303 (Online)

Species Specific Primer Designing – An Easy Method for Identification of *Bacillus thuringiensis.*

Mangesh More, Chetan Narkhede, Shivaji Deshmukh, Aniket Gade and Mahendra Rai*
Department of Biotechnology, Sant Gadge Baba Amravati University
Amravati-444 602, Maharashtra India.
*For Correspondence - mkrai123@rediffmail.com

Abstract

Identification and differentiation of *Bacillus thuringiensis* from *B. cereus* which causes food poisoning and *B. anthracis,* a causal agent of anthrax is not easy. The three *Bacilli* species share a great number of phenotypic and biochemical characteristics therefore, their authentic identification remains a problem. In the present study, we have applied newly developed methodology of the species-specific primer designing and use of polymerase chain reaction for identification and differentiation among commercial *B. thuringiensis* from *B. cereus* and *B. anthracis*. We have designed species-specific primers successfully by comparing different *cry* sequence using the primer designing tool Ampliconb 09. The forward primer was found to be ccactacttacagccgtag whereas, the reverse primer was agttgatatgcgtctaggtggt there was no self complementarities and Hairpin shown by the primers. By using this set of primers it is easy to differentiate *B. thuringiensis* from *B. anthracis* and *B. cereus*. However, results need to be confirmed by wet lab techniques.

Keywords: *Bacillus thuringiensis;* Ampliconb09 and *cry* sequences

Introduction

Bacillus thuringiensis is a Gram positive, spore-forming, rod-shaped bacterium and only the source of *cry* gene for transformation of normal crop into insecticidal Bt crop. *B. anthracis, B. cereus* and *B. thuriengiensis* are morphologically similar but have different virulence nature (4, 5, 7). *B. anthracis* causes anthrax while *B. cereus* causes food poisoning in human (3). Differentiation of B. *thuringiensis* from rest of two species on the basis of biochemical and morphological is not easy there is much need of molecular techniques (8, 15). Polymerase chain reaction (PCR) is one of the molecular tools, widely used for characterization of gene coding for *cry* protein and analysis of *B. thuringiensis*. This technique was first introduced by Carozzi *et al.* (11). Juarez-Prez *et al*. (14) has reported the PCR and E-PCR based approach for detection of *Bacillus thuringiensis* based on cry1 genes only.

Presently, the molecular methods used are difficult, tedious and time-consuming because different primers are used for different genotype. In the present study, we have attempted to design species-specific PCR primers which could amplify all *cry* genes and hence very useful for easy, one step identification of *B. thuringiensis.* Tools for designing group-specific PCR primers are in demand because these type of primer sets are becoming popular for investigating species diversity in environmental samples (12, 13, 10).

Vol. 5 (4) 1469-1472 October 2011, ISSN 0973-8916 (Print), 2230-7303 (Online)

Amplicon is a primer design program specifically for the group-specific primer design on sets of aligned DNA sequences. Amplicon is controlled with a graphical interface that allows the user to view, edit and select sequences from multiple sequence alignment files. Amplicon can read multiple sequence alignments produced by CLUSTALW (10). Sequences can be selected from the alignment and transferred into 'target group' and 'excluded group' windows. Differences between the target and excluded group sequences are then highlighted. These differences may allow the user to design PCR primers that will produce an amplification product from the target group and not from the excluded group. The user may either select primer binding sites directly or use Amplicon's search functions to find binding sites for which the primer will have a set of features determined by the user. Primers properties such as, their TM, GC%, degeneracy, potential for false priming and binding to 'excluded' group sequences should be estimated. The implementations of these estimations are outlined in the Amplicon manual that can be downloaded from the same site as the software. Amplicon is the only free, open source, stand-alone software for group-specific primer design and includes several features not available in any of the other similar programs.

Material and Methods

Fifteen relatively similar length *cry* gene sequences were selected for design of primer. Then the 15 sequences were downloaded from the NCBI website i.e www.ncbi.nlm.nih.gov in FASTA format.

Accession no. of those sequences is as follows gi/2228579,gi/3668334, gi/142868, gi/862636, gi/142773,gi/142731,gi/40283,gi/971346,gi/142729,gi/15721992,gi/40351,gi/143228.gi/17977980,gi/2624004,gi/5689048.

Alignment of the Sequences **:** Alignment was done by using software MEGA 3.1. Aligned sequences were used for designing primers.

Designing of primers **:** It is very necessary to choose correct primers, for proper amplification of target region.

Criteria for designing primers GC Content: The GC content of primer should be 40-60%.

Primer Length: The optimal length of PCR primers is 18-25 bp. These primer lengths are enough for adequate specificity, and short enough for primers to bind easily to the template at the annealing temperature.

Primer Melting Temperature(Tm): Melting Temperature (T_m) of primer is the temperature at which one half of the DNA duplex dissociate to single stranded, which also indicates the duplex stability. Primers with melting temperatures ranging 52-58 ^oC produce the best results. Primers having melting temperatures above 65^oC have a tendency for secondary annealing.

Runs: Primers with long runs of a single base should be avoided as their mispriming chances are more. A maximum number of runs of single base is up to 4 bp is acceptable.

Primer Secondary Structures: Primer secondary structures are produced by intermolecular or intra-molecular interactions, and can lead to poor or no yield product. They adversely affect primer template annealing and thus the amplification. They greatly reduce the availability of primers to the reaction.

i) Hairpins: It is formed by intra-molecular interaction within the primer and should be avoided.

Vol. 5 (4) 1330-1332 October 2011, ISSN 0973-8916 (Print), 2230-7303 (Online)

ii) Self Dimer: A primer self-dimer is formed by intermolecular interactions between the two (same sense) primers, where the primer is homologous to it self, it should avoided.

iii) Cross Dimer: Primer cross dimers are formed by intermolecular interaction between sense and antisense primers, where they are homologous, it should avoid (1, 2)

Repeats: A repeat is a di-nucleotide occurring many times consecutively and should be avoided because they can misprime. For example, ATATATAT. A maximum number of di-nucleotide repeats acceptable in an oligo is 4 di-nucleotides (1, 2)

Software used : Designing primers was carried out by using Ampliconb09. First step was to open the aligned sequences into Amplicon window. Then aligned sequences can be viewed in amplicon window. Thereafter, the target group was selected; in this case it is conserved sequences of *cry* genes. After that the primers were picked up with the help of software. Then various parameters like GC content, Tm, self annealing etc. were checked. The length of PCR product was obtained by using the online software sequence manipulation suites.

Results and Discussion

Forward primer : ccactacttacagccgtag Sequence length: 19, Base counts: G=3; A=5; T=4; C=7; Other=0; GC content (%): 52.63 Molecular weight (Daltons): 5732.78, nmol/A260: 5.59, micrograms/A260: 32.03, Basic Tm (degrees C): 51,

Reverse Primer : agttgatatgcgtctaggtggt Sequence length: 22, Base counts: G=8; A=4; T=8; C=2; Other=0; GC content (%): 45.45, Molecular weight (Daltons): 6836.52 nmol/A260: 4.59 Micrograms/A260: 31.40 Basic Tm (degrees C): 53

PCR suitability tests of above primer was shown that there Tm is less than 58, No GC clamp present, No, Self-annealing, No, Hairpin formation, conforming that primers are having the high degrees of suitability.

PCR product: The PCR product of 2168 bp were obtained by amplifying the consensus sequences with the above primer pair.

Conclusion

Species-specific primer was designed by taking result of multiple sequence alignment of selected 15 *cry* genes. Conserved sequences were selected as target. The DNA fragment of 1614 bp will be amplified by using this set of primer. This is relatively easy, cheap and one step method. However, verification by wet lab technique is required. It may be concluded from the above results that most of the *cry* type of genes may be amplified with the help of the primers, which we have designed, by Ampliconb09. This study will be very useful for the agriculture field and also need of the rapidly growing population.

References

1. Linhart, C. (2005). The degenerate primer design problem: Theory and Application. journal of computational biology, 12(4):432-456.

2. Dieffenbach, C.W., Lowe, T.M.J. and Dveksler, G.S. (1993). General Concepts for PCR Primer Design. *Genome Res,* 3: S30-S37.

3. Rasko, D. A., Altherr, M. R., Han C. S. and Ravel J. (2005). Genomics of the *Bacillus cereus* group of organisms. FEMS Microbiol.Reviews, 29:303-329.

4. Daffonchio, D., Cherif, A. and Borin, S. (2000). Homoduplex and Heteroduplex polymorphisms of the amplified ribosomal 16S–23S internal transcribed spacers describegenetic relationships in the ''*Bacillus cereus* group''. Appl. Environ. Microbiol. 66: 5460– 5468.

5. Helgason, F., Okstad, O.A., Caugant, D.A., Johansen, H.A., Fouet, A, Mock, M, Hegna, I. and Kolstø A. B. (2000). *Bacillus anthracis*, *Bacillus cereus*, and *Bacillus thuringiensis*—one species on the basis of genetic evidence. Appl. Environ. Microbiol. 66:12627–2630.

6. Thompson, J.D., Jeanmougin, F., Gouy, M., Higgins, D.G. and Gibson T.J. (1998). Multiple sequence alignment with clustal X. Trends Biochem.sci. 23:403-405.

7. Vilas-Boas, G.V., Lereclus D.S. and Lemos M.V. (2002). Genetic differentiation between sympatric populations of *Bacillus cereus* and *Bacillus thuringiensis*. Appl. Environ.Microbiol. 68: 1414–1424.

8. Ceron, J.L., Ortiz, A., Quintero, R., Guereca L. and Bravo, A. (1995). Specific primers directed to identify *cry*I and *cry* III genes within a bacillus train collection.Appl.Environ.Microbiol.61:3826-3831.

9. Ceron, J.L., Covarrubias, R., Quintero, A., Ortiz, E., Aranda, L. and Bravo, A. (1994). PCR analysis of the *cry*I insecticidal family genes from Bacillus thuringiensis. Appl.Environ.Microbiol.60:353-356.

10. Thompson, J. D., Toby J. G., Plewniak P., Jeanmougin F. and Jarman S.N. (2004) Amplicon: software for designing PCR primers on aligned DNA sequences. Bioinformatics, 20: 10 2004, 1644–1645.

11. Carozzi, N.B., Kramer, V. C., Warren G. W., Evola, S. and Koziel M.G. (1991), Prediction of insecticidal activity of Bacillus thuringiensis strains by PCR product rofiles.Appl.Environ.Microbiol. 57:3057-3061.

12. Boom, N., De W.W., Verstraete, W. and Top, E. M. (2002) Evaluation of nested PCR-DGGE (denaturing gradient gel electrophoresis) with group-specific 16S rRNA primers for the analysis of bacterial communities from different wastewater treatment plants. FEMS Microbiol. Ecol., 39:101–112.

13. Borm, S. V. and Boomsma J.J. (2002) Group-specific polymerase chain reaction amplification of SSU rRNA-encoding gene fragments from 12 microbial taxa. Mol. Ecol. Notes, 2:356–359.1645

14. Juarez-Prez, V.M., Ferrandis, M.D. and Frutos, R.(1997). PCR based approach for detection of novel Bacillus thuringiensis genes.Appl.Environ.Microbiol.63:2997-3002.

15. Wenwan Z., Yulin S., Thomas M.Y. and Babetta L. M. (2007). *Bacillus anthracis*, *B. cereus* and *B. thuringiensis* Differentiation Using Pulsed Field Gel Electrophoresis. Appl. Environ. Microbiol., 73 (10) :3440-3449

Current Trends in Biotechnology and Pharmacy
Vol. 5 (4) 1473-1479 October 2011, ISSN 0973-8916 (Print), 2230-7303 (Online)

Enhanced Hyaluronic Acid Production by a Mutant Strain, 3523-7 of *Streptococcus zooepidemicus*

K. Jagadeeswara Reddy[1,2], K.T. Karunakaran[2*] and K.R.S. Sambasiva Rao[1]
[1]Department of Biotechnology, Acharya Nagarjuna University, Guntur, India
[2]MM Biolabs Private Limited, 274 Fortuna Glade B3/A, VB Layout, Bangalore, India
*For Correspondence - mmbiolabsindia@yahoo.com

Abstract

Hyaluronic acid (HA) is a hydrated gel and comprises repeating units of glucuronic acid and *N*-acetylglucosamine. HA has been of considerable interest due to its clinical application. This study reports the optimization of fermentation conditions for HA production by *Streptococcus zooepidemicus* 3523-7, a mutant derived from MTCC 3523. In shake flask fermentation, CDM containing 2% glucose and 1.5% yeast extract at pH 7.2 and temperature 36°C with 1% inoculums favored maximum HA production by the strain 3523-7. Enhanced HA production (1.89 g/l) by 3534-7 was seen when the fermentation was carried out in a 10 L bioreactor under optimal conditions such as 400 rpm and aeration 0.6 vvm.

Key words: Hyaluronic acid production, fed-batch fermentation, *Streptococcus ooepidemicus* mutant strain 3523-7.

Introduction

Hyaluronic acid (HA) is a mucopolysaccharide, ubiquitously expressed in human and animal tissues as hydrated gel, which comprises repeating units of glucuronic acid and *N*-acetyl glucosamine (17, 20). It is widely used in biomedical, healthcare, food and cosmetics because of its unique physicochemical properties such as hydrophobicity, lubrication and biocompatibility (7). Many clinical applications of HA however, depends on its molecular size and there are several studies that focus on this aspect. HA has been conventionally extracted from animal tissues such as rooster combs and bovine vitreous humor (18). Since the isolation of HA from animal sources is economically difficult, technology has been developed to produce HA from microbial source through fermentation (13). HA is synthesized by many strains of group A and C *Streptococci* (1, 5, 14, 15, and 17) and number of separation procedures such as protease digestion, HA ion-pair precipitation (with e.g., acetyl-pyridinium chloride), membrane ultrafiltration, HA non-solvent precipitation and lyophilization (8, 9, 10, 12, and 16) have been employed to obtain a highly pure HA suitable for clinical application. Recently Patil *et al* (14) have shown that *S. equi* subsp. *zooepidemicus* MTCC 3523 is capable of producing exopolysaccharide, HA. The present study describes optimal conditions for enhanced production of HA by a mutant strain 3523-7 derived from *S. zooepidemicus* MTCC 3523 using a chemically defined medium.

Materials and Methods

Bacteria and media **:** A spontaneous mutant, 3523-7 derived from *Streptococcus equi* subsp.

zooepidemicus MTCC 3523 (obtained from Institute of Microbial Technology, Chandigarh, India) was defective in pathogenic factor, produced more than tenfold higher HA compared to its parent strain in shake flask fermentation (data not shown). Both the strains 3523 and its derivative 3523-7 used in this study were maintained as freeze dried cultures and stored at 4ºC. Bacteria were sub cultured and grown as described by John *et al*. (4). One percent inoculum was used to propagate *S. zooepidemicus* in Todd Hewitt broth (THB), Brain heart infusion broth (BHI), Veal infusion broth (VIB) as recommended by the manufacturer (Difco) or a chemically defined medium (CDM, 19) containing carbon and nitrogen sources to determine the optimal media for cultivation.

HA production in shake flask fermentation **:** A multifactor experiment was carried out to optimize conditions for production of HA by the strain 3523-7 of *S. zooepidemicus*. Batch culture experiments were performed aerobically in 500 ml flask with a working volume of 100 ml for optimizing various conditions of pH (6.0-8.0), temperature (30-40ºC), glucose (10-60 g/l), agitation (200-300 rpm) and harvesting time (16-24 h). The pH of the culture media was maintained by adding sterile 5 M sodium hydroxide for every 3-5 h (1). Different experiments were conducted to investigate the optimal concentrations of glucose, yeast extract, percentage of inoculum and favorable culture conditions to enhance hyaluronic acid yield.

HA production in fermenter**:** HA fermentation experiments were performed in 10 L fermenter (Scigenics, India) with a working volume of 4 L. Agitation was provided by three, four-bladed turbines, the pH of culture media was maintained as 7.2 ± 0.2 by automatic addition of 5 N sodium hydroxide and temperature at 36ºC. As for the established conditions in shake flask experiments, and maintaining initial glucose concentration of 20 g/l by adding glucose from the stock (220 g/l) from the 8-10th h onwards. The impeller speed (300-800 rpm) and aeration (0.2 to 1.8 vvm) were optimized in the bioreactor for defined culture conditions.

Cell growth**:** The growth of the culture was determined by measuring optical density (OD) at A_{530} nm (1) with UV-Visible Spectrophotometer (Labomed Inc, USA) by using the medium without inoculation as reference blank. The culture samples were diluted with distilled water to give less than 1 OD at A_{530} nm.

Isolation and purification of hyaluronic acid **:** HA produced by *S. zooepidemicus* in fermentation broth was purified as described in literature (2) and some modifications in purification steps as indicated were done to improve the recovery. Purity of HA present in fermented broth during the growth and fermentation was estimated by the carbazole method (2). The fermentation broth containing HA was precipitated by addition of isopropyl alcohol (19). The precipitated HA was redissolved in 0.15 M sodium chloride solution. This solution was treated with activated charcoal (0.5-2%), and stirred for 1 h followed by centrifugation at 7000 rpm for 30 min at 4ºC.

After centrifugation, HA solution was passed through 0.45 µ filters (Millipore, USA). The filtered HA solution was further purified by ultrafiltration in diafiltration mode after two dilutions with pyrogen-free water. Finally the retentate containing HA sample was concentrated to original volume. The concentrated HA solution was precipitated with isopropyl alcohol and vacuum (Biotron, Korea) dried.

Statistical analysis **:** Data were expressed as mean ± SD obtained from at least three independent experiments. Statistical significance of the obtained results was verified by Student's t-test and one way ANOVA using a commercial package (Sigma Plot 5.05). $p < 0.05$ in comparisons to controls was considered as significant.

Results and Discussion

Several studies have reported the optimum culture conditions for exopolysaccharide, HA production in batch mode (1, 3, 13, 14, and 17). Patil *et al* (14) have recently reported HA production by *S. zooepidemicus* MTCC 3523 and the yields were low. The present study reports the optimal conditions for efficient production of HA by a mutant strain, 3523-7 derived from *S. zooepidemicus* MTCC 3523 in a chemically defined medium (CDM)**.** Effect of culture variables like pH, temperature, agitation rate and aeration, and CDM containing various media additives on HA production were also studied. HA production in shake flasks has been scaled up in 10 L bioreactor for enhancing HA production.

Hyaluronic acid production **:** The glucose concentration in the media for growing the organism might play a role in HA production. Initially, effects of glucose concentration in CDM on HA production in shake flask studies were compared. Maximum HA production (444 ± 11.3 mg/l) was obtained at 2% glucose (Fig. 1) and increasing concentration reduced HA production. Glucose molecules are converted into phosphohexoses such as glucose-6-phosphate and fructose-6-phosphate and further utilized for the synthesis of D-glucuronic acid and N-acetyl glucosamine moieties of HA (10). HA production of 506 ± 14.1 mg/l was obtained with 1.5 % of yeast extract and further increase had no significant effect on HA production. Similarly adding 1% inoculum resulted in HA production of 605 ± 12.7 mg/l (Fig. 1) but no significant increase in HA was seen upon increasing inoculum size.

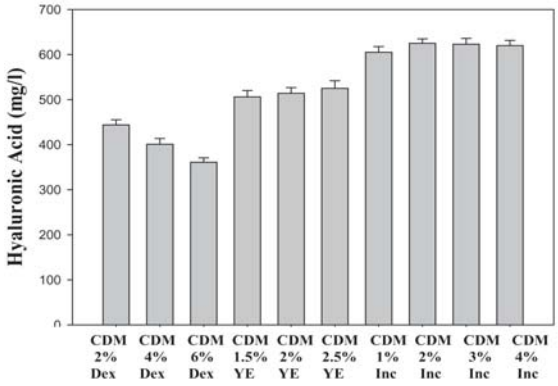

Fig. 1. Effect of initial glucose (Dextrose, Dex) concentration, yeast extract (YE) and inoculum (Inc) size on hyaluronic acid production by *S. zooepidemicus* 3523-7 in shake flasks.

Effect of culture conditions on hyaluronic acid production **:** Since, the pH and temperature are the critical factors that play a major role in cell growth and favor the organism to produce the metabolites, the effect of pH and temperature on culture condition of S. *zooepidemicus* 3523-7 was compared for production of HA. The culture pH exerted a considerable influence on cell growth and HA yields (4). The maximum HA production (834 ± 10.6 mg/l) was obtained at pH 7.2 (Fig. 2A). This is inconsistent with that of Patil *et al.* (14) that they have reported the optimum pH as 7.5 for HA production. Further change in culture pH reduced HA production which is consistent with that of Johns *et al.,* (4) as they have observed similar decline of HA yield at pH 6.0 and pH 7.9. Experiments were performed by varying the culture incubation temperature and this resulted in maximum cell growth and HA production (863 ± 3.5 mg/l) at 36 ºC (Figure. 2B). HA production was less at lower temperatures and this suggest that this effect is result of a reduced growth rate of S. *zooepidemicus* 3523-7 at other temperatures (1).

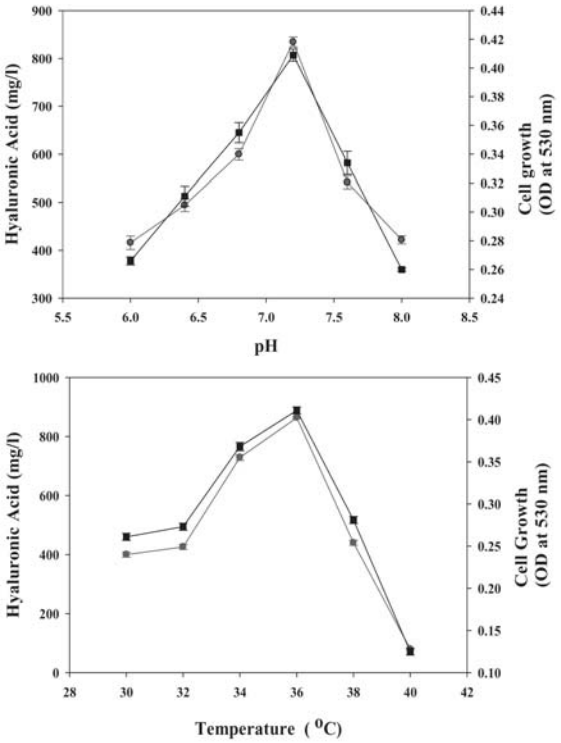

Fig. 2A. Effect of pH on hyaluronic acid production by *S. zooepidemicus* 3523-7 in shake flasks. The change in hyaluronic acid yield (- ● -) along with cell growth indicated by OD_{530} (- ■ -) are shown in line graph. **B.** Effect of temperature on hyaluronic acid production by *S. zooepidemicus* 3523-7in shake flasks. The change in hyaluronic acid yield (- ● -) along with cell growth indicated by OD_{530} (- ■ -) are shown in line graph.

Furthermore, the effect of aeration on HA production was compared and HA production was affected by different levels of agitation (200-300 rpm) in the shake flask cultures. Maximum HA production was achieved (939 ± 9.9 mg/l) when the agitation speed was at 250 rpm (Fig. 3A). Growth time also had a profound influence on HA production and maximum (990 ± 7 mg/l) was observed at 20th of fermentation (Fig. 3B).

***Effect of media on hyaluronic acid production*:** In order to determine the influence of the media on HA production under optimal conditions, *S. zooepidemicus* 3523-7 was grown in different media such as THB, BHI, VIB and CDM (Table. 1) and HA production was compared. Maxium HA production was observed in CDM followed by THB, BHI and VIB. In CDM more HA production was seen compared to THB and BHI. In addition, HA production at various time intervals was also studied and maximum HA production was seen at 24 h of fermentation in CDM and HA concentration decreased beyond 24 hrs (Table 1) in all media possibly due to degradation.

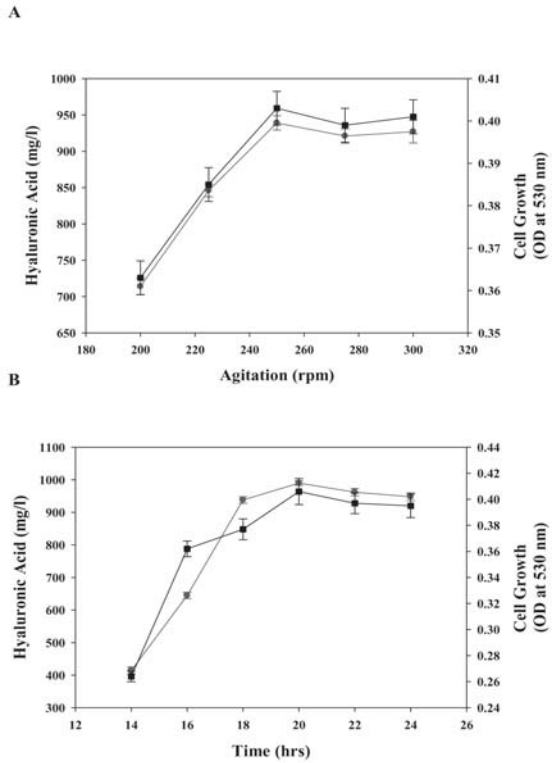

Fig. 3A. Effect of agitation (rpm) on hyaluronic acid production by *S. zooepidemicus* 3523-7 in shake flasks. The change in hyaluronic acid yield (- ● -) along with cell growth indicated by OD_{530} (- ■ -) are shown in line graph. **B.** Effect of growth on hyaluronic acid production by *S. zooepidemicus* 3523-7 in shake flasks. The change in hyaluronic acid yield (- ● -) along with cell growth indicated by OD_{530} (- ■ -) are shown in line graph.

Enhanced hyaluronic production by S. zooepidemicus 3523-7 in fermenter **:** As we have obtained maximum HA production in CDM, fermentation process under optimal conditions was carried out in 10 L fermenter with CDM to enhance HA production by *S. zooepidemicus* 3523-7. Earlier studies have reported that aeration in bioreactor favors the growth of the organism as well as higher HA production compared to anaerobic fermentation (6). Although there are several studies reporting the use of aeration for increasing the yield in hyaluronic acid fermentations, the described aeration and agitation conditions are vague. The need for vigorous agitation is found to enhance oxygen transfer, yet the polymer chain is reportedly susceptible to mechanical stress (3). Very high agitation speeds may be deleterious to HA quality, since a high shear rate may also damage the polymer (4). In present study, maximum HA production of 1.82 ± 0.098 g/l (Fig. 4) was attained at an agitation rate of 400 rpm. Further, increase of the agitation speed from 400 to 800 rpm decreases cell growth and HA production that coincides with earlier reports which observed reduced HA production at high agitation speed (6). The cultures in 10 L bioreactor with aeration of 0.6 vvm resulted in HA production of 1.89 ± 0.042 g/l (Fig. 5). This higher HA concentration in aerated culture is probably due to the superior energy yield obtained by the use of molecular oxygen to oxidize nicotinamide metabolites and the diversion of pyruvate to acetate, rather than lactate (4, 11).

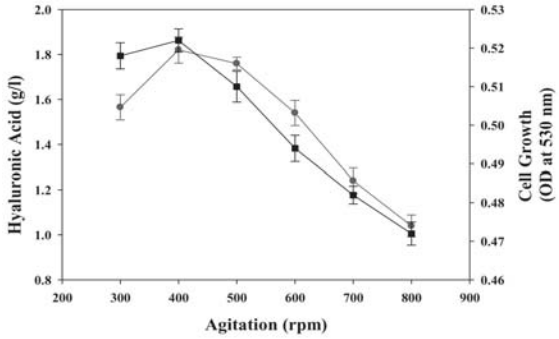

Fig. 4. Effect of agitation (rpm) on hyaluronic acid production by *S. zooepidemicus* 3523-7 in 10 L fermenter. The change in hyaluronic acid yield (- •-) along with cell growth indicated by OD_{530} (- ■-) are shown in line graph.

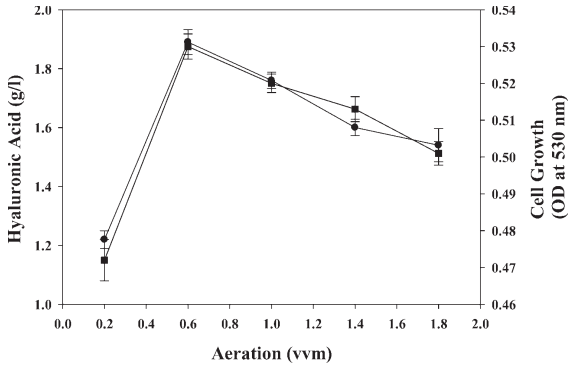

Fig. 5. Effect of aeration (vvm) on hyaluronic acid production by *S. zooepidemicus* 3523-7 in 10 L fermenter. The change in hyaluronic acid yield (- •-) along with cell growth indicated by OD_{530} (- ■-) are shown in line graph.

Table 1. Comparison of HA (g/l) production by *S. zooepidemicus* 3523-7 in various media

Media	24 h	48 h	72 h
THB	98.1	96.3	32.3
BHI	87.8	78.3	32.7
CDM	134.1	121.0	53.7
VIB	69.1	62.9	43.2

Conclusion

A spontaneous mutant, 3523-7 derived from *Streptococcus equi* subsp. *zooepidemicus* MTCC 3523 produced more than tenfold higher HA compared to its parent strain (data not

shown). Therefore, strain 3523-7 was used throughout our studies to optimize fermentation condition for HA production. The present study optimized the media composition and growth conditions of 3523-7 for HA production in shake flask fermentation. CDM containing 2% glucose, 1.5% yeast extract at pH 7.2, temperature 36°C and 1% inoculums seem to favour HA production by the strain 3523-7. Further, we have optimized fermentation conditions (400 rpm and 0.6 vvm) in a 10 L fermenter for 3523-7 to obtain maximum HA production.

References

1. Armstrong, D.C. and Johns, M.R. (1997). Culture conditions affect the molecular weight properties of hyaluronic acid produced by *Streptococcus zooepidemicus*. Appl. Environ. Microbiol., 63(7): 2759-2764.

2. Bitter, T. and Muir, H. M. (1962). A modified uronic acid carbazole reaction. Anal Biochem., 4(4): 330-334.

3. Chabrecek, P., Soltes, L. and Orvisky, E. (1991). Comparative depolymerization of sodium hyaluronate by ultrasonic and enzymatic treatments. J Appl Polym Sci., 48: 233–241.

4. Johns, M.R., Goh, L.T. and Oeggerli, A (1994). Effect of pH, agitation and aeration on hyaluronic-acid production by *Streptococcus zooepidemicus*. Biotechnol. Lett. 16(5): 507-512.

5. Jeong-Hyun Kim, Seung-Jong Yoo, Deok-Kun Oh, Young-Gi Kweon, Dong-Woo Park, Chul-Hoon Lee and Gwang-Hoon Gil (1996). Selection of a Streptococcus equi mutant and optimization of culture conditions for the production of high molecular weight hyaluronic acid. Enzyme Microb Technol. , 19(6): 440-445.

6. Kim, J.H., Yoo, S.J., Oh, D.K. and Kweon, Y.G. (1996). Selection of a *Streptococcus equi* mutant and optimization of culture conditions for the production of high molecular weight hyaluronic acid. Enzyme Microb. Technol.,19: 440-445.

7. Kogan, G., Soltes, L., Stern, R. and Gemeiner, P. (2007). Hyaluronic acid: a natural biopolymer with a broad range of biomedical and industrial applications. Biotechnol. Lett., 29(1): 17–25.

8. Laurent, T. C., Ryan, M. and Pietruszkiewicz, A. (1960). Fractionation of hyaluronic acid. The polydispersity of hyaluronic acid from the bovine vitreous body. Biochim Biophys Acta., 42: 476-485.

9. Martin, A.F. (1953). Towards a referee viscosity method for cellulose. TAPPI. 34:363-366.

10. Matsubara, C., Kajiwara, M., Akasaka, H. and Haze, S. (1991). Carbon-13 nuclear magnetic resonance studies on the biosynthesis of hyaluronic acid. Chem. Pharm. Bull., 39:2446-2448

11. Mausolf, A., Jungmann, J. Robenek, H. and Prehm, P. (1990). Shedding of hyaluronate synthase from Streptococci. Biochem. J., 267: 191-196.

12. Mendichi, R. and Soltes, L. (2002) Hyaluronan molecular weight and polydispersity in some commercial intra-articular injectable preparations and in synovial fluid. Inflamm. Res., 51(3): 115–116.

13. O'Regan, M., Martini, I., Crescenzi, F., De Luca, C. and Lansing, M. (1994) Molecular mechanisms and genetics of hyaluronan

biosynthesis. Int. J. Biol. Macromol., 16(6): 283-286.

14. Patil, K.P., Chaudhari, B.L. and Chincholkar, S.B. (2009). Screening for pharmaceutically important exopolysacchardie producing *Streptococci* and partial optimization for EPS production. Curr Trends Biotechnol Pharma 3(3): 329-340.

15. Rangaswamy, V. and Jain, D. (2008). An efficient process for production and purification of hyaluronic acid from *Streptococcus equi* subsp. *zooepidemicus*. Biotechnol. Letters., 30(3): 493-496.

16. Soltes, L. and Mendichi, R. (2003). Molecular characterization of two host–guest associating hyaluronan derivatives. Biomed. Chromatogr., 17(6): 376–384.

17. Swann, D.A. and Kuo, J.W. (1991). Hyaluronic acid. In: Byrom, D. (ed) Biomaterials-novel materials from biological sources. Stockton Press, New York, pp 286–305.

18. Van Brunt, J. (1986). More to hyaluronic acid than meets the eye. Biotechnology. 4(9): 780–782.

19. Van de Rijn, I. and Kessler, R.E. (1980). Growth characteristics of group A streptococci in a new chemically defined medium. Infect. Immun., 27(2): 444-448.

20. Wessels, M.R., Moses, A.E., Goldberg, J.B. and DiCesare, T.J. (1991). Hyaluronic acid capsule is a virulence factor for mucoid group *A streptococci*. Proc Natl Acad Sci.USA. 88(19): 8317-8321.

NEWS ITEM

Quality Primary Education Leads India's Future: Abdul Kalam

Former President of India Dr A.P.J. Abdul Kalam while emphasizing the importance of education at the seminar titled "Evolution of the Unique", said that the future of India is depended on the quality of primary education given to them. The primary education must be made a fundamental right of Indian citizens. Primary education needs to be approached more creatively where dedicated teachers develop young children who can prepare themselves for the challenges of the future. He said that the syllabi should engage the children and lead them to enjoy the process of learning. Dr. Abdul Kalam also stressed on time management as a rule for achieving success and said that children must be taught to set a goal for themselves and be motivated to work hard to achieve it.

India to raise UK education standards: David Cameron

Britain Prime Minister David Cameron cited the example of India to caution schools not to be complacent and strive for excellence to raise education standards in the country, particularly in Science and Mathematics. In a speech at a school Mr Cameron said, "When China is going through an educational renaissance, when India is churning out science graduates, any complacency now would be fatal for our prosperity. And we've got to be ambitious, too, if we want to mend our broken society". Reminding education leaders and others that Britain was a "modern, developed country", Mr Cameron said that his government had a three-point plan to drive education standards which included ramping up standards, bringing back the values of a good education and changing the structure of education providing more choice, more competition, and greater independence.

Be role models against graft: Prathibha Patil

President of India Pratibha Patil urged teachers to be "role models" by instructing students to fight corruption and be honest citizens. Patil said after giving the national teachers awards that in present times, values such as hard work, integrity, honesty and fighting against corruption are very essential amongst our population. She said that teachers must be role models who instill good habits amongst the upcoming generation. "You may not be leaders, however, you have the capabilities of creating leaders of the future," she added. She also stressed that moral education was as important as conventional subjects. Knowledge without values is incomplete. It is a value system that can prepare the younger generation to become responsible citizens who contribute to the welfare of society and advancement of the human race.

US and Indian Universities will collaborate each other

American consul general Ms. Catherine S. Dhanani, Speaking to presspersons, at the Hyderabad consulate, said that President Barak Obama wants the extension of collaboration between India and US in education field, apart from the economic and industrial sectors. She said that The United States of America will soon collaborate with Indian Universities in the education field. As part of the programme, faculty exchange will start first, followed by student exchange in the near future. Commenting on the one way route of Indians seeking employment and educational opportunities in the US, Ms. Dhanani replied that reciprocation will also take place soon. Addressing the students at the Adikavi Nannaya University, Ms. Dhanani promised to use her good offices for collaboration of Indian Universities with universities in the US to give students the much needed international exposure.

Collaborative Projects in Scientific Research for Advanced Research between India and UK

Dr. Ashwani Kumar, Minister of State for Planning, Science & Technology and Earth Sciences, India and Mr. Gordon Brown, former Prime Minister of Britain discussed perspectives of ways and means to further consolidate cooperation between UK and India through Science & Technology and Innovation space in the margins of the Summer Davos conference in Dalian, China. Mr. Brown offered assistance in marshalling the resources of international business and philanthropic community for facilitating the achievement of universal education targets set by India and the achievement of millennium development goals. While appreciating the huge efforts being made by India, in this area Mr. Brown offered to facilitate the availability of teachers and technology to realize this goal.

SCIENTIFIC NEWS

Papillomavirus Protein Fragment Blocks Spread of the Virus in Tissue Culture

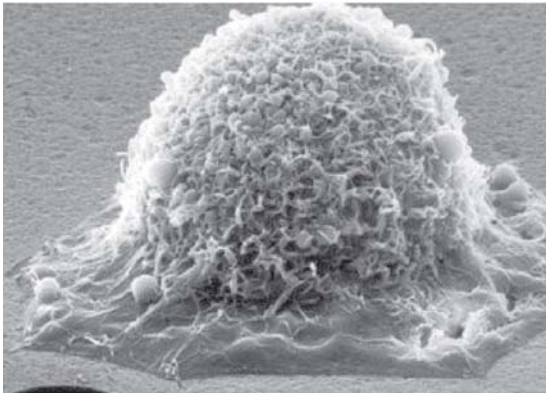

A protein fragment generated from an integral human papillomavirus (HPV) protein prevents transcription of viral genes and blocks spread of the HPV virus, which is the causative agent of cervical and anogenital cancers. Investigators at Tufts University, Boston prepared a truncated version of the HPV E2 protein. This E2R fragment contained only the protein's C-terminal dimerization domain, and repressed the normal function of E2 due to formation of an inactive heterodimer. When tested in a mammalian cell cultures system, E2R was found to inhibit theE2 protein of HPV-16, the high risk strain of the virus that is most commonly associated with cancers. As HPV infects epithelial cells, the outermost layer of the skin, and the mucous membranes, protein inhibitors such as E2R may be adaptable to application in a topical form. Dr. James Baleja, Associate professor of Biochemistry at Tufts University said, "Social and economic challenges make widespread administration of a vaccine difficult, particularly in developing countries, A topical treatment for HPV could provide an economical option".

M. Murali

Biodegradable Nanoparticles Kill Drug Resistant Gram-Positive Bacteria

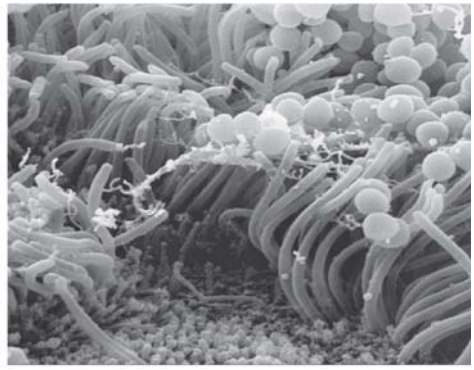

Investigators at the IBM Almaden research Laboratory, USA focused on types of nanoparticles that would be able to disrupt bacterial cell membranes. In their study, they prepared polymer nanoparticles synthesized by metal-free organo catalytic ring-opening polymerization of functional cyclic carbonate. These nanoparticles were biodegradable and possessed a secondary structure that could insert into and disintegrate bacterial and fungal cell membranes. Data obtained in collaboration with researchers at the Singapore Institute of Bioengineering and Nanotechnology, Singapore showed that the nanoparticles disrupted microbial walls and membranes selectively and efficiently, thus inhibiting the growth of Gram-positive bacteria,

including methicillin-resistant *Staphylococcus aureus* (MRSA), and fungi, without inducing significant hemolysis over wide range of concentrations. The biodegradable nanoparticles, which can be synthesized in large quantities and at low cost, represent a promising new class of antimicrobial drugs.

V. V. N. Yaswanth

Lavender Oil Demonstrates Impressive Antifungal Activity

Essential oils distilled from *Lavandula viridis* demonstrated potent antifungal activity in studies carried out on laboratory cultures of dermatophytes and *Candida* species. Investigators at the University of Coimbra, Portugal isolated essential oils from *L.viridis* by hydro distillation and analyzed them by gas chromatography and mass spectrometry. The MIC (minimal inhibitory concentration) and the minimal lethal concentration (MLC) of the essential oils and its major compounds were determined against several pathogenic fungi. The effects of short exposure to the oils on *Candida albicans* cells were examined by flow cytometry. Results revealed that the oils were characterized by a high content of oxygen-containing monoterpenes, with 1,8-cineole being the main constituent. Monoterpene hydrocarbons were present at lower concentrations. According to the determined MIC and MLC values, the dermatophytes and *Cryptococcus neoformans* were the most sensitive fungi followed by *Candida* species. For most of these strains, MICs were equivalent to MLCs, indicating a fungicidal effect of the essential oil. The oil was under further shown to inhibit completely filamentation in *Candida albicans* at concentrations well below the respective MICs. Flow cytometry results suggested a mechanism of action ultimately leading to cytoplasmic membrane disruption and cell death. *Lavandulka* oil shows wide-spectrum antifungal activity and is highly potent. This is a good starting point for developing this oil for clinical use to manage fungal infections. Research has shown that essential oils may be cheap, efficient alternatives that have minimal side effects.

S. Arvind Kumar

Newly Identified Cytokine Blocks Inflammatory Bowel Disease in Mouse Model

A recently identified cytokine, interleukin 37 (IL-37) was found to prevent the development of inflammatory bowel disease (colitis) in a mouse model. Basing their work on previous findings that IL-37 functioned as a fundamental inhibitor of innate immunity and inflammation, investigators at the University of California, San Diego (USA) and their colleagues at the University of Colorado (Boulder, USA) examined a role for IL-37 during experimental colitis. For this study, they genetically engineered a transgenic mouse strain that expressed human IL-37 (hIL-37tg). These mice and a matching wild type population were subjected to dextran sulfate sodium (DSS)-induced colitis. Results revealed that during the development of colitis, clinical disease scores were reduced by 50%, and histological indices of colitis were one-third less in hIL-37tg mice compared with wild type counterparts. Reduced inflammation was associated with decreased leukocyte recruitment into the thin layer of loose connective tissue that lies beneath the colonic epithelium (lamina propria). Dr. Jesus Rivera-Nieves, Professor of gastroenterology at the University of California, San Diego, said that while the mechanism of action was not understood, in the future, scientists may be able to engineer cells to overproduce IL-37 and use it to treat or control an overactive immune system in humans.

T. S. N. Lakshmi

EDUCATION

PhD/Post Doctoral Programs

Admission to Ph.D. Programme: Applications are invited for admission to Ph.D programmes in Central Drug Research Institute (CDRI), P.B.No.173, Chattar Manzil, Lucknow - 226001, India in the relevant areas of research in the Institute like Biochemistry, Botany, Clinical & Experimental Medicine, Drug Target Discovery & Development, Endocrinology, Fermentation Technology, Medicinal & Process Chemistry Division, Microbiology, Molecular & Structural Biology, Parasitology, Pharmaceutics, Pharmacokinetics & Metabolism, Pharmacology & Toxicology. Candidates with M.Sc. in Life Sciences/ Biotechnology/Chemical/Pharmaceutical sciences) and qualified in CSIR-UGC-NET, ICMR, DBT examination or M.Pharm in Pharmaceutical/ Pharmacology disciplines are eligible. Applications should be submitted online and a print out of the system generated page containing the ID ticket along with their photograph, photocopies of certificates of date of birth, educational qualifications and proof for qualifying JRF/GPAT must be sent to Scientist-in-Charge, Academic Affairs Division, Central Drug Research Institute (CSIR), Chattar Manzil, Lucknow-226 001, India on or before 12th October 2011. Email: academic_unit@cdri.res.in. Information can also be obtained from the website: www.cdriindia.org.

OPPORTUNITIES

Centre for Cellular and Molecular Biology (Council of Scientific & Industrial Research), Uppal Road, Hyderabad - 500 007, India. Applications are invited from eligible candidates for 2 positions of Project JRF in research projects entitled "Study of some important signaling and metabolic pathways in T-cell and glioma" funded by DBT Project GAP0372 under 'R&D in Bioinformatics' and 1 position of Project JRF in research projects entitled "Modelling spatiotemporal distribution of host-parasite populations and disease spread" funded by DST Project GAP0304. Candidates with MSc/MTech in Biotechnology/Bioinformatics with Physics/ Mathematics/Statistics as major in Undergraduate level OR BTech in Bioinformatics/Biotechnology with sound knowledge of Physics, Mathematics, and Statistics. Eligible candidates may download the application form from website www.ccmb.res.in and appear for Interview along with the duly filled in application form supported by Bio-data and one set of attested photo copies of Certificates of educational qualification, age, experience, caste (in case of SC/ ST/OBC candidates), latest passport size photograph. Date of Walk-in-Interview: 10th October, 2011 at CCMB, Habsiguda, Uppal Road, Hyderabad - 500 007.

Centre for Genetic Disorders, **Banaras Hindu University, Varanasi –** 221005, India. Applications are invited from eligible candidates for the post of Junior Research Fellow (JRF) in DBT funded project entitled "Genetics of Tooth Development: Genes underlying tooth agenesis in Human" at Centre for Genetic Disorders, Banaras Hindu University, Varanasi – 221005, India. NET/GATE qualified candidates with atleast 55% marks in M.Sc. in Human Genetics / Life Science / Biotechnology / Biochemistry / Zoology are eligible. Application on plain paper with biodata along with qualifications, research experience etc. suppoted by attested documents, a recent passport size photograph, contact no. and email ID should reach to Dr. Parimal Das, Principal Investigator, DBT Project (P-07-455), Centre for Genetic Disorders, Faculty of Science, Banaras Hindu University, Varanasi – 221005, India. Email: parimal@bhu.ac.in.

SEMINARS/WORKSHOPS/CONFERENCES

International Symposium on Innovations in Free Radical Research and Experimental Therapeutics & 5th Annual Convention of Association of Biotechnology and Pharmacy: An International Symposium on Innovations in Free Radical Research and Experimental Therapeutics was going to held on 7th- 9th December, 2011 at Karunya University, Karunya Nagar, Coimbatore - 641114 Tamil Nadu, India organized by Department of Biotechnology, School of Biotechnology and Health Sciences, Karunya University, Karunya Nagar, Coimbatore - 641114 Tamil Nadu, India. Two hard copies of abstract can be submitted to Dr.Guruvayoorappan Chandrasekaran, Organising Secretary, Department of Biotechnology, School of Biotechnology and Health Sciences, Karunya University, Karunya Nagar, Coimbatore - 641114 Tamil Nadu. Email: immunologykarunya@gmail.com. Awards and Gold medals are presented to winning participants in Oral/ Poster Presentations. Registration fee for Research scholars/students is Rs.850 and for others it is Rs.1500. For further details contact: Dr.Guruvayoorappan Chandrasekaran, Organising Secretary, Department of Biotechnology, School of Biotechnology and Health Sciences, Karunya University, Karunya Nagar, Coimbatore - 641114 Tamil Nadu. Mobile: 09894337418, Email: immunologykarunya@gmail.com.

Young Scientists Convention–2011 (YSC-2011): A Young Scientists Convention (YSC) was going to held on October 27-28, 2011 at Acharya Nagarjuna University organized by Andhra Pradesh Academy of Sciences in association with Acharya Nagarjuna University, Guntur, Andhra Pradesh, India. The young scientists below the age of 35 are encouraged to participate in the annual convention choosing the related branch of science like Physical Sciences, Chemical Sciences, Life Sciences, Earth, Ocean & Atmospheric Sciences. Abstract can be submitted online through E-mail: anudbt@yahoo.co.in with a copy to raokrss@yahoo.in and apas1963@yahoo.co.in on or before October 15, 2011. Registration Fee: For participants from colleges & universities - Rs.800/- and for members from national laboratories - Rs.1200/- (DD drawn in favor of Organising Secretary in place of Treasurer). For further details contact: Dr. P.Sudhakar, Convener, YSC-2011, Department of Biotechnology, Acharya Nagarjuna University, Guntur – 522 510, A.P, India. Phone: 9000122929, 2346172. and Prof. K.R.S. Sambasiva Rao, Organising Secretary, Department of Biotechnology, Acharya Nagarjuna University, Guntur, A.P., India – 522 510. Phone – 0863-2346355.

Hands on Training Workshop on Molecular Techniques for Identification of Biocontrol Agents: A workshop on Molecular Techniques for Identification of Biocontrol Agents was going to held on October 18-20, 2011 at Bharathidasan University, Tiruchirapalli, India organized by Department of Plant Sciences, Bharathidasan University, Tiruchirapalli-24, India. Registration Fee- Rs. 1200/- in the form of DD drawn in favour of "Organizing Secretary, Mol.Tech.Iden.ofBiocontrol agents". Last date of receipt of application: Oct 10, 2011. For further details contact: Dr.M.Sathiyabama, Organizing Secretary, Department of Plant Sciences, Bharathidasan University, Tiruchirapalli-620024, India. Phone – 09443893527. Email: bamakvs@gmail.com.

Workshop on Fundamentals Of Nanoscience & Biotechnology - Present and Future Prospects: A workshop on Fundamentals Of Nanoscience & Biotechnology - Present and Future Prospects was going to held on November 22-25, 2011 at Department of Nanobiotechnology, Life Science Foundation India, Karnataka, India organized jointly by Department of Nanobiotechnology, Life Science Foundation India, Karnataka and Department of Biotechnology, Meerut Institute of Engineering and Technology, Meerut, Uttarapradesh, India. Registration Fee- Rs. 2000/- in the form of Demand Draft in favour of "LSF India". Last date of receipt of application: Oct 15, 2011. For further details contact: Dr. Hiregoudra B, Executive Director, Life Science Foundation India, Admin. Office: Morigeri, Bellary – 583220, Karnataka.Tel: 08970177844 / 9880420600. Email: nanobiotek@yahoo.com. and Prof Dr. A. Subrahmanyam, Ph.D., (Ind.Micr.) D.Sc, Professor and Head, Department of Biotechnology, Meerut Institute of Engineering & technology, Off.,

NH 58, Baghpat Crossing Byepass Road, Meerut – 250005, Uttara Pradesh, India.Tel: 0121-2439019 / 2439057.

International Conference on Medical Genetics and Genomics: An International conference on Medical Genetics and Genomics was going to held on December 12-14, 2011 at Bharathidasan University, Tiruchirapalli, India organized by Department of Biomedical Science, School of Basic Medical Sciences, Bharathidasan University, Tiruchirapalli, India. Abstract can be submitted online through E-mail: icmg2k11@gmail.com on or before November 10, 2011. Registration Fee: For Faculty &Professionals - Rs.2500/- and for Research Scholars - Rs.1500/- and for Students - Rs.1000/- (DD drawn in favor of The Organizing Secretary, ICMG-2011, payable at Tiruchirapalli). For further details contact: Dr. K.Prem Kumar, Organizing Secretary, ICMG-2011, Department of Biotechnology, Acharya Nagarjuna University, Guntur – 522 510, A.P, India. Phone: 9000122929, 2346172. and Prof. K.R.S. Sambasiva Rao, Organising Secretary, Department of Biomedical Science, School of Basic Medical Sciences, Bharathidasan University, Tiruchirapalli, India– 620024. Phone –08056589893.

Andhra Pradesh Akademi of Sciences
in association with
Acharya Nagarjuna University

Young Scientists CONVENTION

October 27-28, 2011

The proposed young scientist convention provides a strong motivation to the researchers with interactions and for developing higher level training in advanced research. The young scienctists below the age of 35 years from the following areas of sciences are encouraged to participate in the annual convention choosing the related branch of science as given under.

* **Physcial Sciences** (Mathematical / Engineering / Technology)
* **Chemical Sciences** (Pharmaceutical / Medical & Health)
* **Life Sciences** (Microbiology / Biochemistry / Biotechnology / Agriculture / Veterinary / Fishery
* **Earth, Ocean & Atmospheric Sciences**

Participation Details

Scientific paper presentation (oral /poster) would be there in all the above categories of Science. The participants need to send their abstracts (below 300 to 500 words in word format) through email - anudbt@yahoo.co.in with a copy to raokrss@yahoo.in and apas1963@yahoo.co.in on or before October 15, 2011. Best papers will be rewarded with suitable prizes during the convention.

Registration Fee

There will be a registration fees of Rs. 800/- for participants from colleges and universities and Rs. 1200/- for members from national laboratories DD should be in favor of Organizing Secretary in place of Treasurer.

For further details contact

Dr. P. Sudhakar, Convener, YSC-2011
Department of Biotechnology
Acharya Nagarjuna University
Nagarjunanagar – 522 510, Guntur, A.P.
Phone : 9000122929, 0863-2346355, 2346172
E-mail: anudbt@gmail.com

Prof. K.R.S. Sambasiva Rao
Organizing Secretary YSC-2011
Department of Biotechnology
Acharya Nagarjuna University
Nagarjuna Nagar - 522 510, Guntur A.P., India
E-mail : raokrss@yahoo.in

VENUE : Deichman Auditorium, ACHARYA NAGARJUNA UNIVERSITY
Nagarjuna Nagar - 522 510, Guntur, A.P. India.

International Symposium on Innovations in Free Radical Research and Experimental Therapeutics
&
5th Annual Convention of Association of Biotechnology and Pharmacy

(December 7-9, 2011)

Venue: Karunya University, Karunya Nagar, Coimbatore – 641 114, Tamilnadu, India

Broad Areas of Focus

Oxidative stress, Free radicals and Antioxidants
Free Radical and Cancer
Life style diseases
Herbal Drugs, Nutraceuticals in experimental therapy
Immunomodulators and Radioprotectors
Immunopharmacology
Toxicology
Translation Research
Pharmaceutical Biology
Drug Metabolism and Drug Interactions
Complementary and Alternative Medicines

Contact for further details

Dr. Guruvayoorappan Chandrasekaran
Organizing Secretary
Department of Biotechnology, Karunya University

Registered with Registrar of News Papers for India
Regn. No. APENG/2008/28877

Association of Biotechnology and Pharmacy

(Regn. No. 28OF 2007)

Executive Council

Advisory Board

Executive Members

Printed, Published and owned by Association of Bio-Technology and Pharmacy # 6-69-64 : 6/19, Brodipet, Guntur - 522 002, Andhra pradesh, India. **Printed at :** Don Bosco Tech. School Press, Ring Road, Guntur - 522 007. A.P., India **Published at :** Association of Bio-Technology and Pharmacy # 6-69-64 : 6/19, Brodipet, Guntur - 522 002, Andhra pradesh, India.
Editors : Prof. K.R.S. Sambasiva Rao, Prof. Karnam S. Murthy